
N
© 2007 Europa Technologies
Image © 2007 DigitalGlobe
©2006 Google™
Pointer 10°31'28.49" N 76°12'52.97" E elev 33 m Streaming |||||||||| 100%
Eye alt 594 m

The Different Colors of Gold

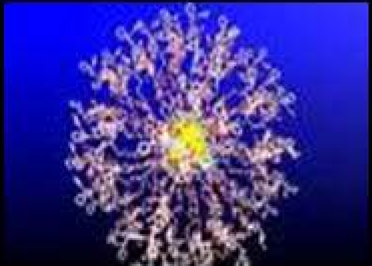

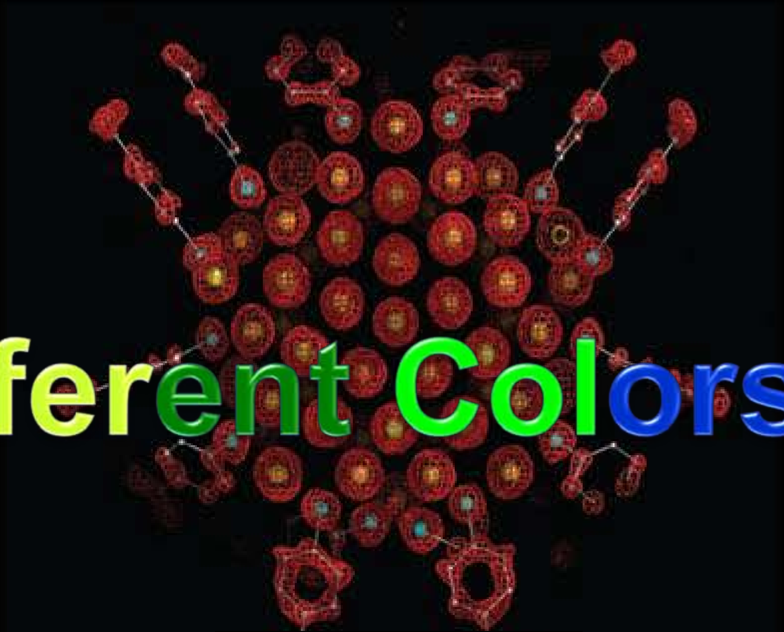

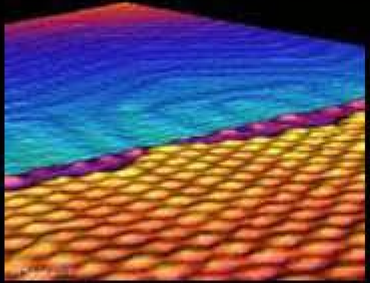

T. Pradeep

http://www.dstuns.iitm.ac.in/pradeep-research-group.php
pradeep@iitm.ac.in

St. Thomas' College, Thrissur, January 5, 2010

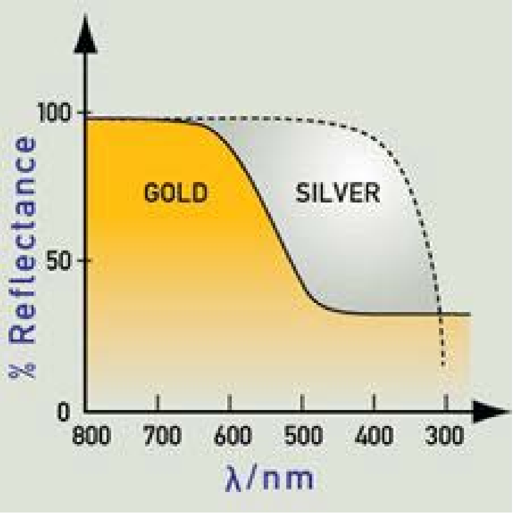

http://www.webexhibits.org/causesofcolor/9.html&usg=__eazWHmio6ubJtFEG_T6NScyGsc=&h=306&w=300&sz=9&hl=en&start=1&um=1&tbnid=g_xdRB5Fe6C6XM:&tbnh=117&tbnw=115&prev=/images%3Fq%3Dgold%2Bnanoparticles%2Bcolor%26hl%3Den%26sa%3DG%26um%3D1

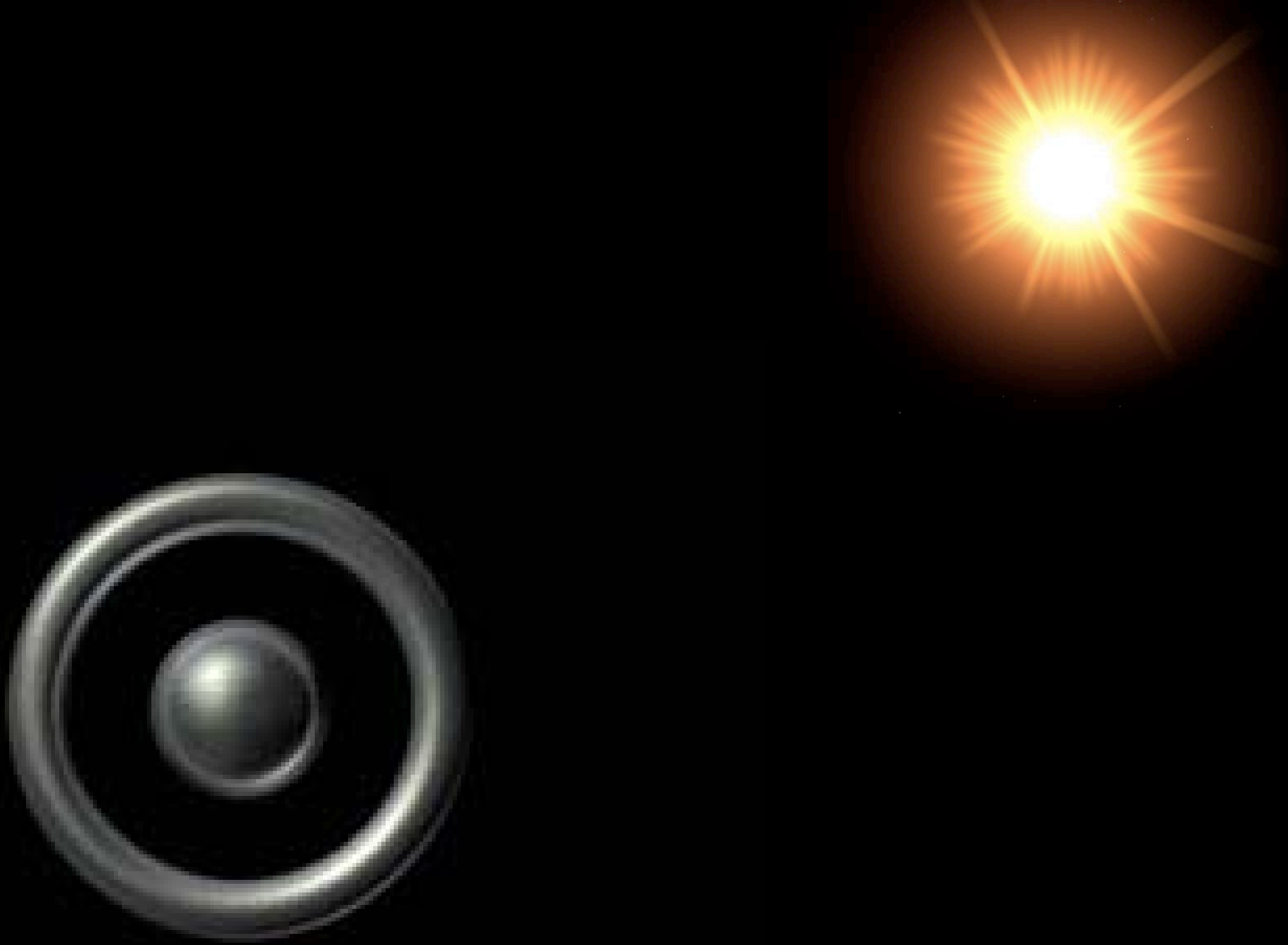


407
408
409
411
414
410
412
413

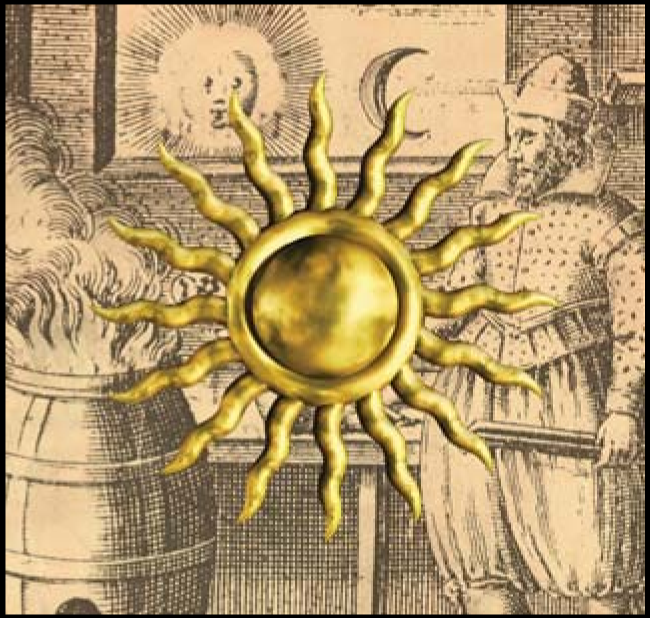

Gold was fascinating for many alchemists.
Copyright Murray Robertson.

Alchemy!

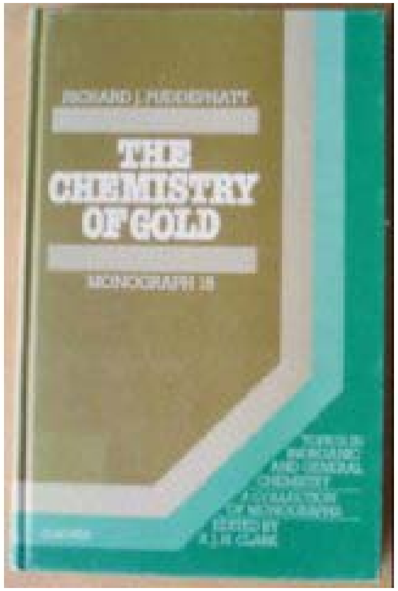

Hardcover: 274 pages
Publisher: Elsevier Science Ltd (June 1978)
Language: English
ISBN-10: 0444416242
ISBN-13: 978-0444416247

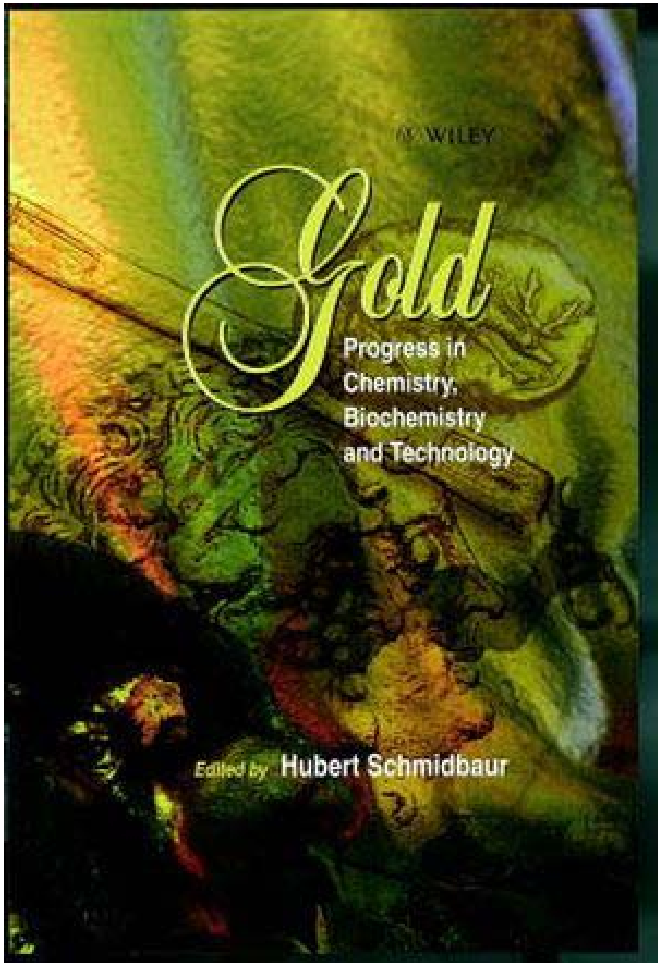

Gold Chemistry
ISBN: 978-0-471-97369-0
Hardcover
908 pages
March 1999

GOLD-CATALYSIS

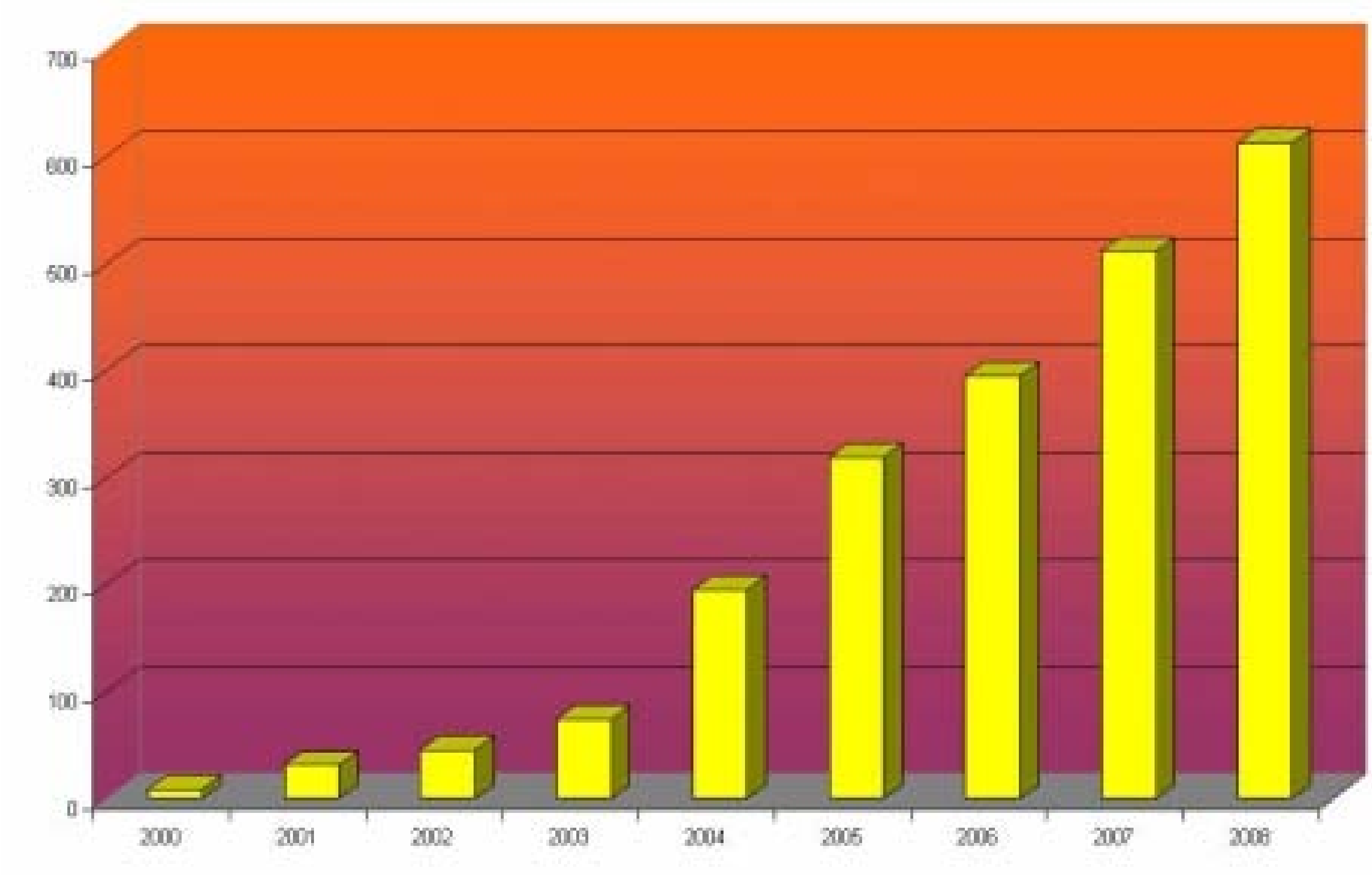

Number of papers published per year after the discovery of gold catalysis.

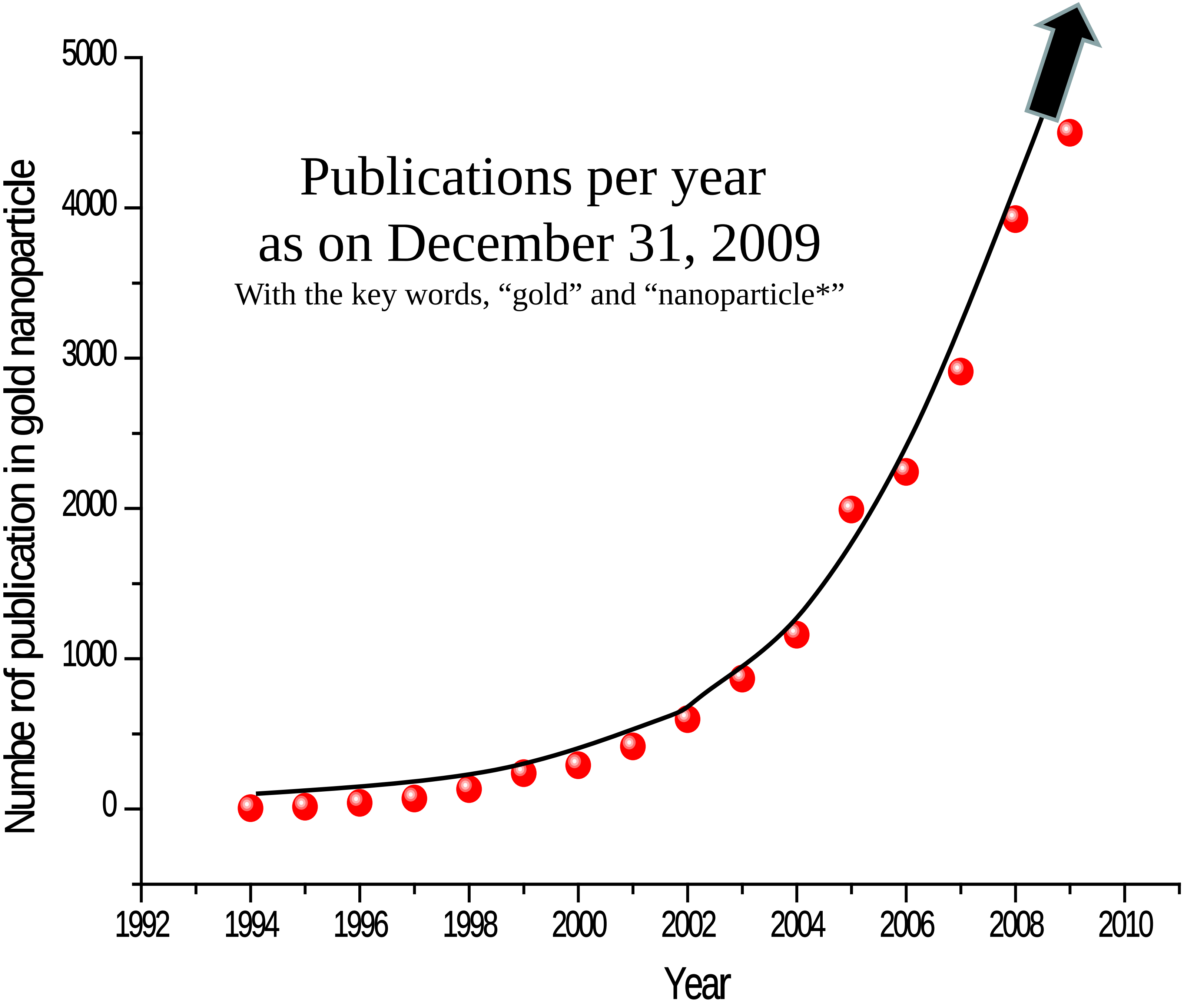

Publications per year
as on December 31, 2009

With the key words, “gold” and “nanoparticle*”

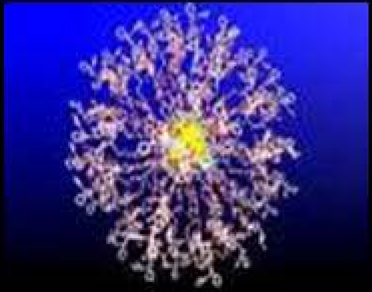

The Different Colors of Gold


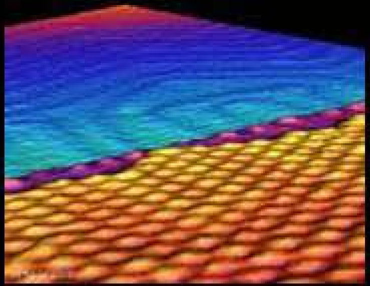

Revisiting gold molecules in the era of nanotechnology


T. Pradeep

http://www.dstuns.iitm.ac.in/pradeep-research-group.php
pradeep@iitm.ac.in

The gold that is not GOLD!

Acknowledgements

M.A. Habeeb Muhammad
E.S. Shibu, P. R. Sajanlal
Udayabhaskar Rao Tummu
K.V. Mrudula

K. Kimura, University of Hyogo, Japan
T. Tsukuda, IMS, Okazaki, Japan
S.K. Pal, SNBS, Kolkata
G.U. Kulkarni, JNCASR, Bangalore
R. V. Omkumar, RGCB, Tiruvananthapuram
Manzoor Koyakutty, Amrita, Kochi

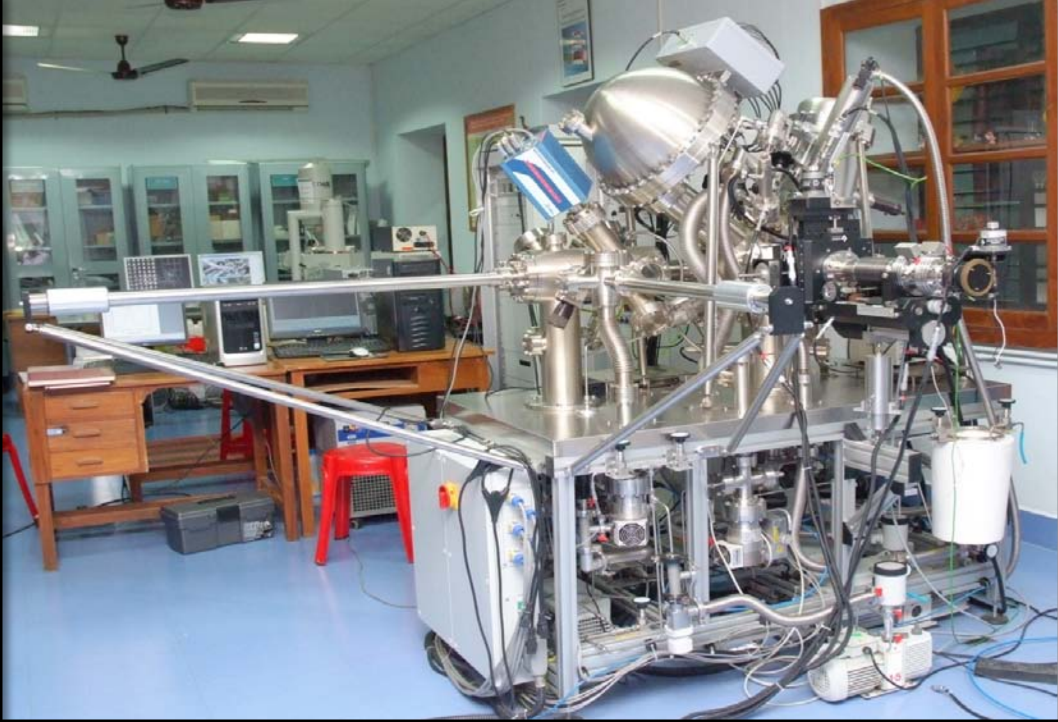

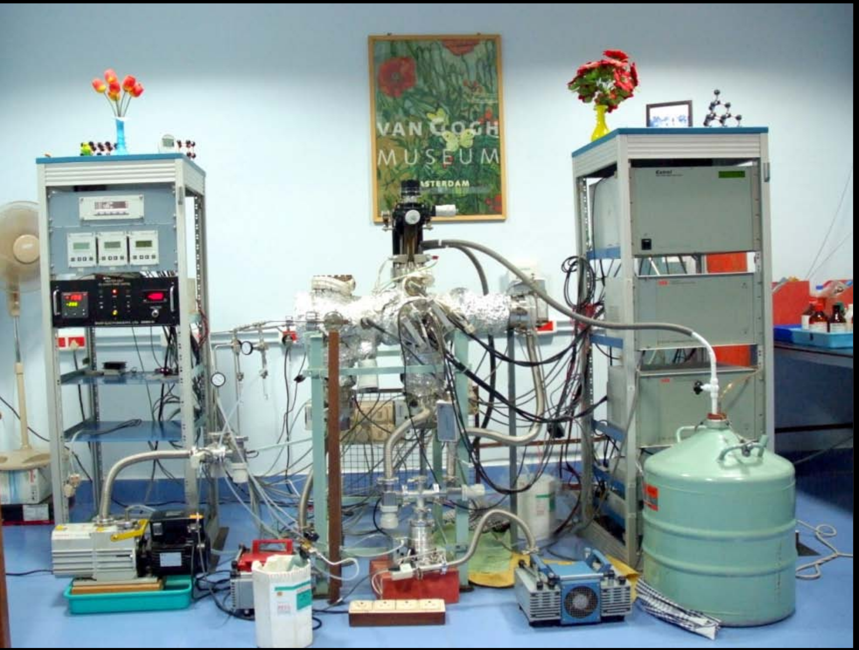
VAN GOGH
MUSEUM
AMSTERDAM


WITec
α

E. S. Shibu

P. R. Sajanlal

E

B

E

T s
e

T th 1845)

22/09/1791-25/08/1867

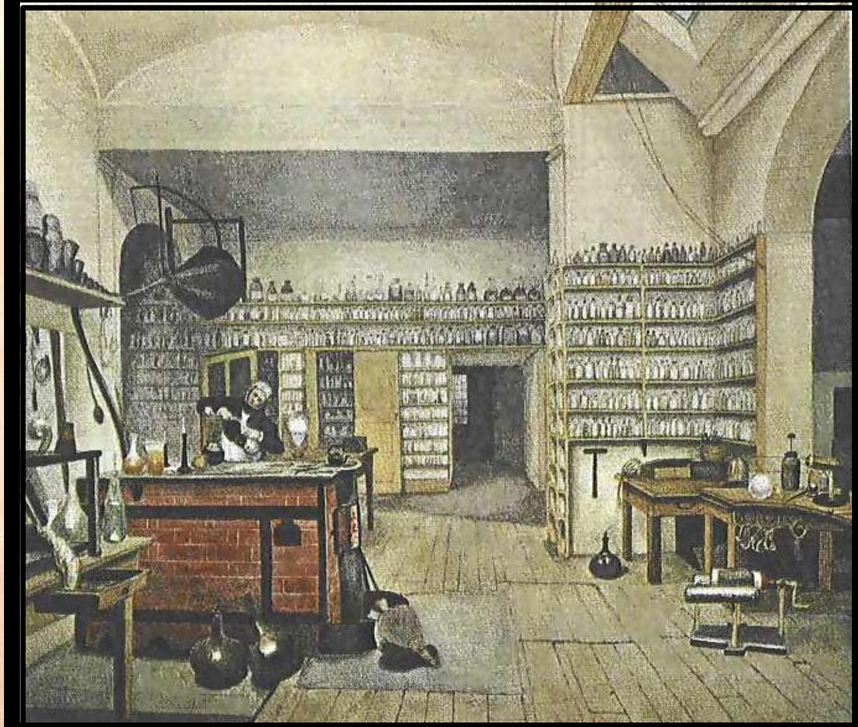

Faraday in his laboratory
Royal Institution

Faraday’s gold preserved in Royal Institution. From the site, http://www.rigb.org/rimain/heritage/faradaypage.jsp

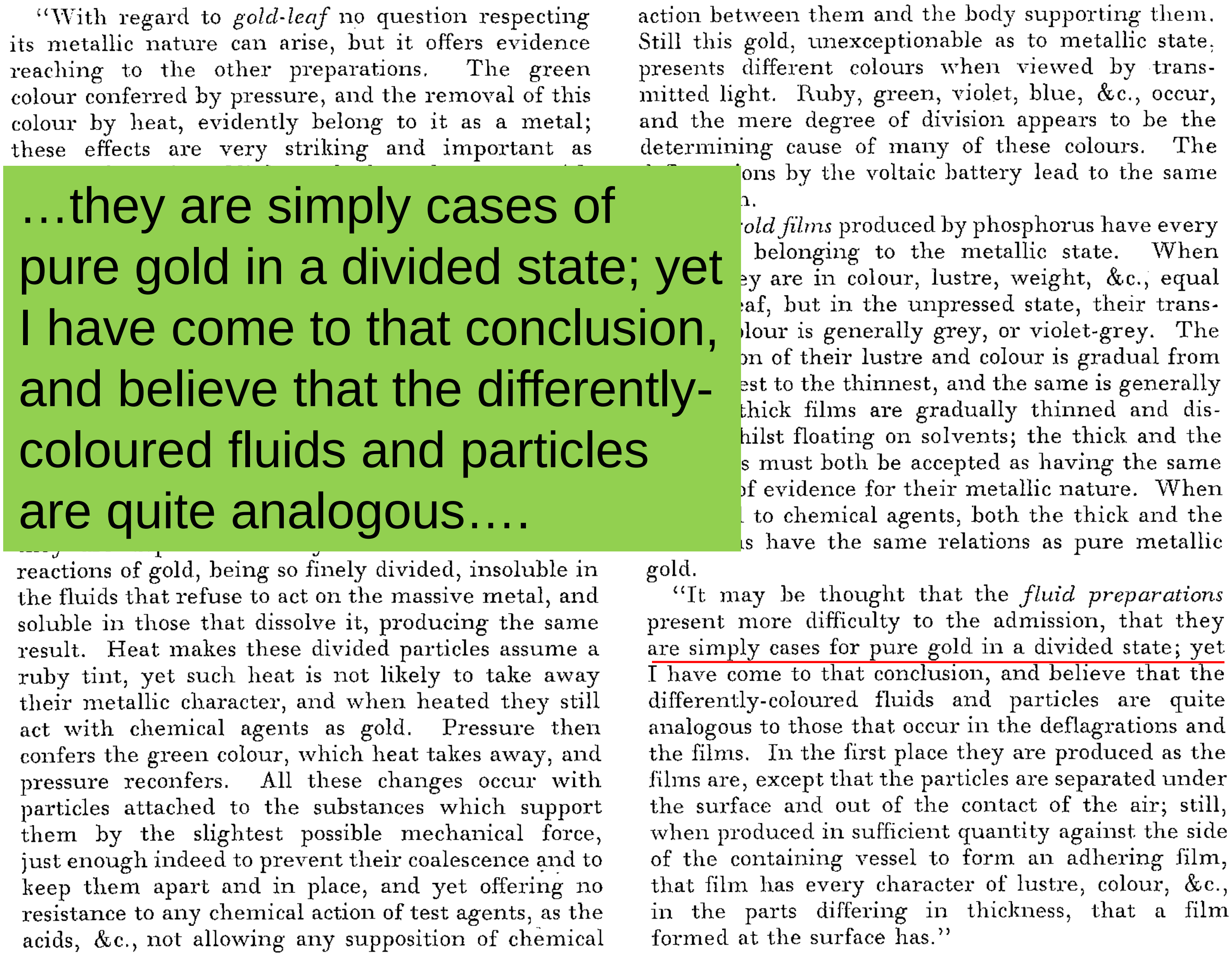

Gustav Mie (1868 - 1957)

Surface plasmons

1905

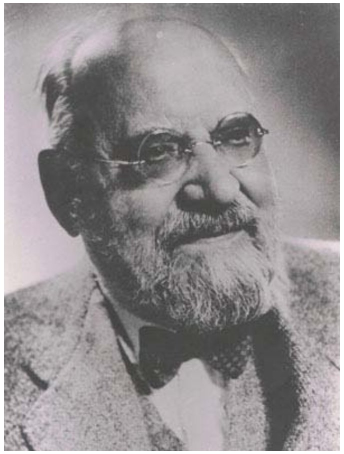

1940

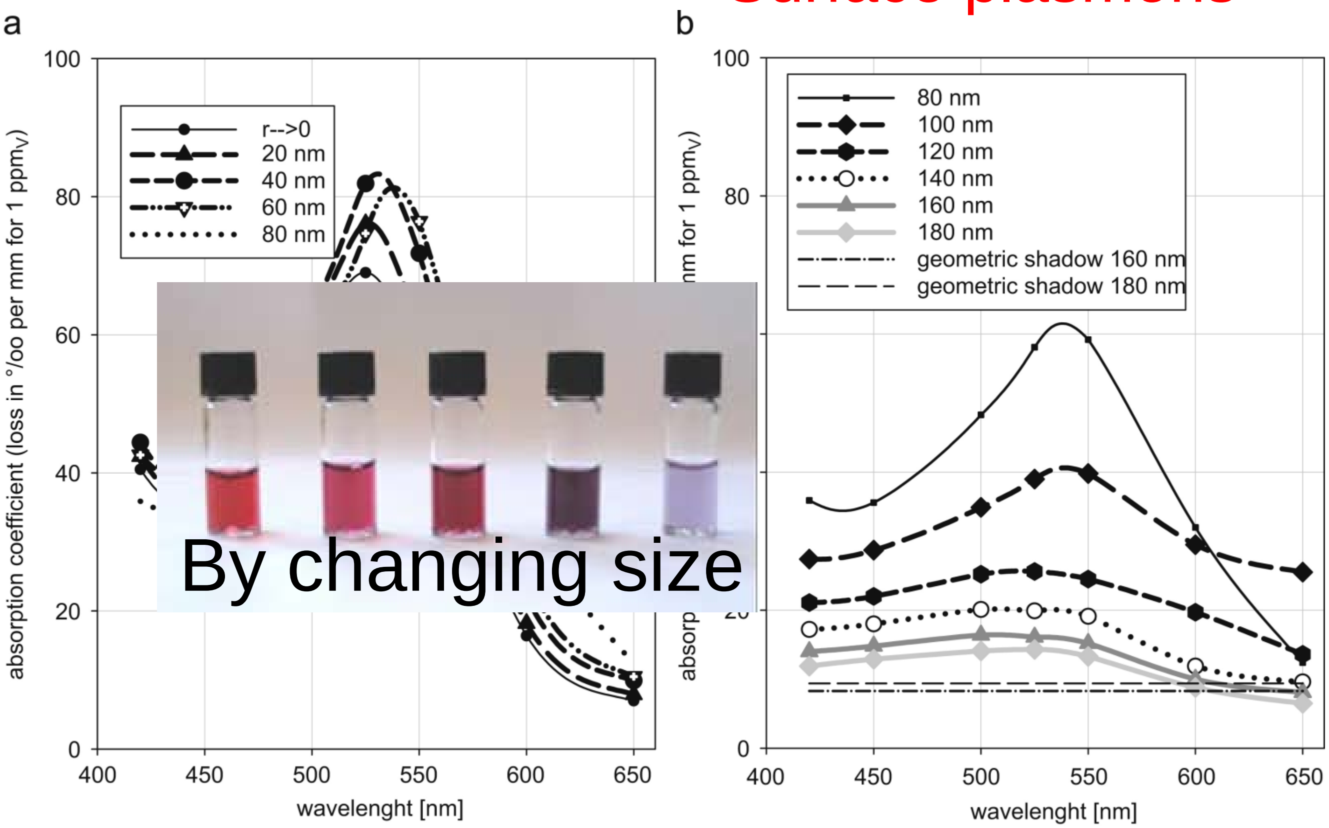

By changing size

Mie G. Beiträge zur Optik trüber Medien speziell kolloidaler Goldlösungen (contributions to the optics of diffuse media, especially colloid metal solutions). Ann Phys 1908;25:377–445. This paper, including an English translation, as well as other historic papers on light scattering and absorption can be found at www.iwt-bremen.de/vt/laser/wriedt/index_ns.html .

Silicon dioxide in Lycurgus cup = 73%
Silicon dioxide in Modern Glass = 70%
Sodium oxide in Lycurgus cup = 14%
Sodium oxide in Modern Glass = 15%
Calcium oxide in Lycurgus cup = 7%
Calcium oxide in Modern Glass = 10%

So why is it coloured? The glass contains very small amounts of gold (about 40 parts per million) and silver (about 300 parts per million)

Lycurgus cup; in transmitting light (left) and in reflected light (right). From the site, http://www.thebritishmuseum.ac.uk.

Colours by changing shape

Shells

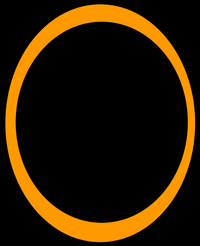

Gold shells. Nanoshells designed to absorb various wavelengths of light (the six vials on the right), including infrared (vial at far right) compared to gold colloid (far left). Used with permission from www.ece.rice.edu/people/faculty/halas.

Colours by changing shape

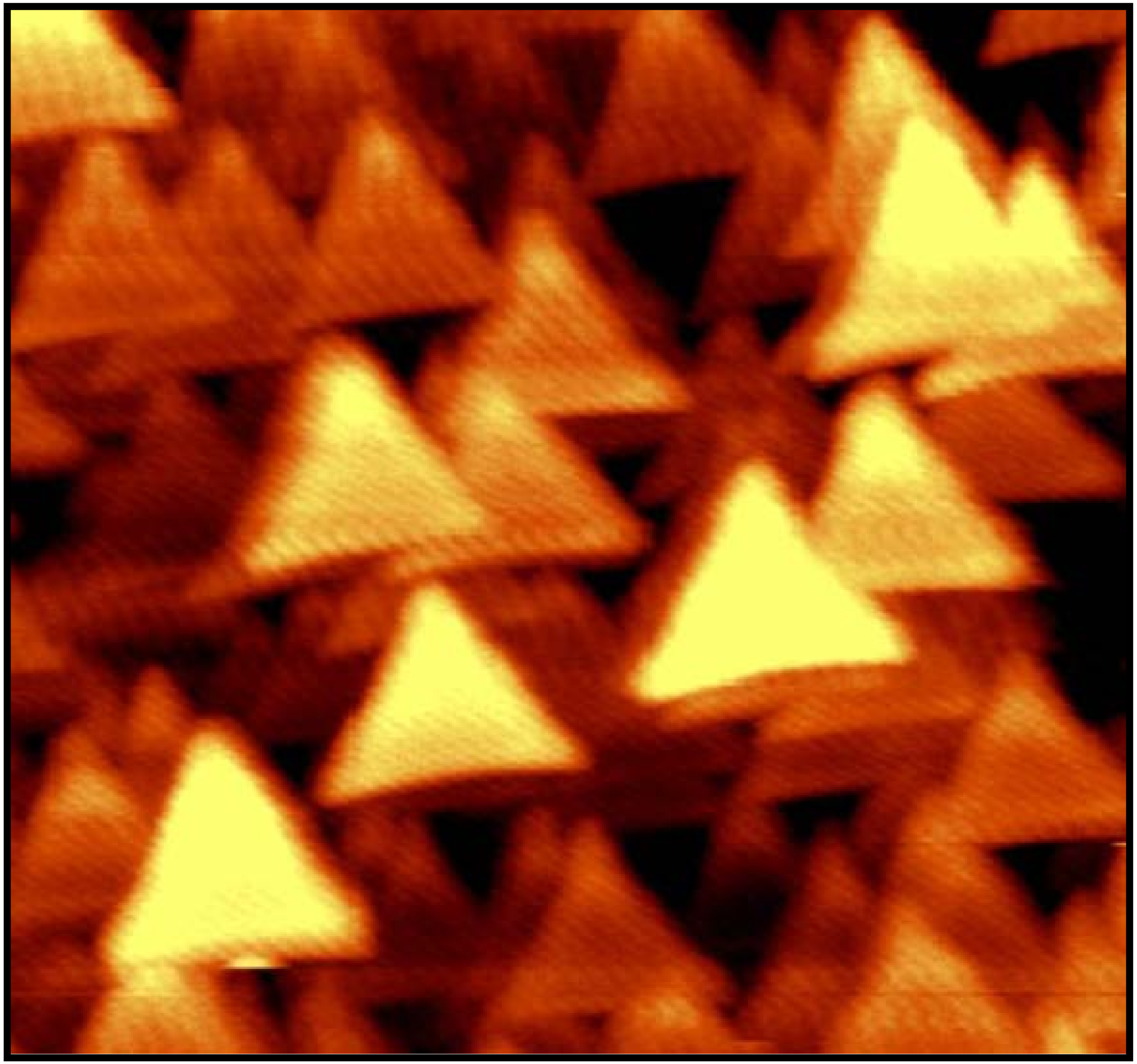

Sajanlal

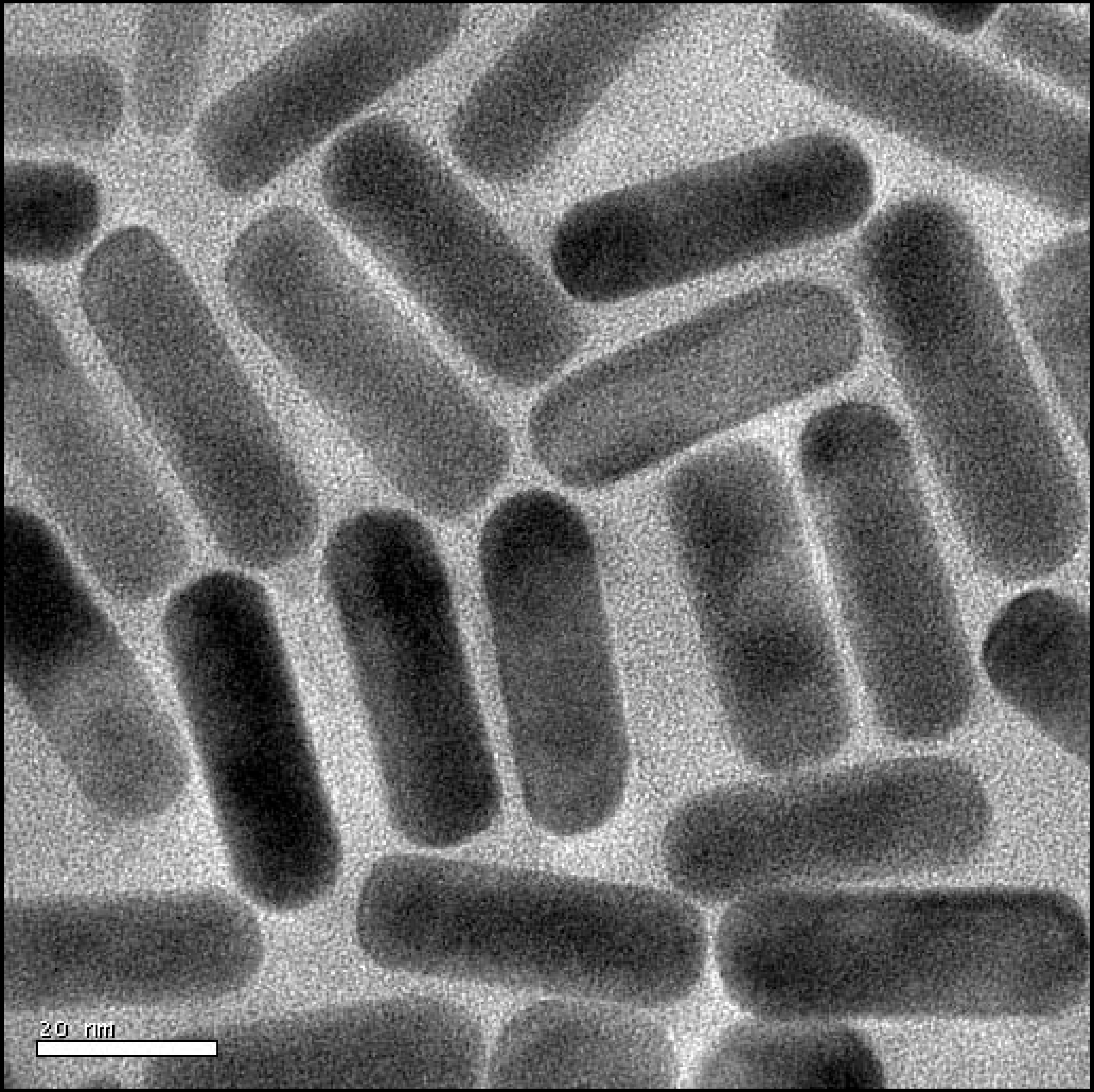

Samal

Materials are needed for chemistry

Nanorod Solution

Nanorod Powder

Changing length by reaction

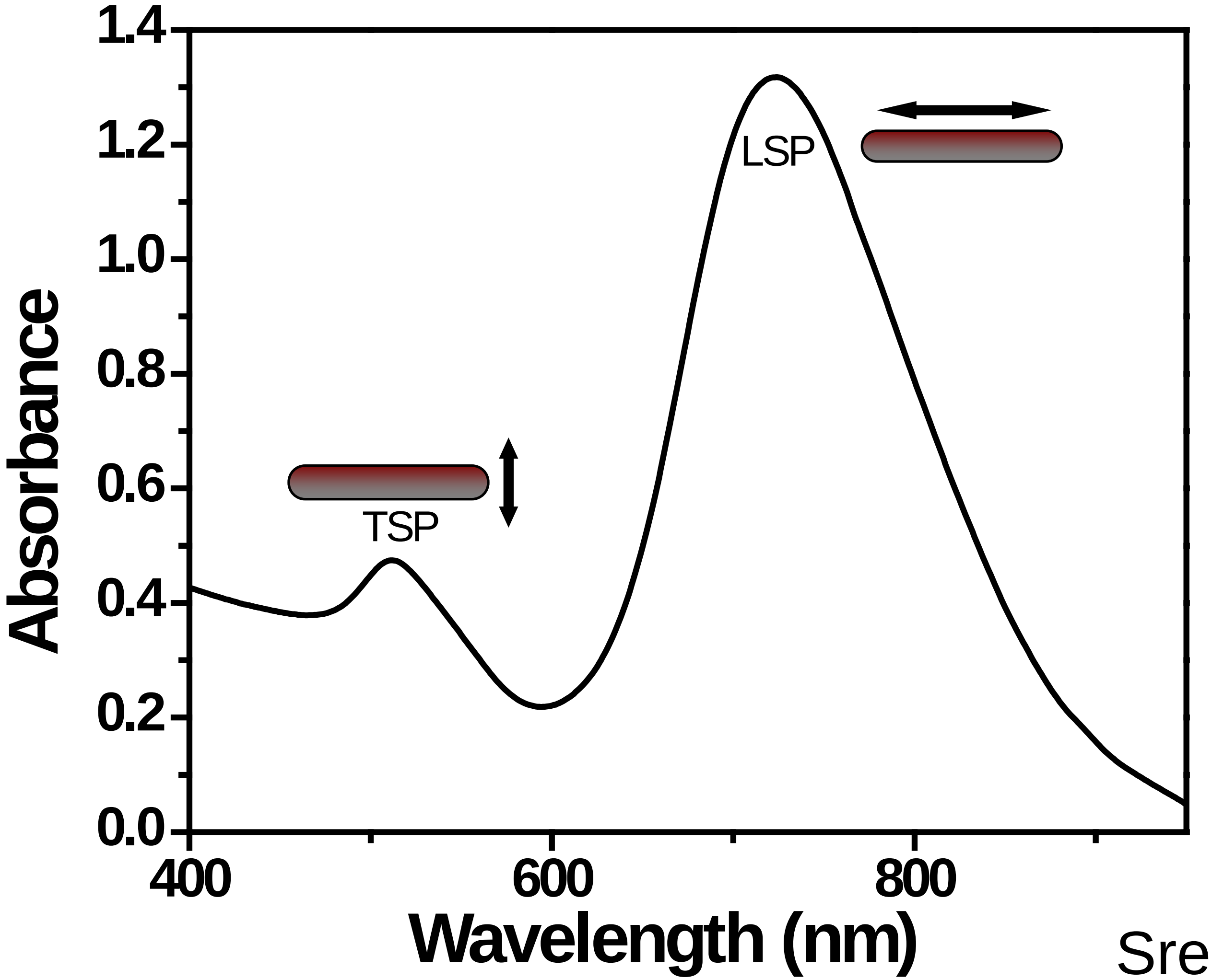

Sreeprasad

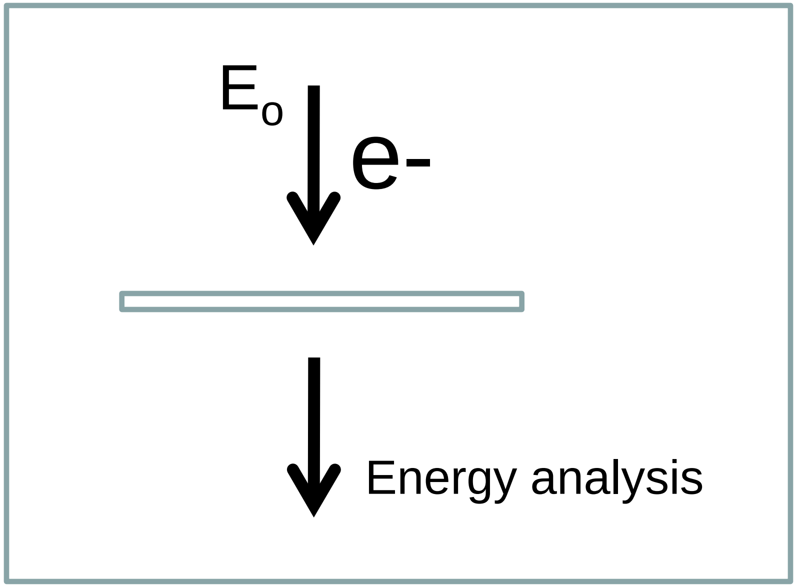

E_o

e-

Energy analysis

EELS

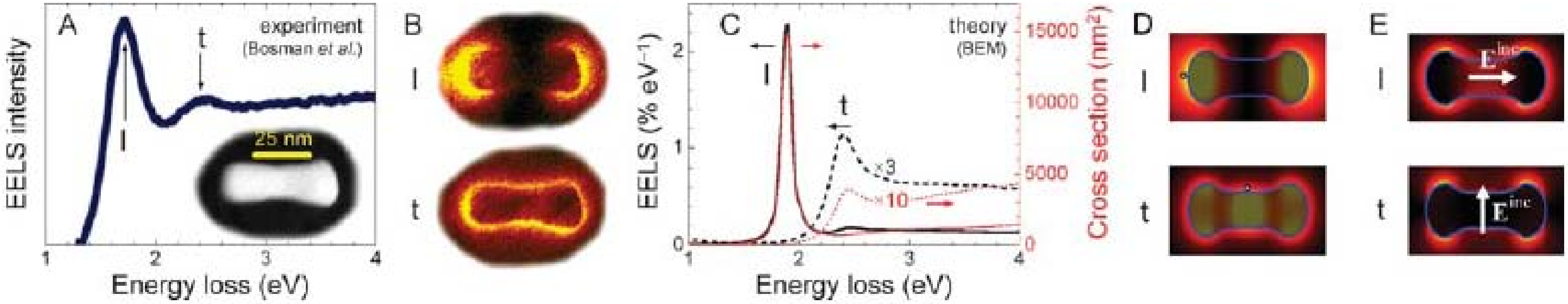

M. Bosman, V. J. Keast, M. Watanabe, A. I. Maaroof, M. B. Cortie, Nanotechnology, 2007, 18, 165505.


n Electron Microscopy (HRTEM) of Nanomaterials
OXFORD
JEOL
DELL

The reaction

$$\xrightarrow[\text{CuCl}_2]{70\ ^{o}\text{C}}\ t$$

T. S. Sreeprasad et al. **2008**

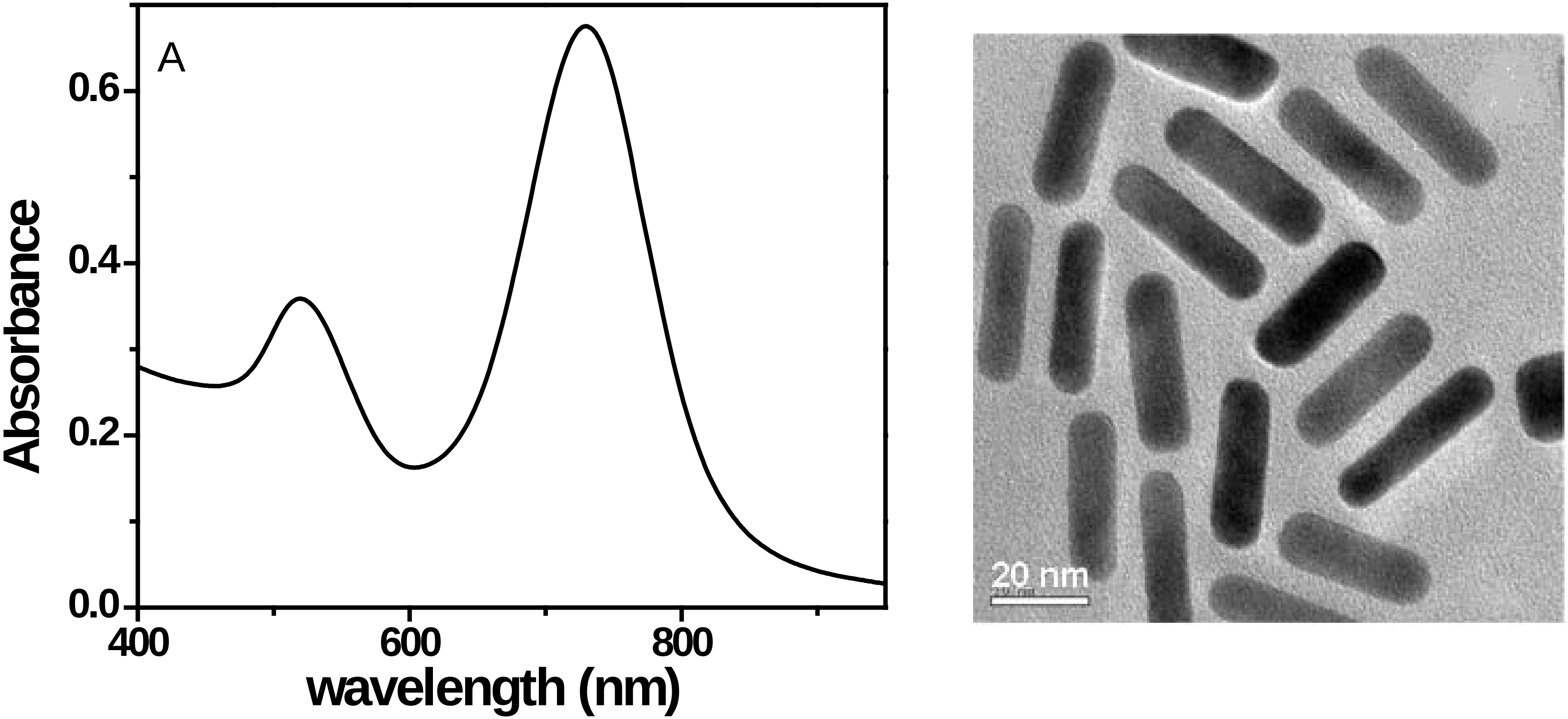

(A)UV-visible spectrum of the starting nanorod and (B) TEM image

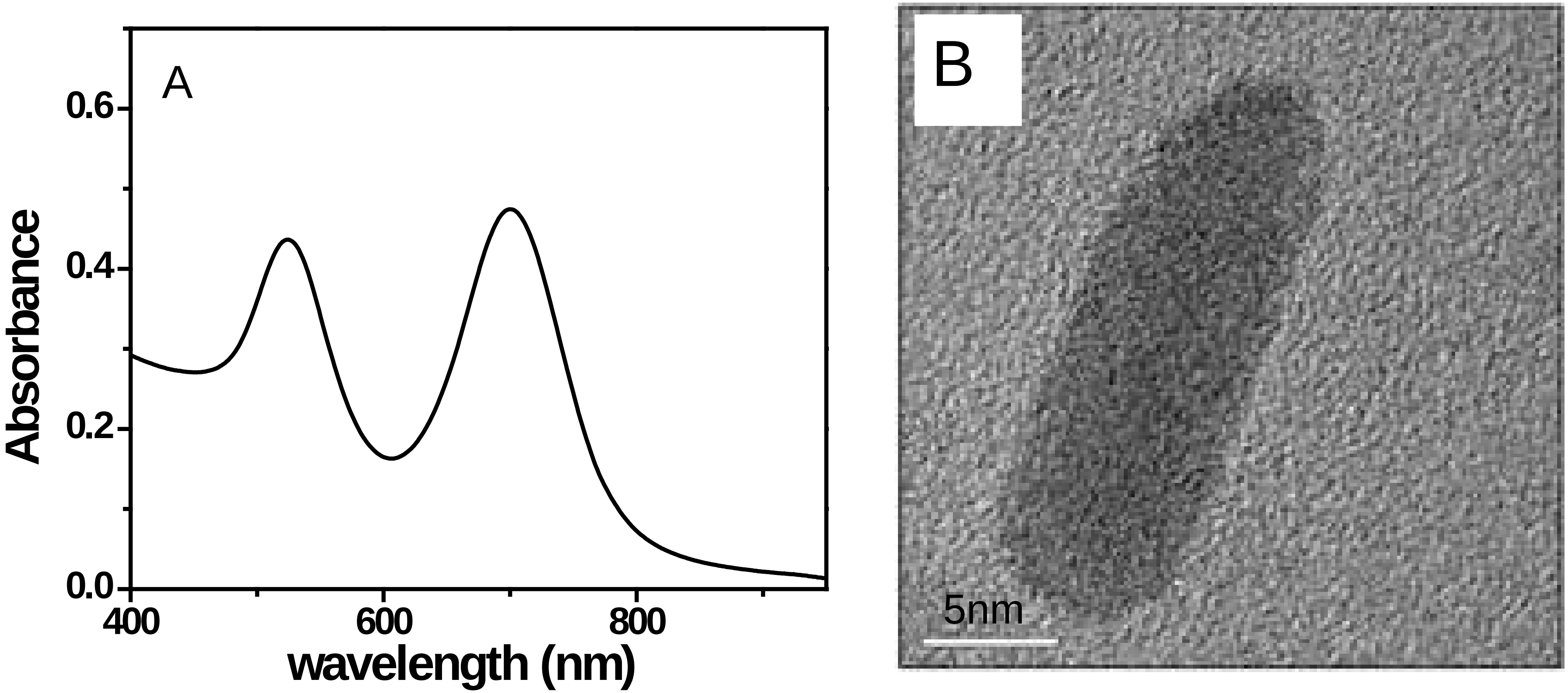

(A) UV-visible spectrum acquired after 1 h of reaction between gold nanorods and $CuCl_2$. TEM taken from the same sample.

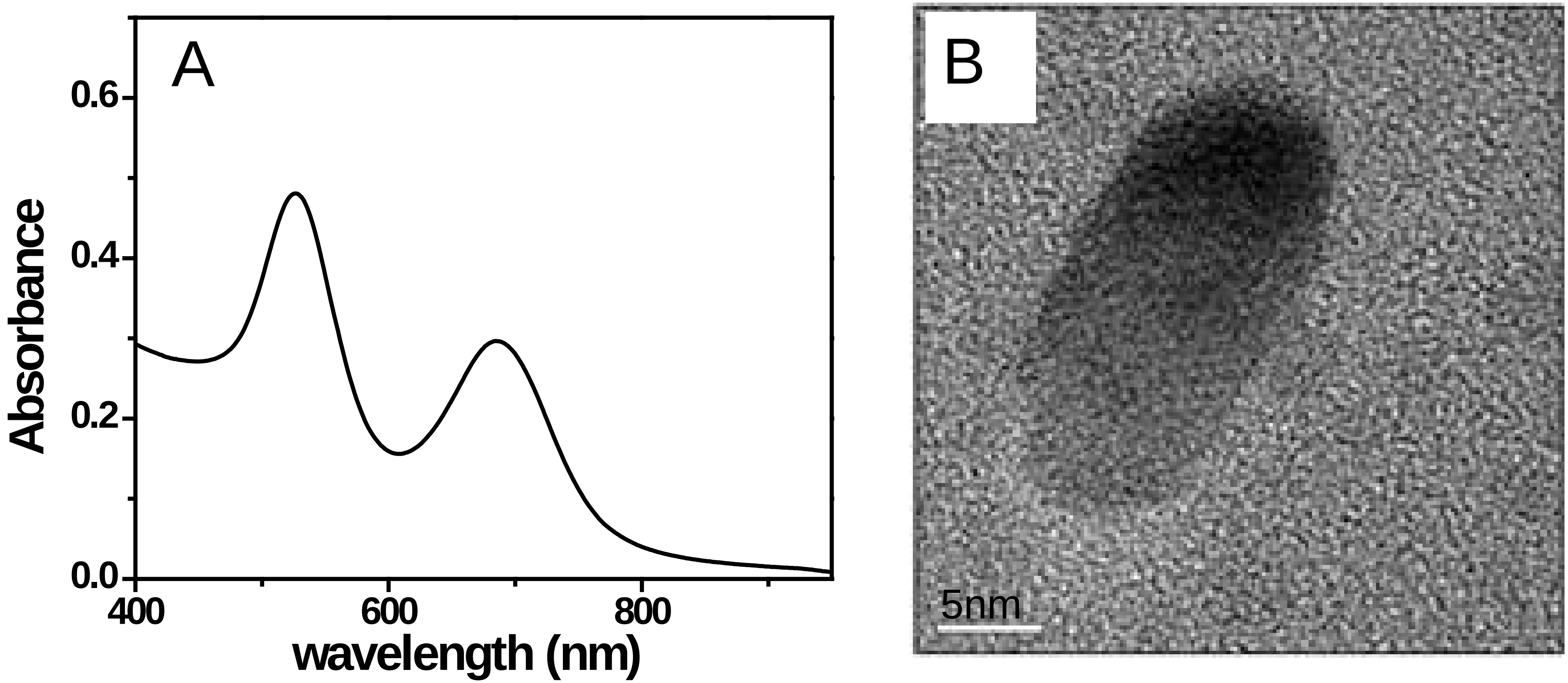

(A) UV-visible spectrum acquired after 2 h of reaction between gold nanorods and $CuCl_2$. TEM taken from the same sample.

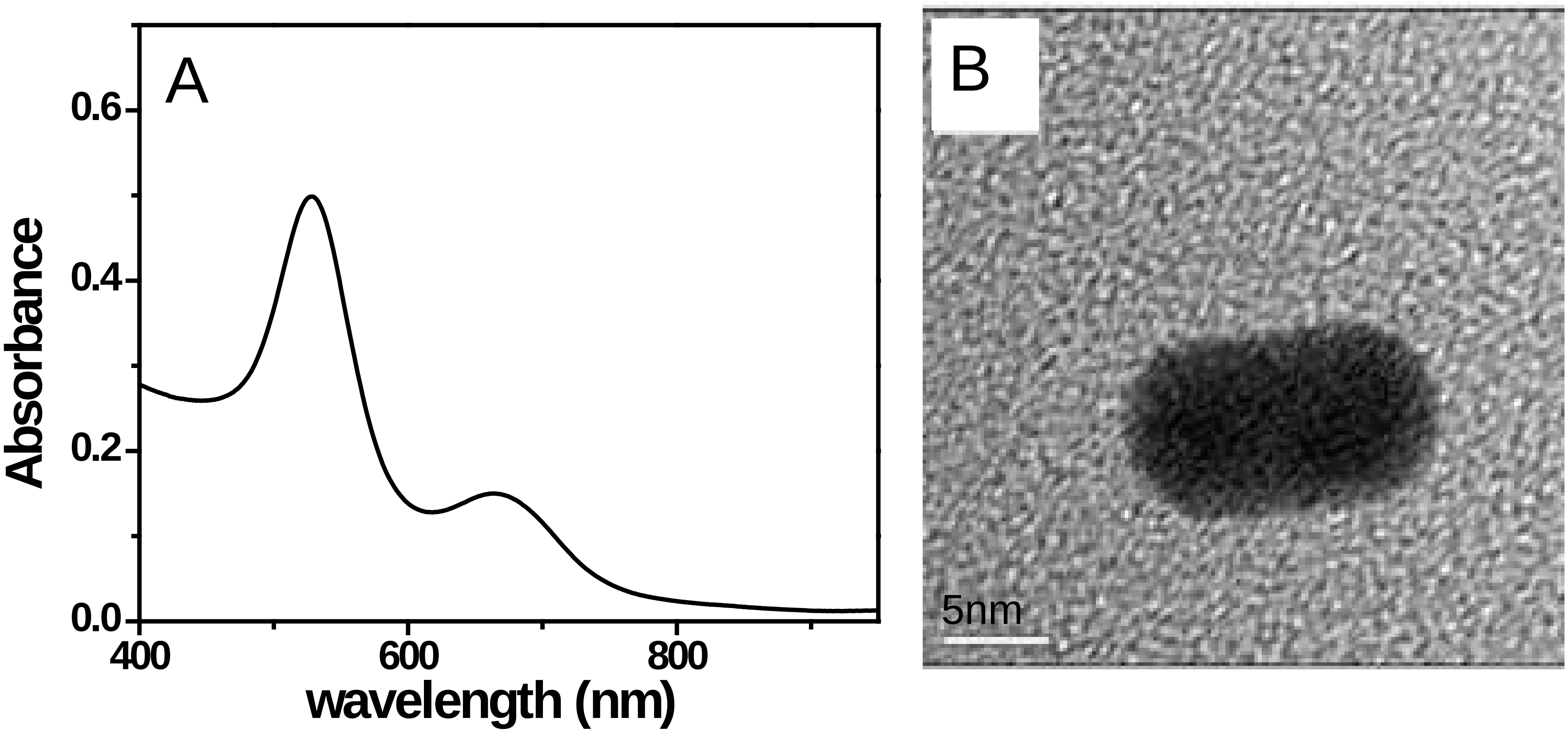

(A) UV-visible spectrum acquired after 3h of reaction between gold nanorods and $CuCl_2$. TEM taken from the same sample.

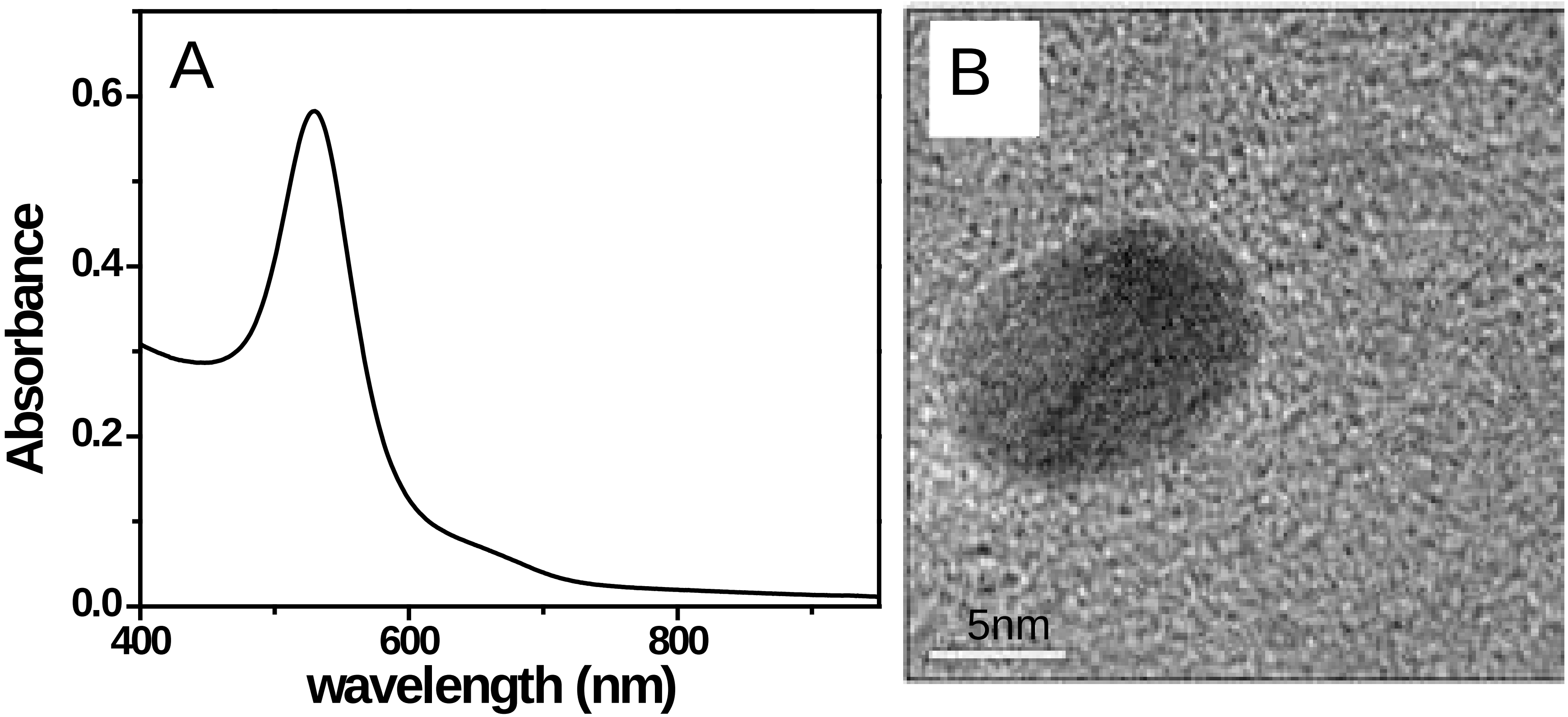

(A) UV-visible spectrum acquired after 4h of reaction between gold nanorods and $CuCl_2$. TEM taken from the same sample.

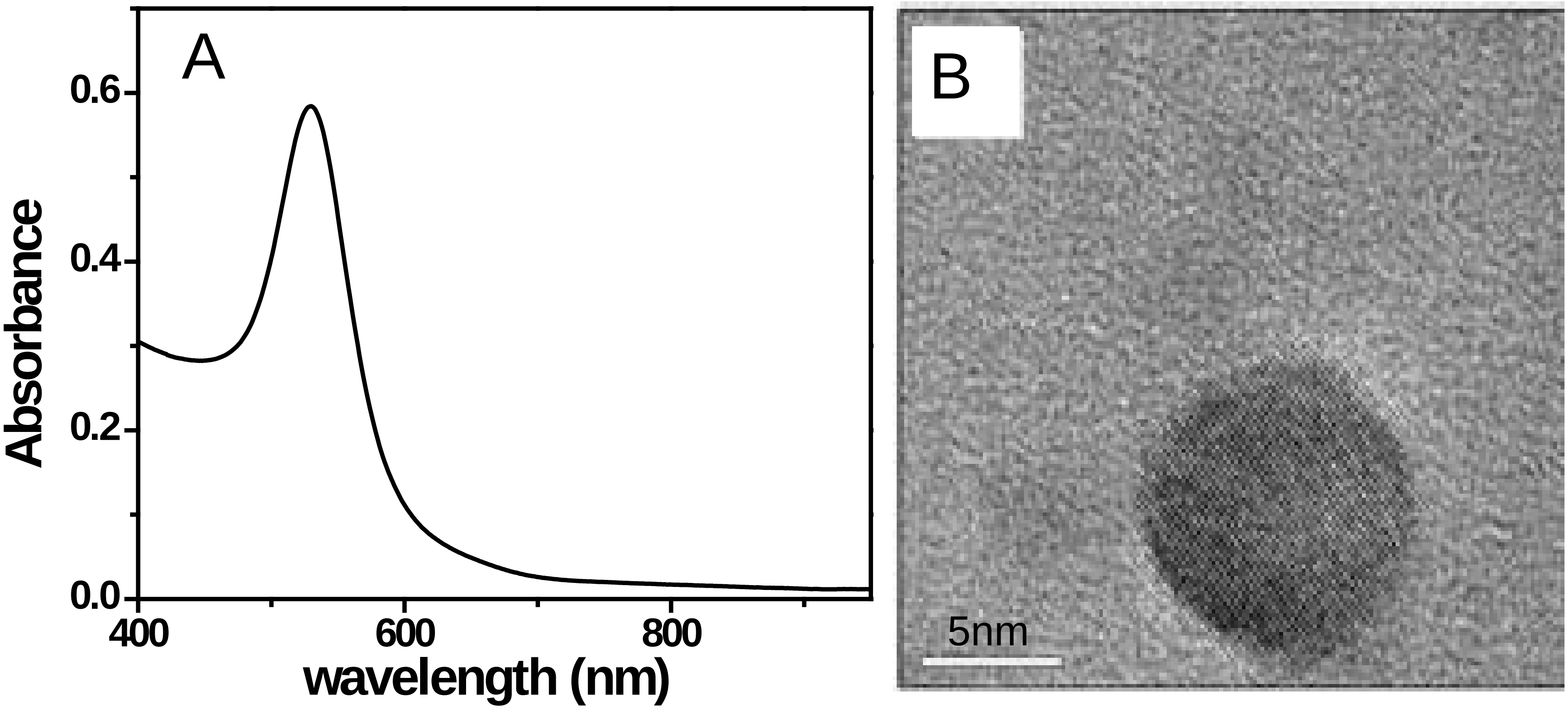

(A) UV-visible spectrum acquired after 5h of reaction between gold nanorods and $CuCl_2$. TEM taken from the same sample.

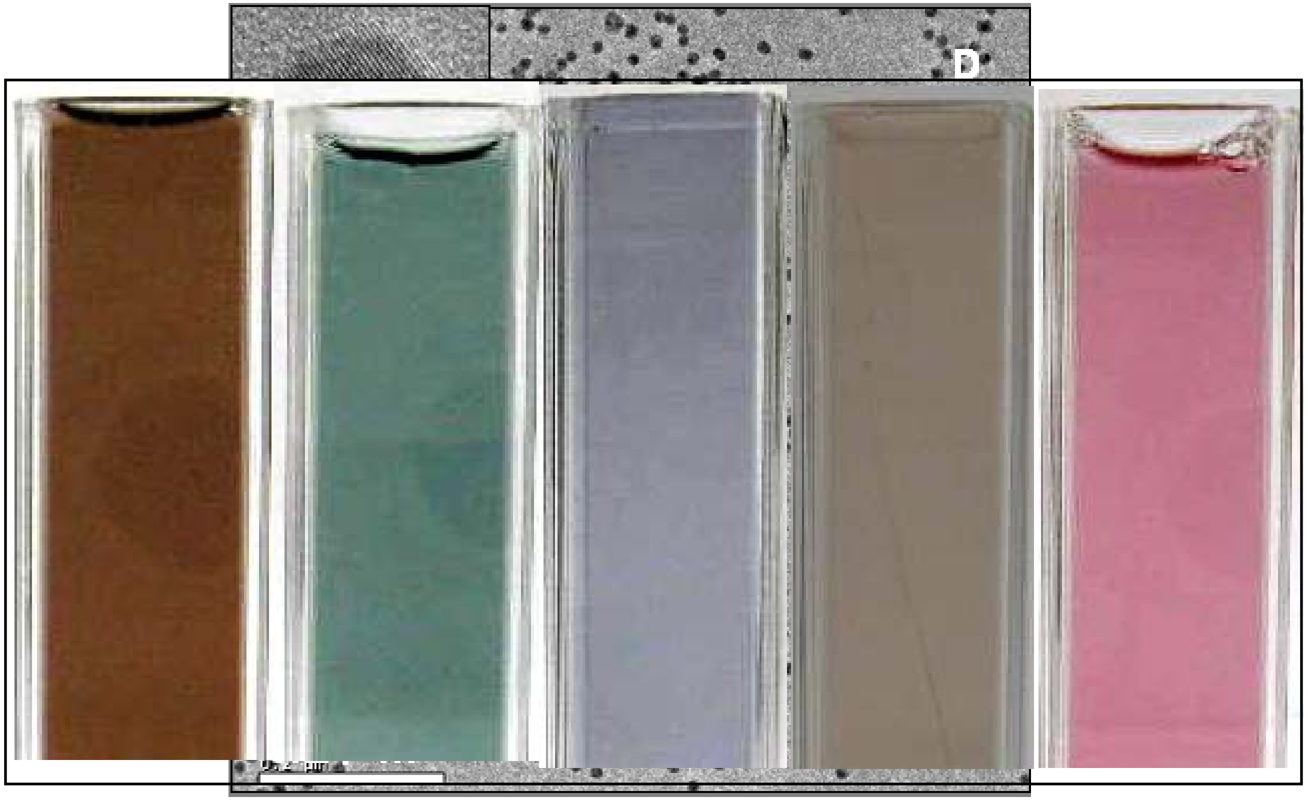

Any shape can be prepared by arresting the reaction

Why should the rod do that?

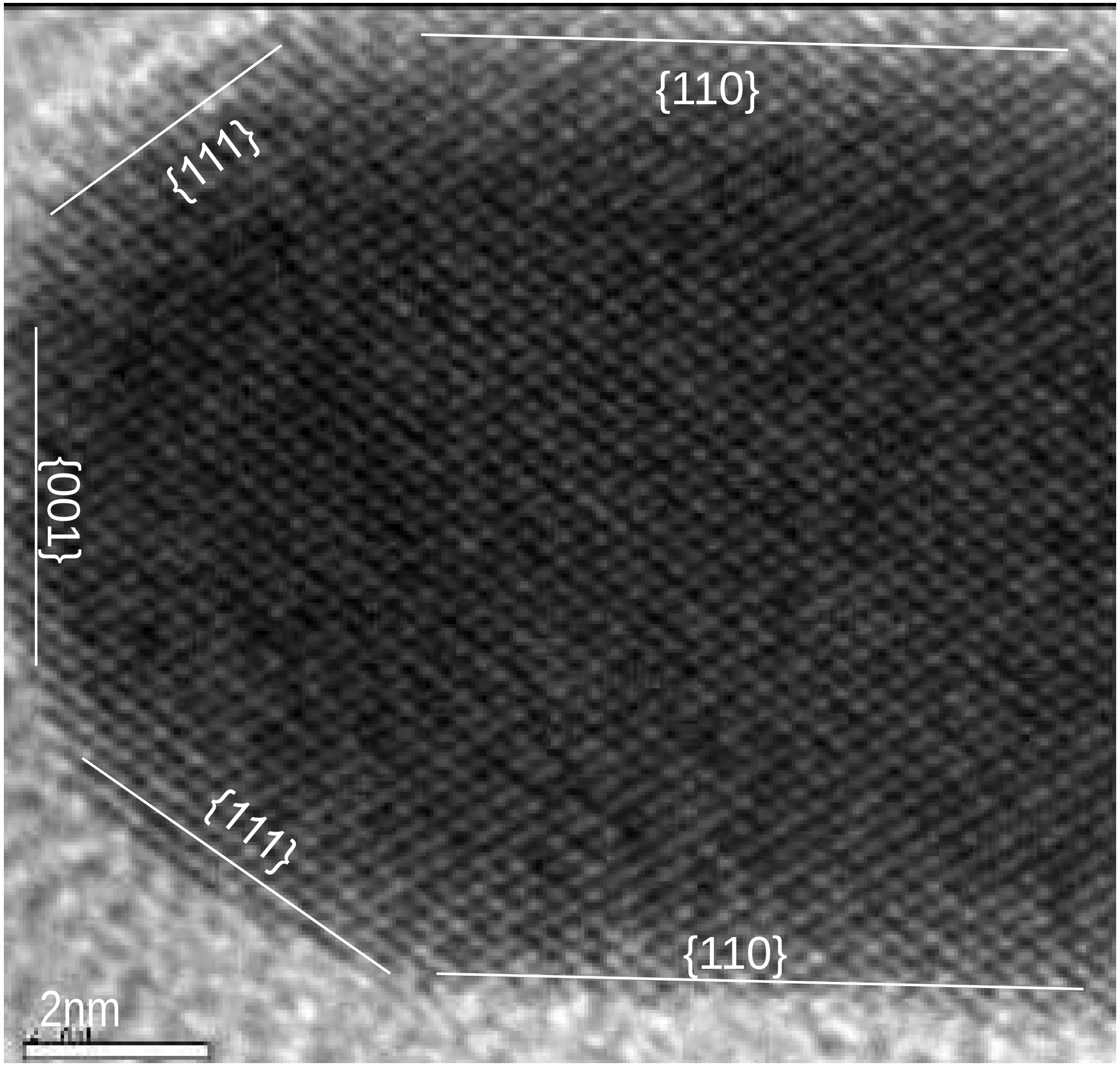

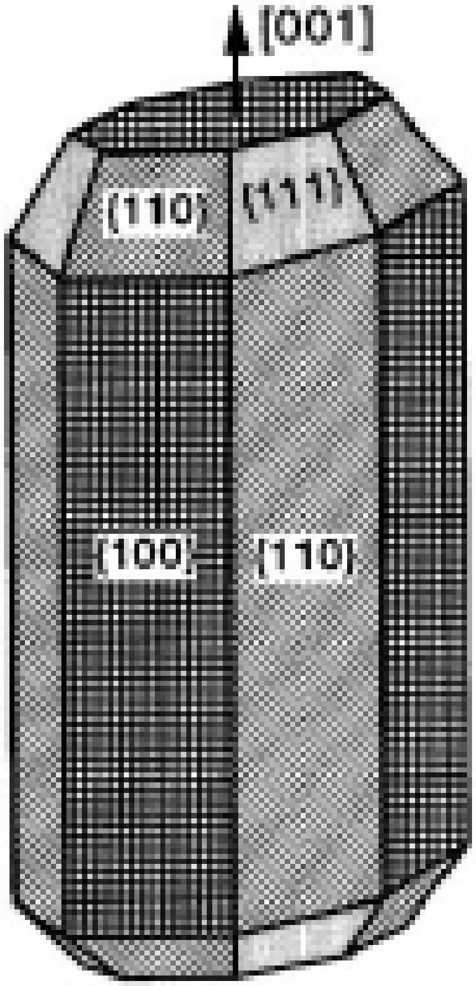

A structural model of the Au nanorod.

Wang, Z. L.; Mohamed, M. B.; Link, S.; El-Sayed, M. A. *Surf.Sci*. 1999, *440*, L809.

Reconstruction

Surface Energies

(100)

(110)

(111)

planes

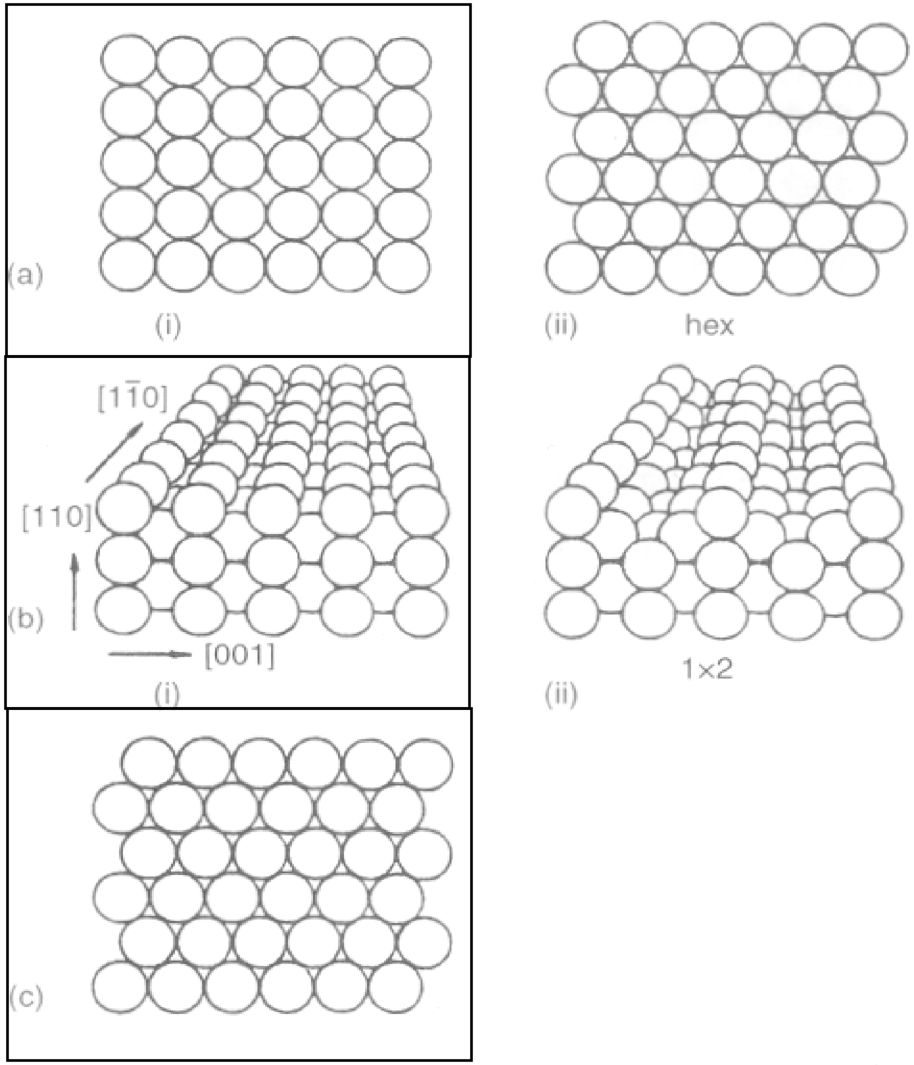

$0.66\ \mathrm{J\ m^{-2}}$

$0.70\ \mathrm{J\ m^{-2}}$

$0.58\ \mathrm{J\ m^{-2}}$

(a) Todd, B. D.; Lynden-Bell, R. M. *Surf. Sci.* 1993, *281*, 191. (b) Uppenbrink, J.; Johnston, R. L.; Murrell, J. N. *Surf. Sci.* 1994, *304*, 223.

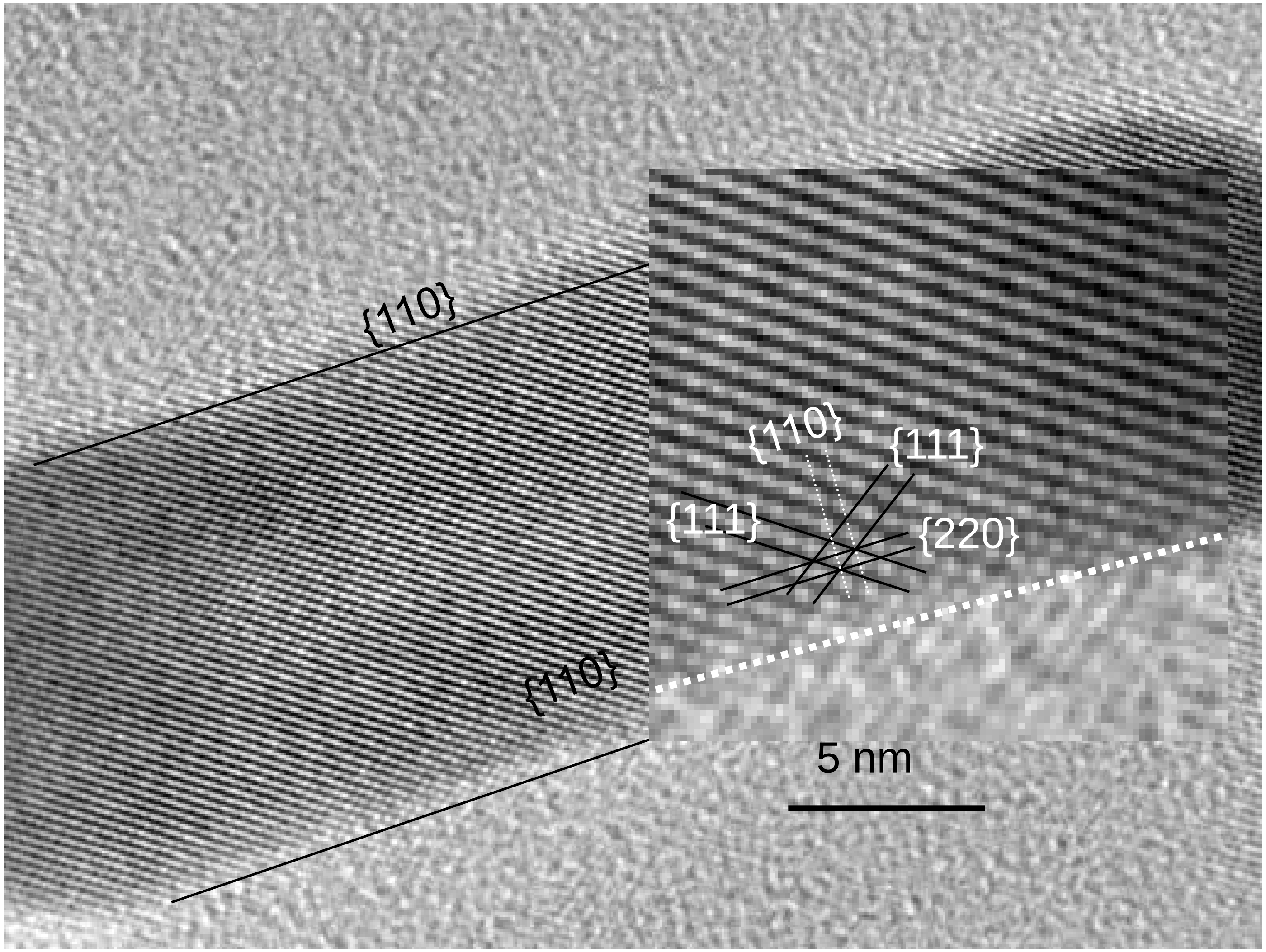
{110}
{110}
{110}
{111}
{111}
{220}
5 nm

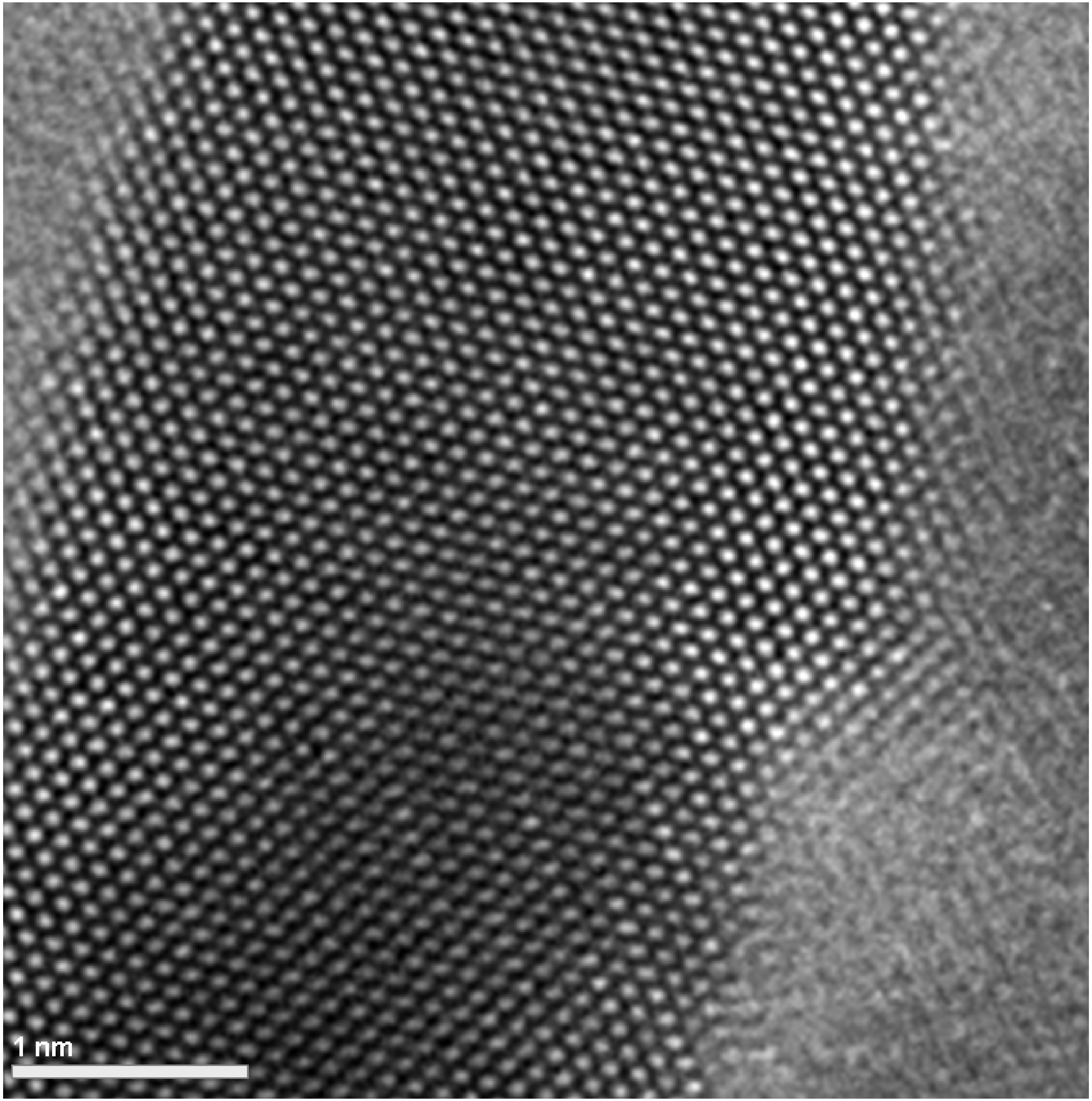
1 nm

Colours with octahedra

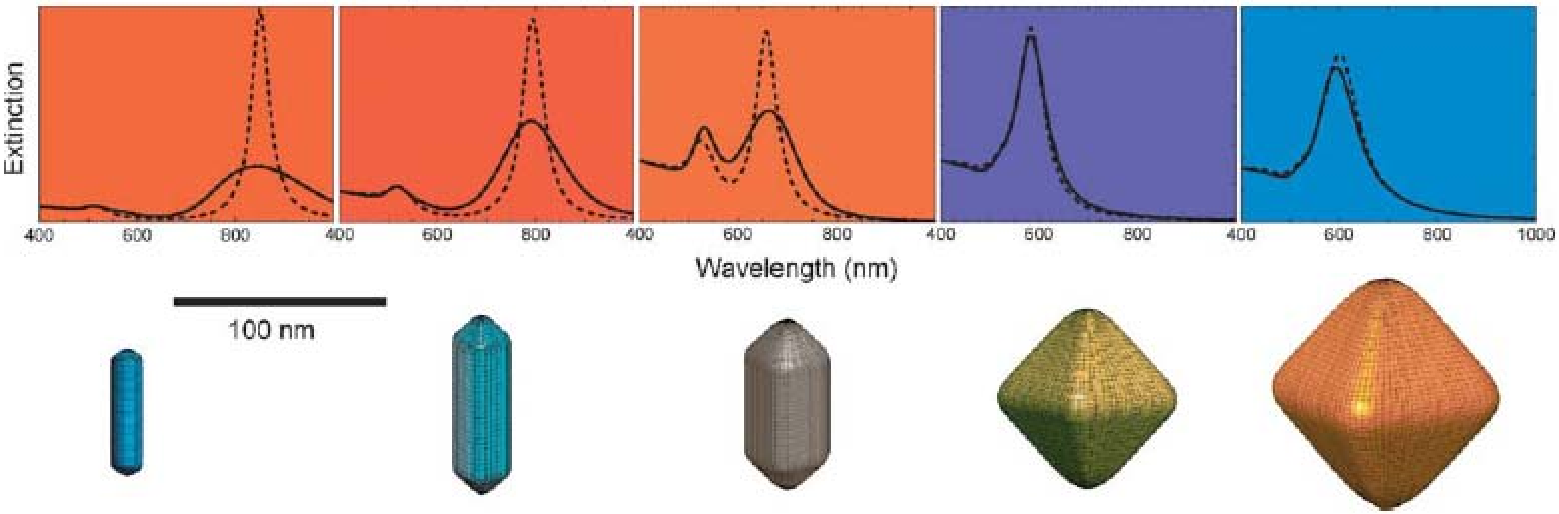

E. Carbo-Argibay, B. Rodriguez-Gonzalez, J. Pacifico, I. Pastoriza-Santos, L. M. Liz-Marzan, Angew. Chem. Int. Ed. 2007, 46, 8983.

Colours by assorted shapes

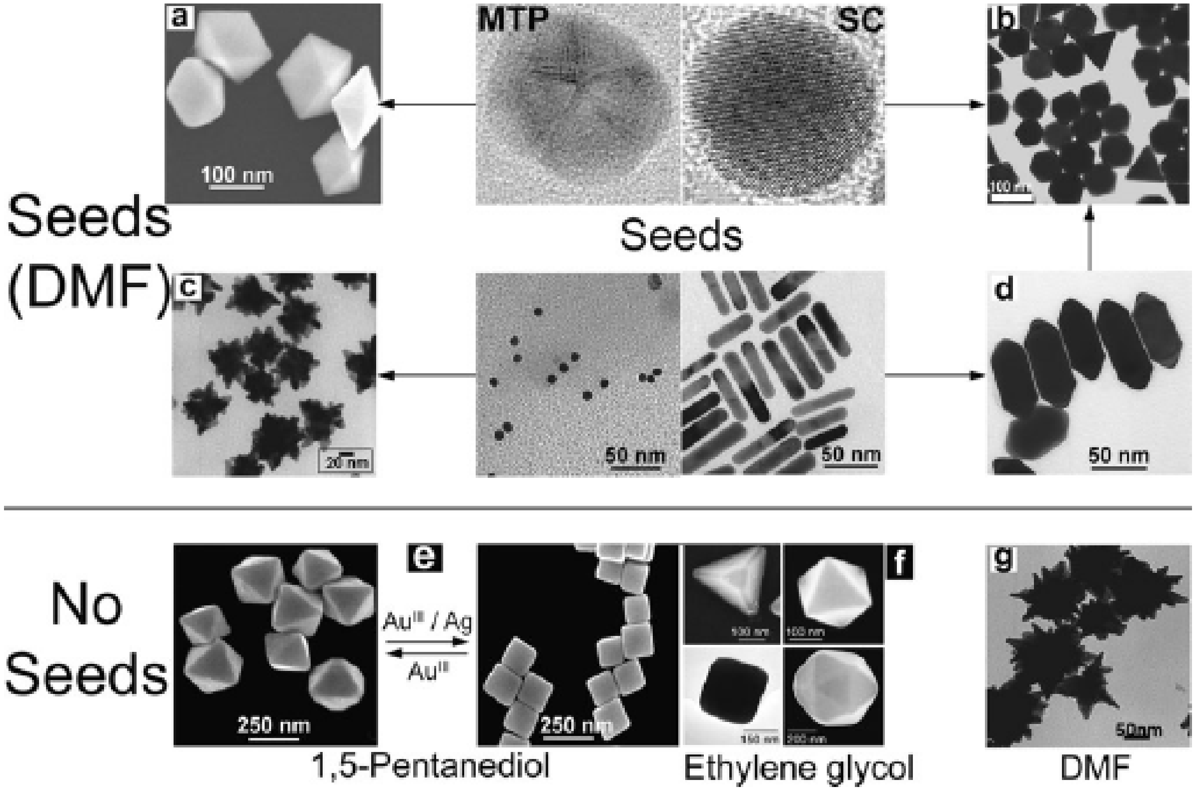

M. Grzelczak, J. Perez-Juste, P. Mulvaney and L. M. Liz-Marzan, Chem. Soc. Rev. 2008, 37, 1783-1791.

Colour by surface modification

Example

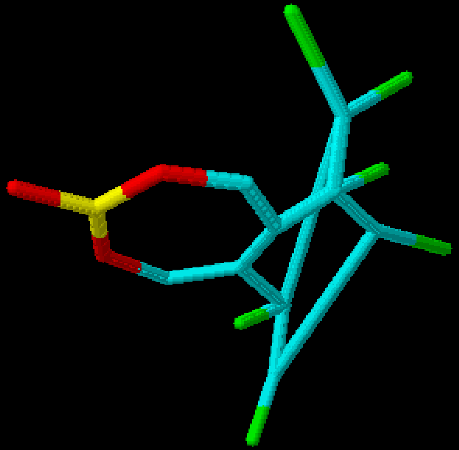

Endosulfan

Color of gold nanoparticles with endosulfan

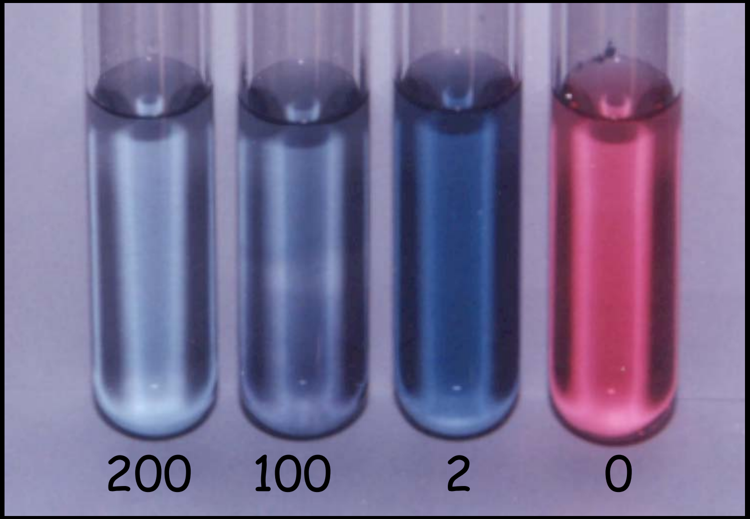

Endosulfan concentration in ppm

Color changes with pesticide concentration
Good response at lower concentrations
Down to 0.1 ppm
Adsorbed pesticides can be removed from solution

J. Environ. Monitoring. 2003

Pesticide removal from drinking water

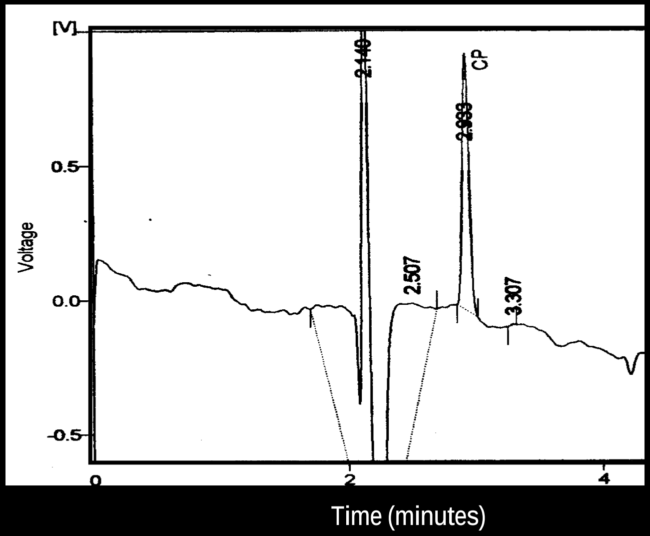

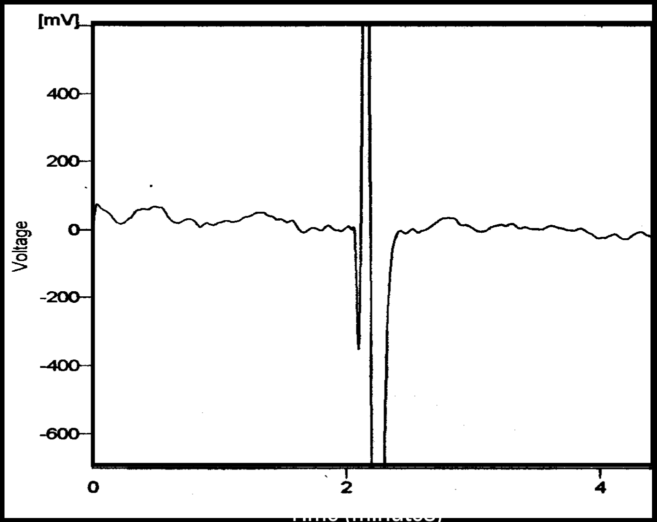

Indian patent granted
PCT application filed
Technology transferred
Product is in the market


HEATING VESSEL
2007 1 16

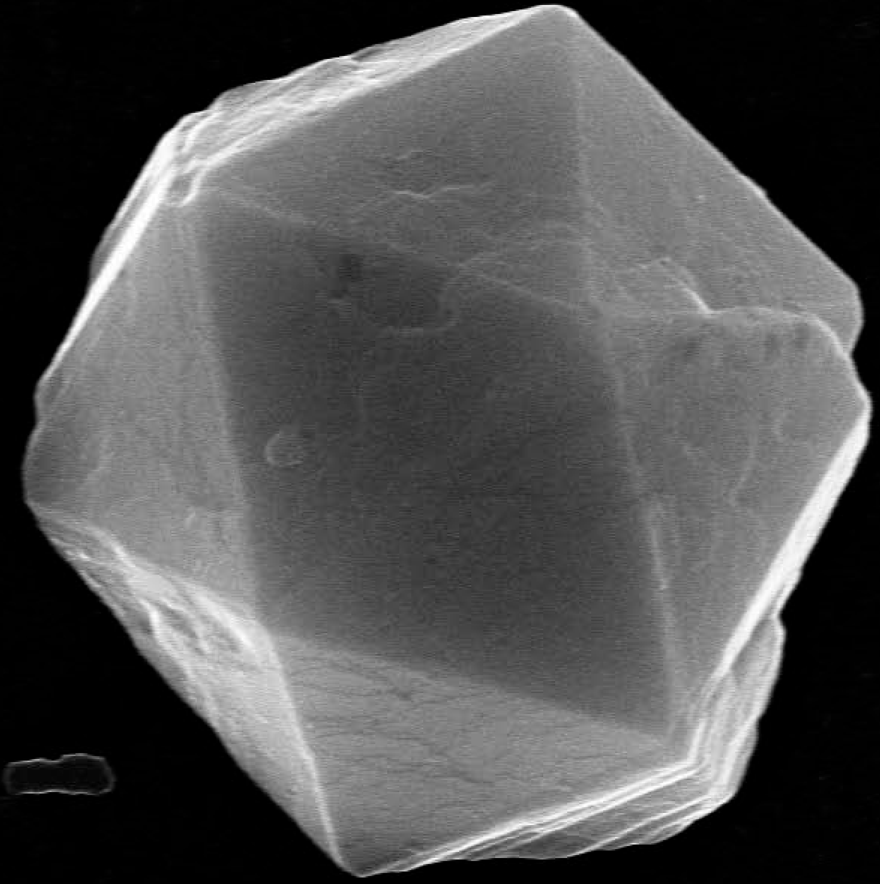

Organised nanostructures

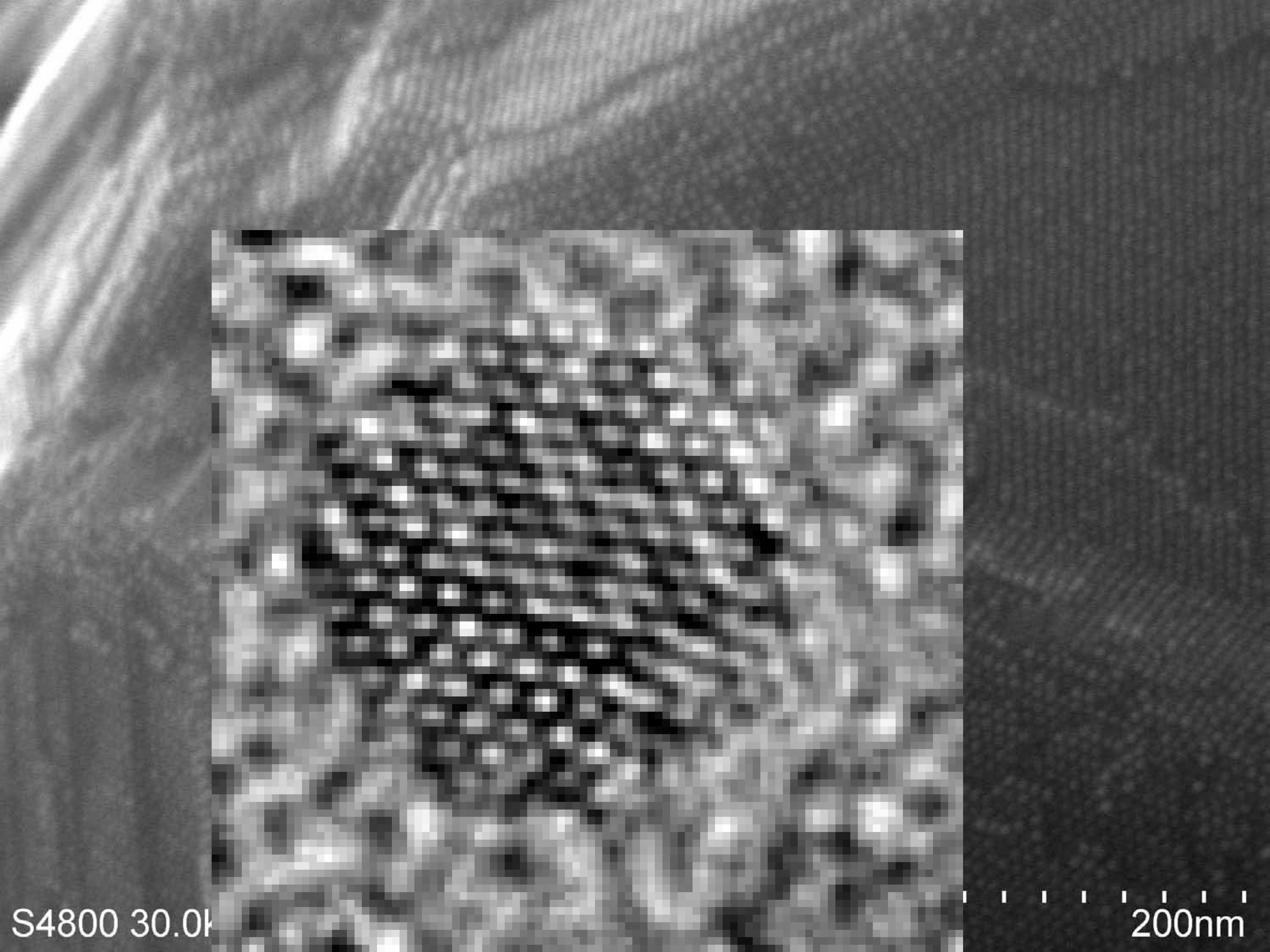
S4800 30.0k
200nm

Colours by organisation

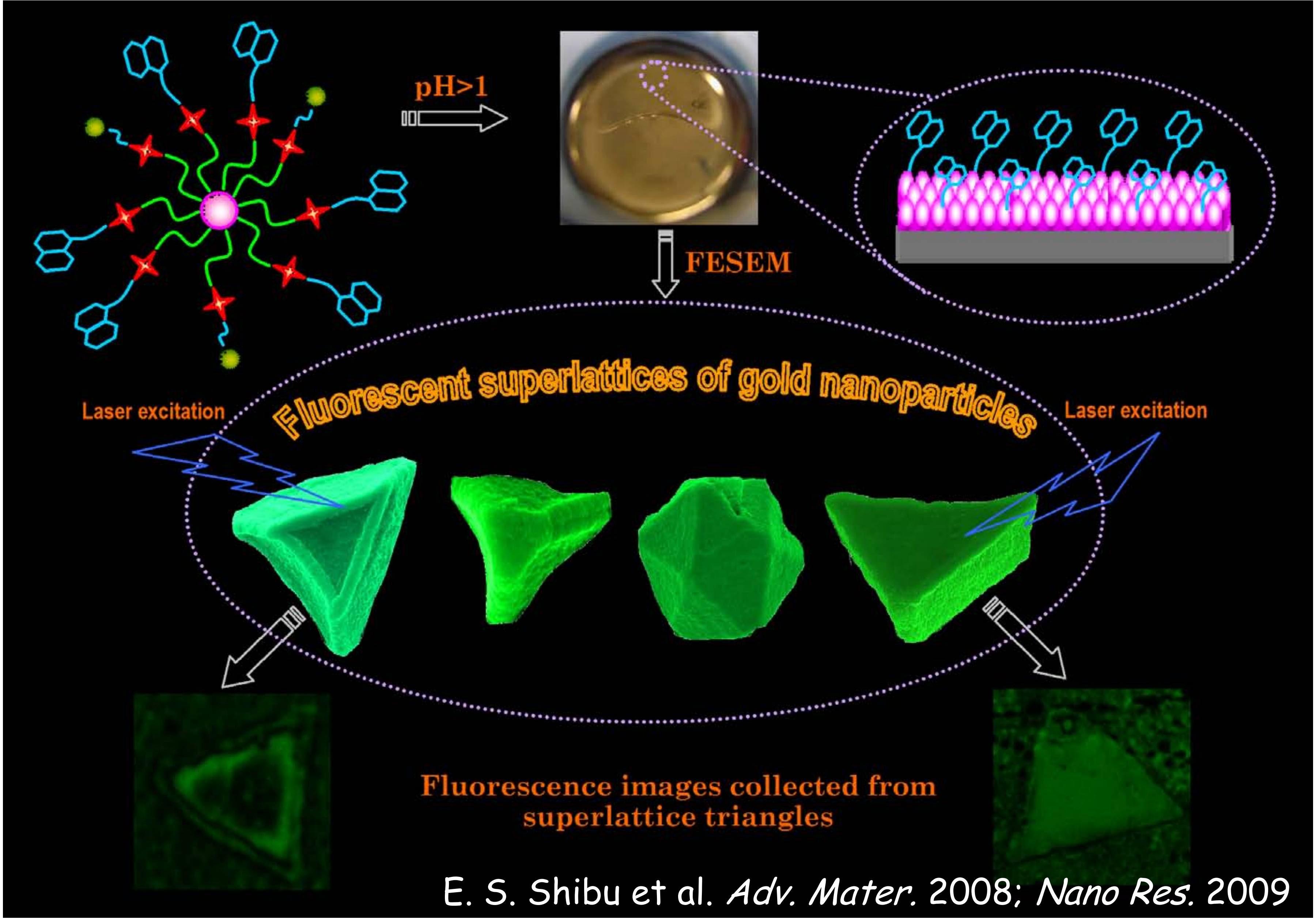

E. S. Shibu et al. *Adv. Mater.* 2008; *Nano Res.* 2009

Mesoflowers

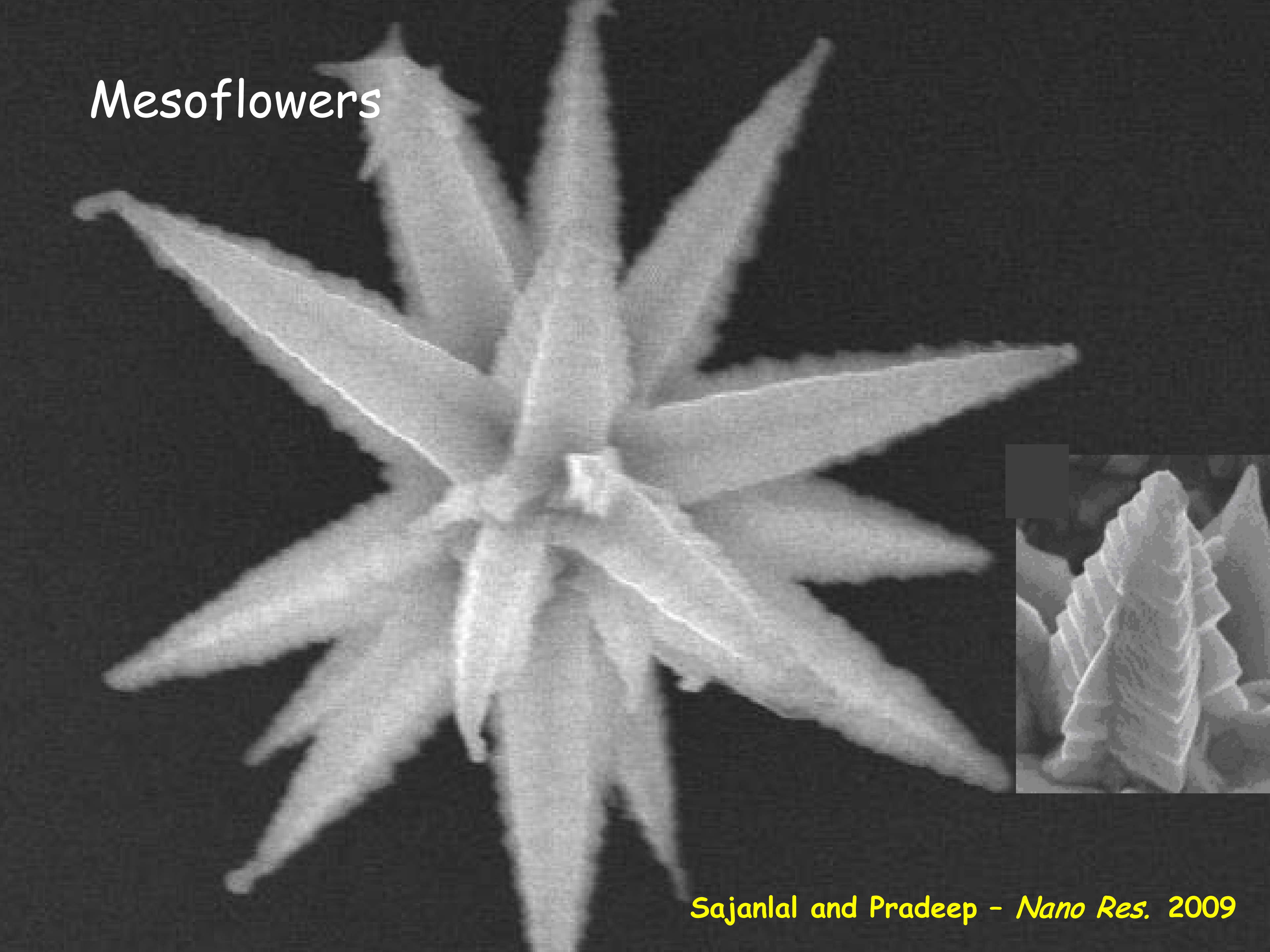

Sajanlal and Pradeep – *Nano Res.* 2009

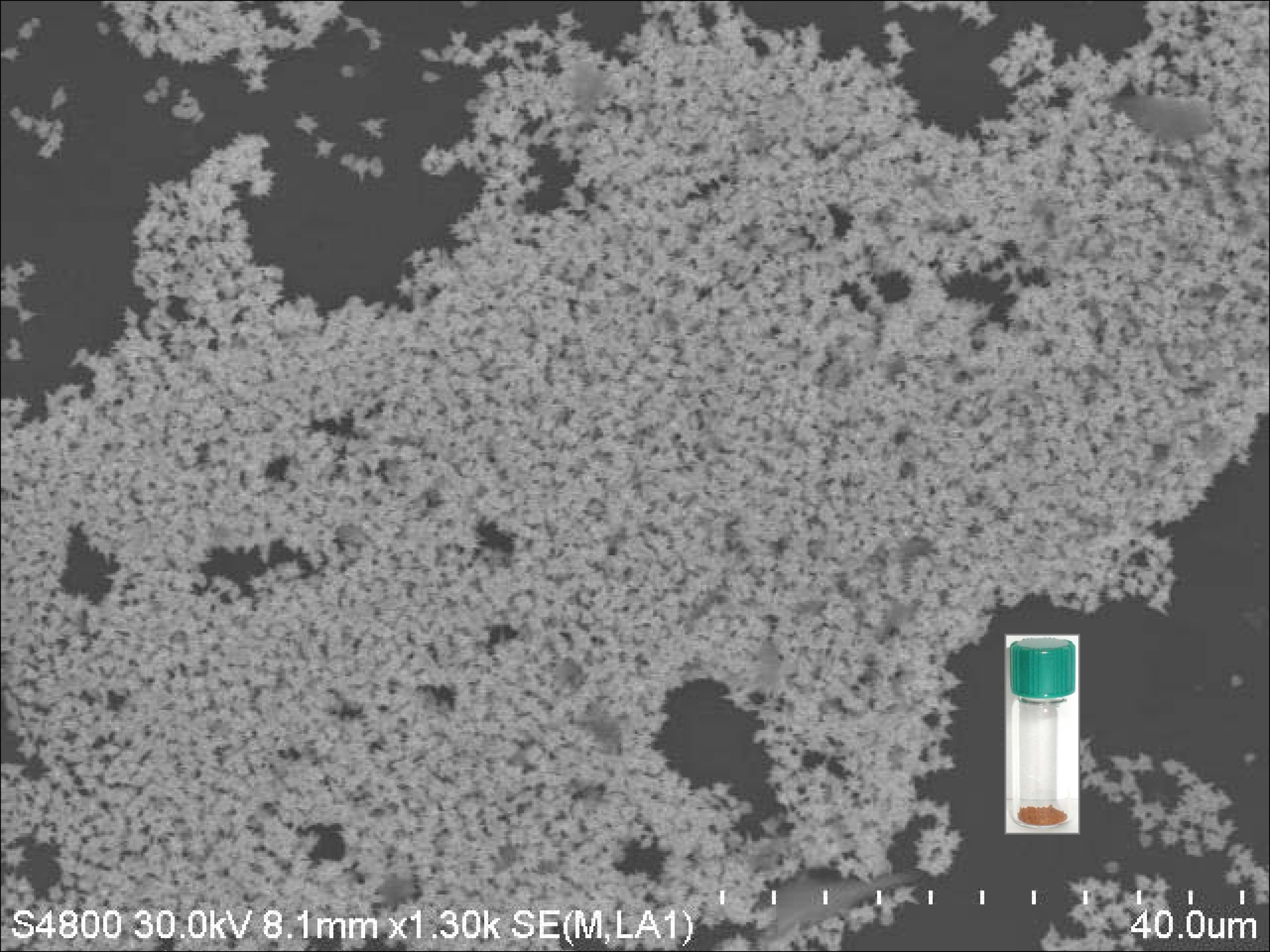
S4800 30.0kV 8.1mm x1.30k SE(M,LA1)
40.0um

Bimetallic mesoflowers

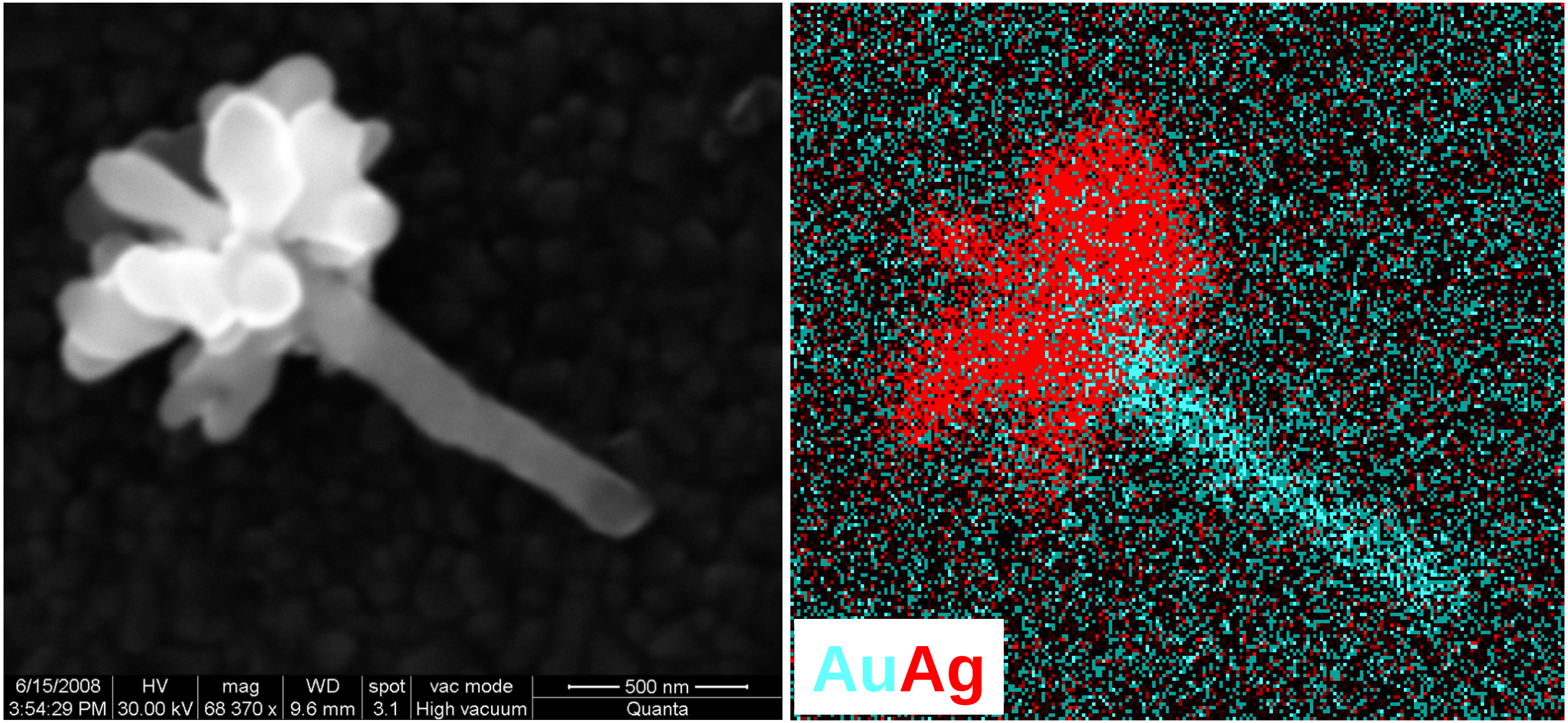

P. R. Sajanlal.; T. Pradeep. *Langmuir* **2010**, *26*, 456.

Wire-like meso/nanostructures

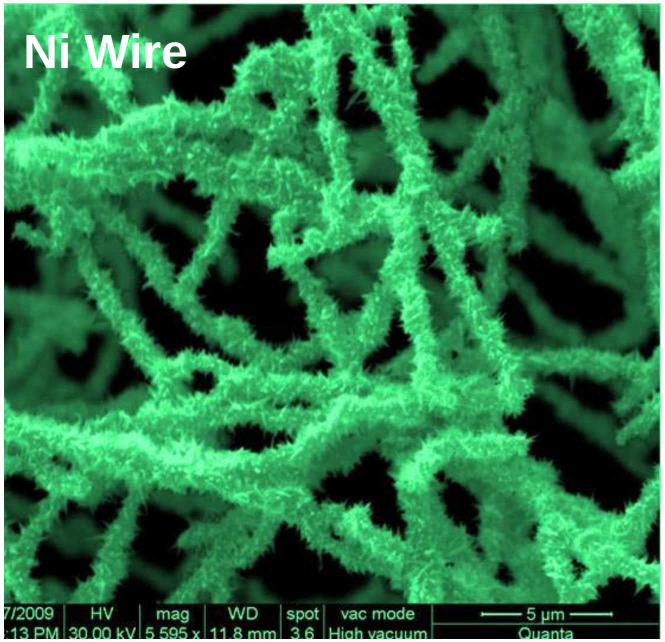

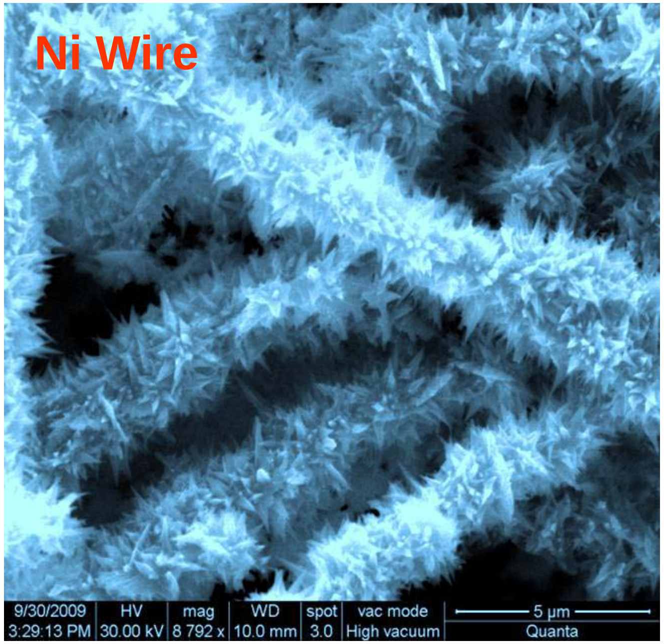

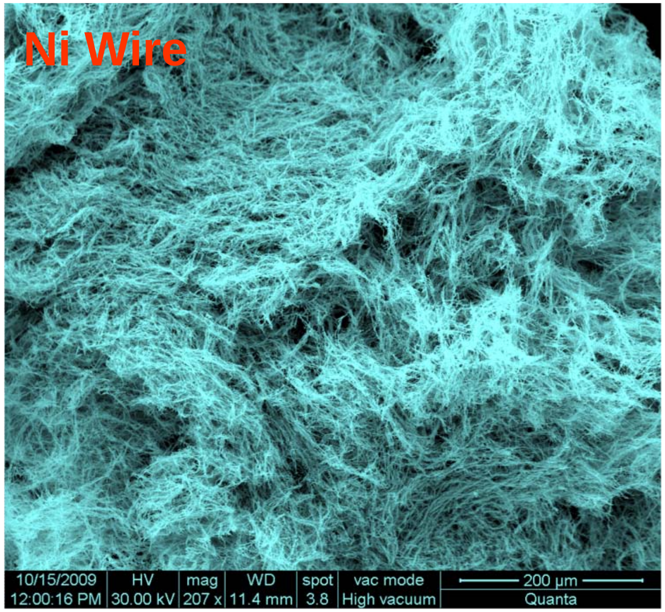

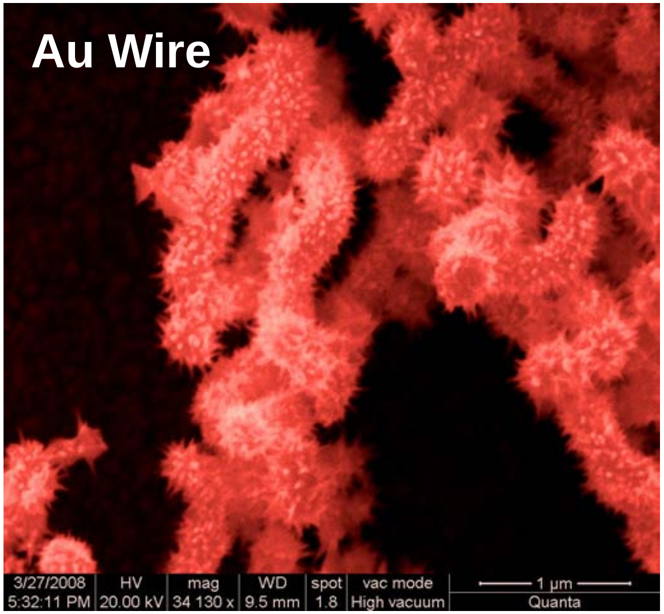

P. R. Sajanlal and T. Pradeep, *Unpublished*

Ni/Au nanotubes

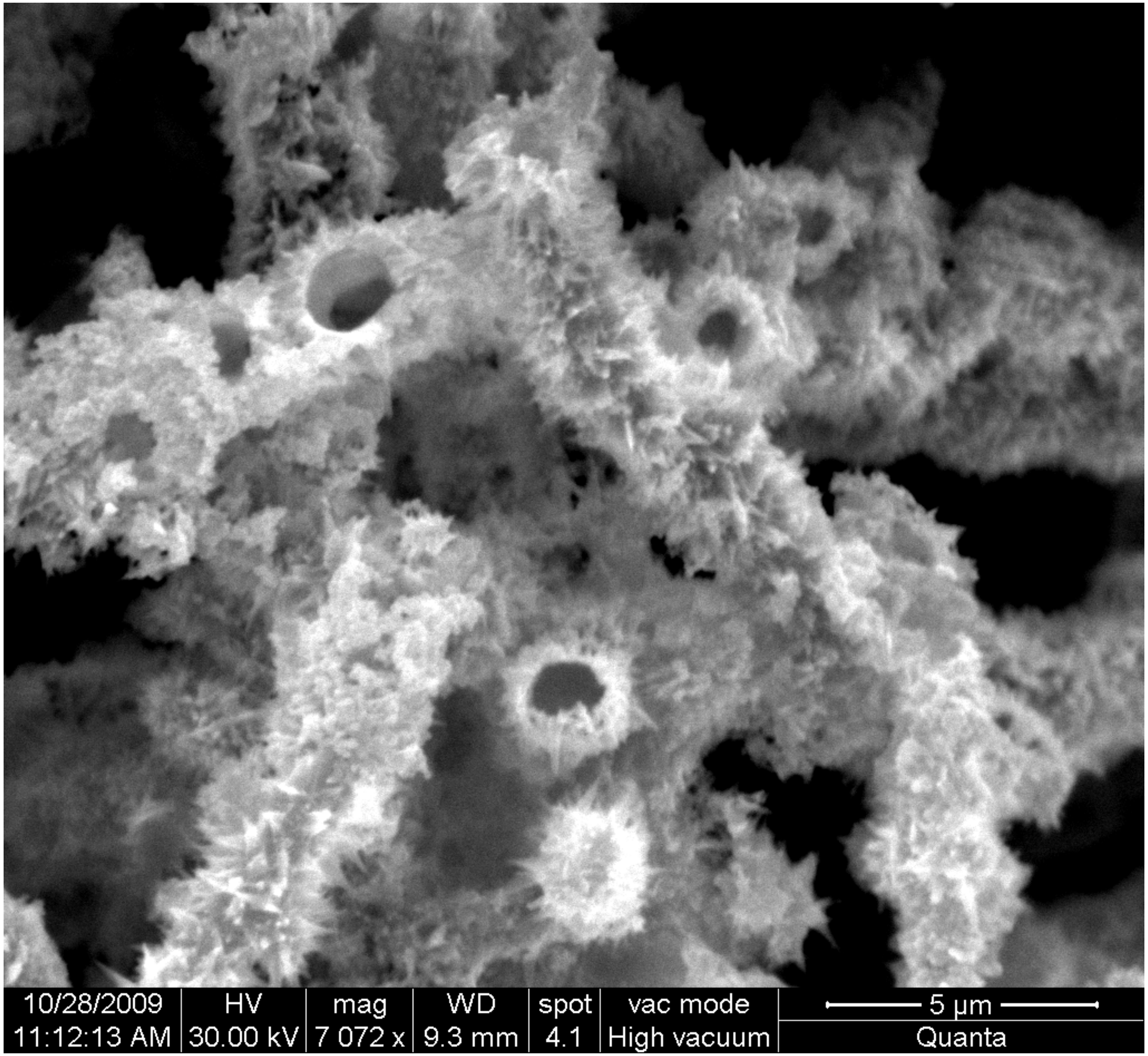

P. R. Sajanlal and T. Pradeep, *Unpublished*

First report- catalysis by gold nanoparticle

M. HARUTA

JOURNAL OF CATALYSIS 115, 301–309 (1989)

Gold Catalysts Prepared by Coprecipitation for Low-Temperature Oxidation of Hydrogen and of Carbon Monoxide

M. Haruta,* N. Yamada,† T. Kobayashi,* and S. Iijima‡,[1]

*Government Industrial Research Institute of Osaka, Midorigaoka 1, Ikeda 563, Japan; †Kishida Chemicals Company, Ltd., Joshoji-machi, Kadoma 571, Japan; and ‡Research Development Corporation of Japan, Science Building, 5-2 Nagata-cho 2-chome, Tokyo 100, Japan

Received October 7, 1987; revised June 6, 1988

Novel gold catalysts were prepared by coprecipitation from an aqueous solution of $HAuCl_4$ and the nitrates of various transition metals. Calcination of the coprecipitates in air at 400°C produced ultrafine gold particles smaller than 10 nm which were uniformly dispersed on the transition metal oxides. Among them, Au/α-Fe_2O_3, Au/Co_3O_4, and Au/NiO were highly active for H_2 and CO oxidation, showing markedly enhanced catalytic activities due to the combined effect of gold and the transition metal oxides. For the oxidation of CO they were active even at a temperature as low as −70°C. © 1989 Academic Press, Inc.

INTRODUCTION

During the course of an investigation into new oxide catalysts useful for the low-temperature catalytic combustion of hydrogen (*1–4*), it became evident that the catalytic activities of transition metal oxides for hydrogen oxidation had a volcano-like relation with the heat of formation of oxides per gram-atom of oxygen (*5*). The volcano relation indicates that the formation of metal–oxygen (*M*–O) bonds is rate determining for the oxides of Ag and Au, which are located on the left side, while the breaking of *M*–O bonds is the slow step for the other metal oxides located on the right side. Therefore, an attempt was made to develop composite oxides of Ag with the 3*d* transition metals, for which an enhancement in both catalytic activity and thermal stability was expected.

Our earlier paper (*5*) reported that an appreciable enhancement in catalytic activity was, in fact, achieved in some composite oxides of silver with 3*d* transition metals which were prepared by coprecipitation. Specifically, a mixed oxide composed of Co, Mn, and Ag (20 : 4 : 1 in atom ratio) was both thermally stable and highly active for the oxidation of H_2 and CO. The successful results obtained for these composite oxides of silver led us to expect that a significant enhancement in catalytic activity might also be exhibited by composites of gold and the other metal oxides. The present investigation into gold-based oxide catalysts was undertaken to test this hypothesis.

Previous work on gold catalysts has been reviewed by several authors (*6–10*). All the gold catalysts investigated so far are gold supported on inactive ceramic oxides, such as SiO_2 (*11–17*), Al_2O_3 (*14–16, 18*), MgO (*15–17, 19*), and TiO_2 (*20*), or unsupported gold filaments (*21*), powder (*22, 23*), sponges (*24*), filings (*25*), and gauze (*26*).

The chemical reactivity of gold catalysts has been studied for the oxidation by oxygen or nitrogen oxides of CO (*11, 22, 24, 26*) and H_2 (*12, 15, 17, 21–23*), selective oxidation of organic compounds by nitrogen dioxide (*13*), hydrogenation of alkenes (*7*), and so on. However, the conventional gold catalysts prepared by impregnation have been reported to be usually far less active than platinum-group metal catalysts, although they are superior in selectivity for only a few reactions such as the oxidation

---

[1] Present address: NEC Corp., Miyazaki 4, Miyamae, Kawasaki 213, Japan.

0021-9517/89 $3.00

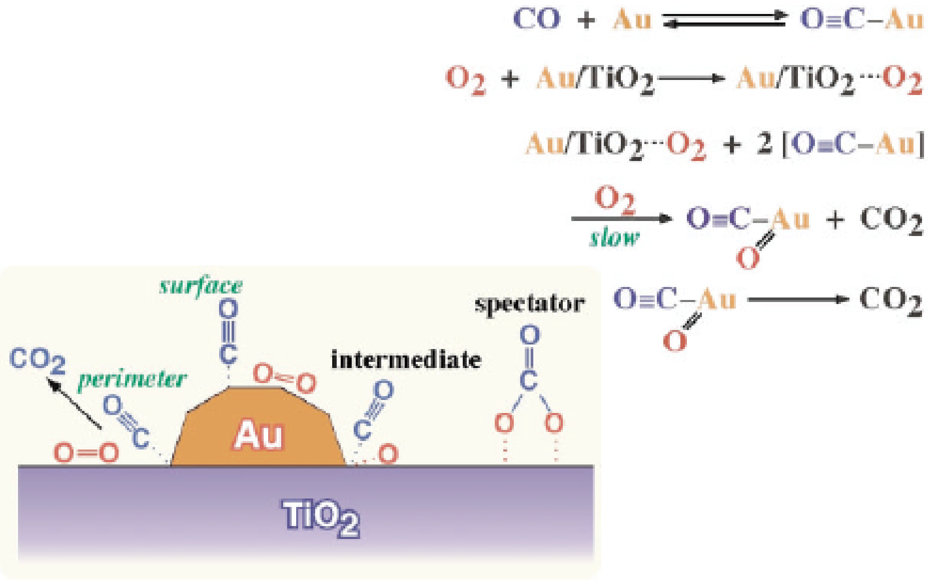

Schematic representation for CO oxidation pathways over Au/TiO2.

M. Haruta. When Gold Is Not Noble: Catalysis by Nanoparticles. *Chem. Rec*. **2003**, *3*, 75.

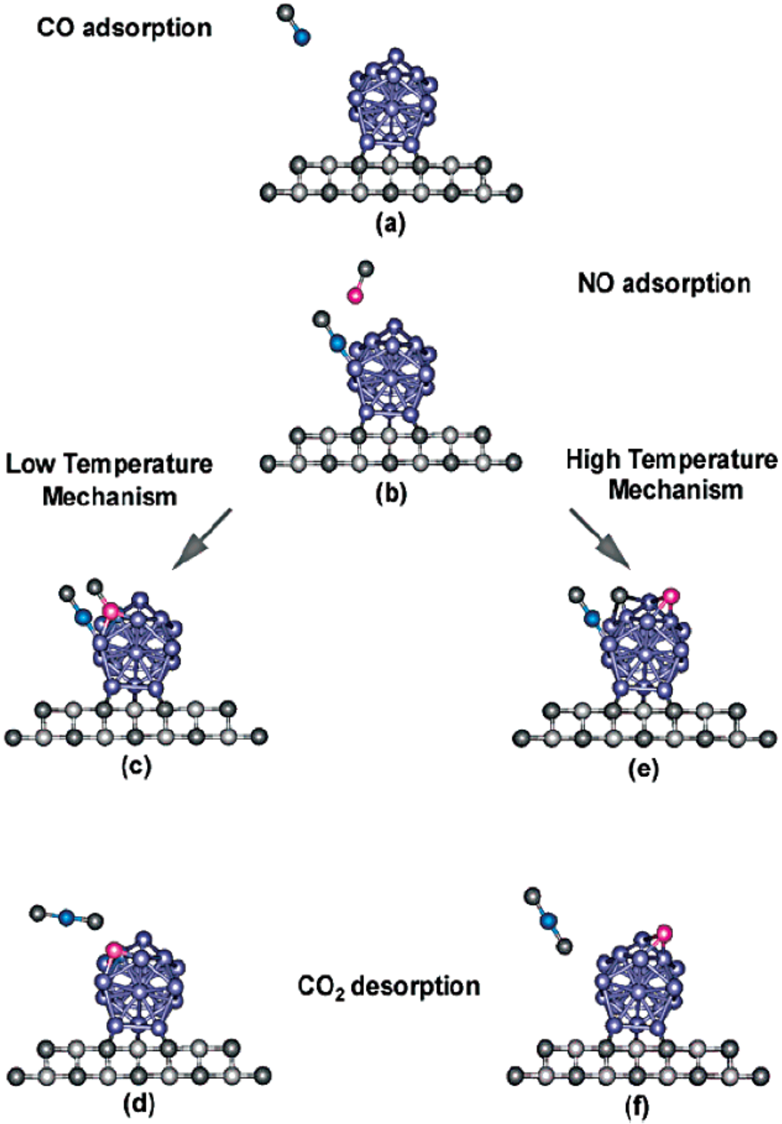

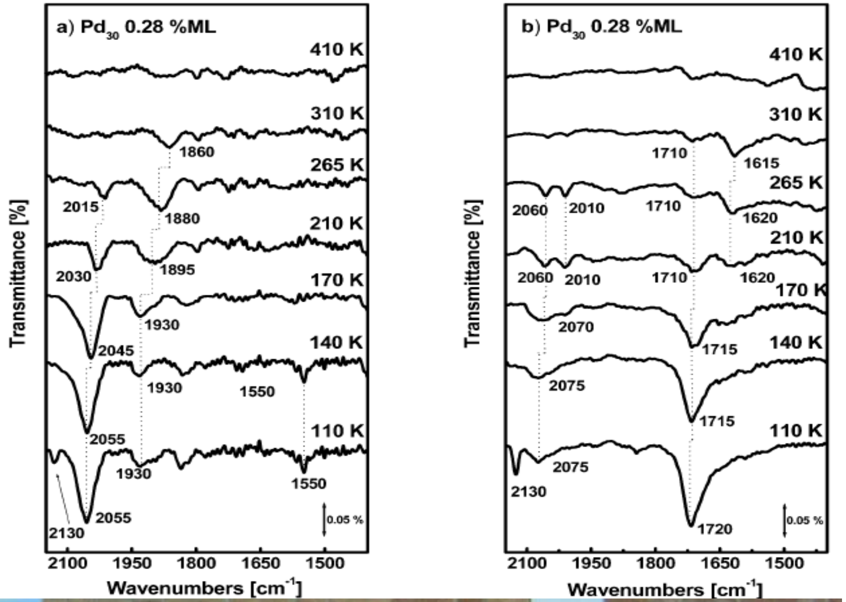

IR-spectra of 13CO and 15NO adsorbed on Pd30 (Figure 3a/b) and Pd8 (Figure 3c/d) clusters. Figure 3a/c shows the spectra if 13CO was predosed for both cluster sizes. Figure 3b/d shows the spectra if 15NO was predosed. All of the spectra were taken at 90 K after annealing the cluster samples to the indicated temperatures.

Wörz, A. S.; Judai, K.; Abbet, S.; Heiz, U. Cluster Size-Dependent Mechanisms of the CO + NO Reaction on Small Pdn (n e 30) Clusters on Oxide Surfaces. *J. Am. Chem. Soc.* **2003**, *125*, 7964.

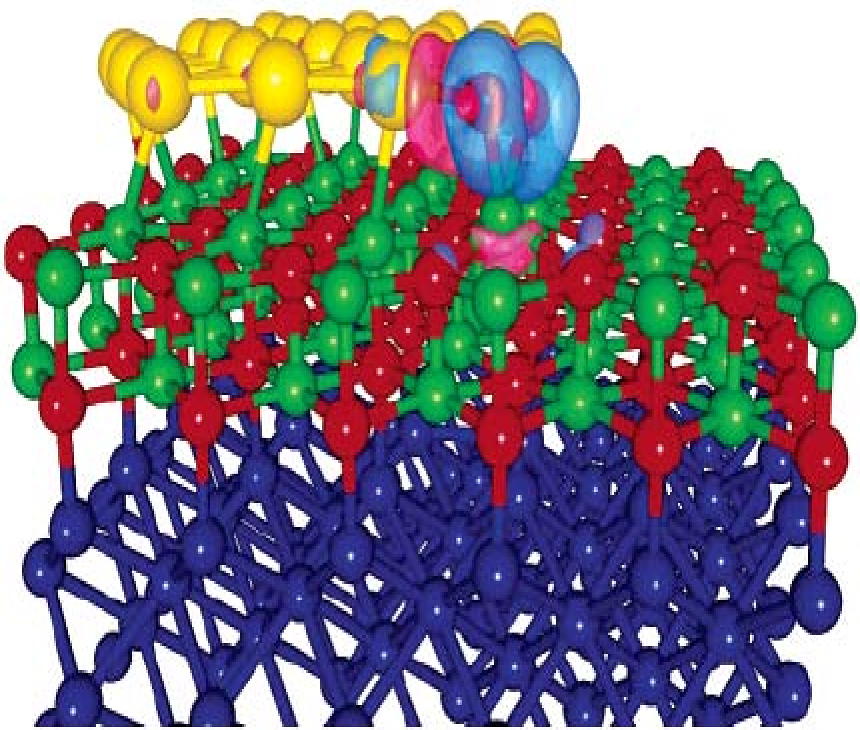

Two-dimensional Au20 island (yellow on line) adsorbs on a two layer MgO film (O atoms in red and Mg in green) supported on Mo(100) (blue on line), with a coadsorbed O2 molecule. Superimposed we show an isosurface of the excess electronic charge (light blue on line) illustrating activation of the adsorbed molecule through population of the antibonding $2\pi^*$ *orbital.*

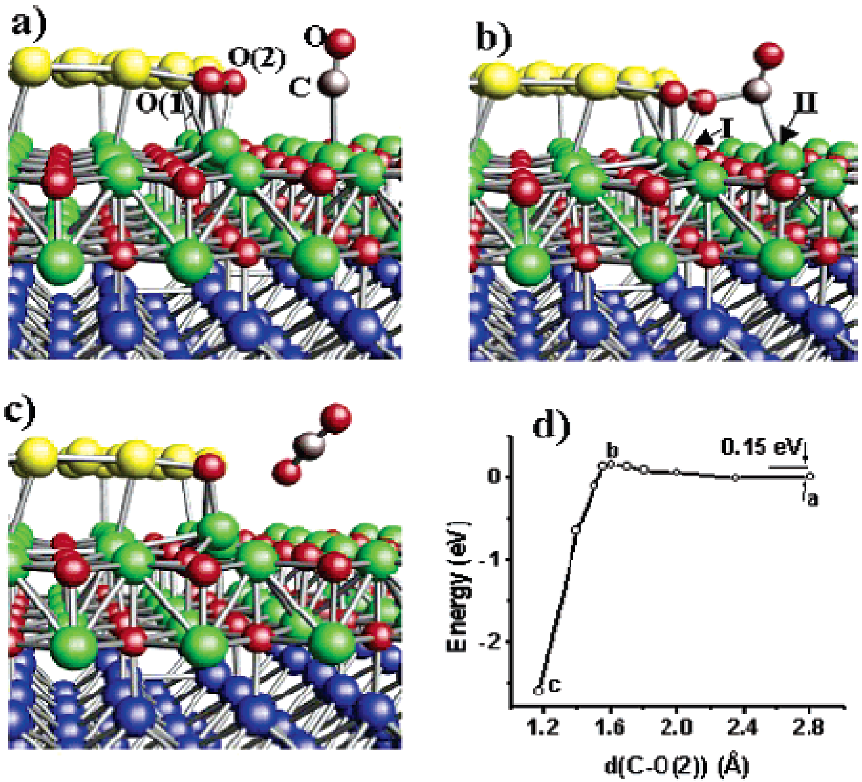

(a-c) Configurations of the two-dimensional Au20 island shown
in Figure 1 Figure 1) with
coadsorbed 2)) and CO (C
atom in g configuration;
d(O(1)-O(2, ransition state
(the neare as I and II);
distances a *60 Å, d(C-O))*
1.18 Å, d(on illustrating
formation energy profile
along the e zero of the
energy scale taken for configuration a. The sharp drop past the
barrier top corresponds to CO2 formation.

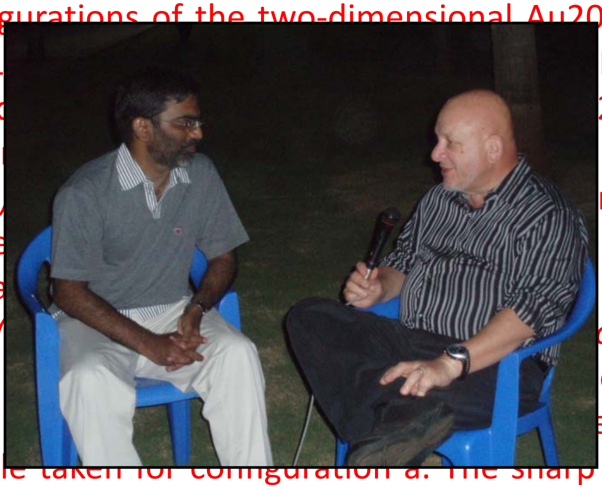

Zhang, C.; Yoon, B.; Landman, U. Predicted Oxidation of CO Catalyzed by Au Nanoclusters on a Thin Defect-Free MgO Film Supported on a Mo(100) Surface . *J. Am. Chem. Soc.* **2007**, *129*, 2228.

Au_{13}

$[Au_{13}(PPhMe_2)_{10}C1_2]^{3+}$

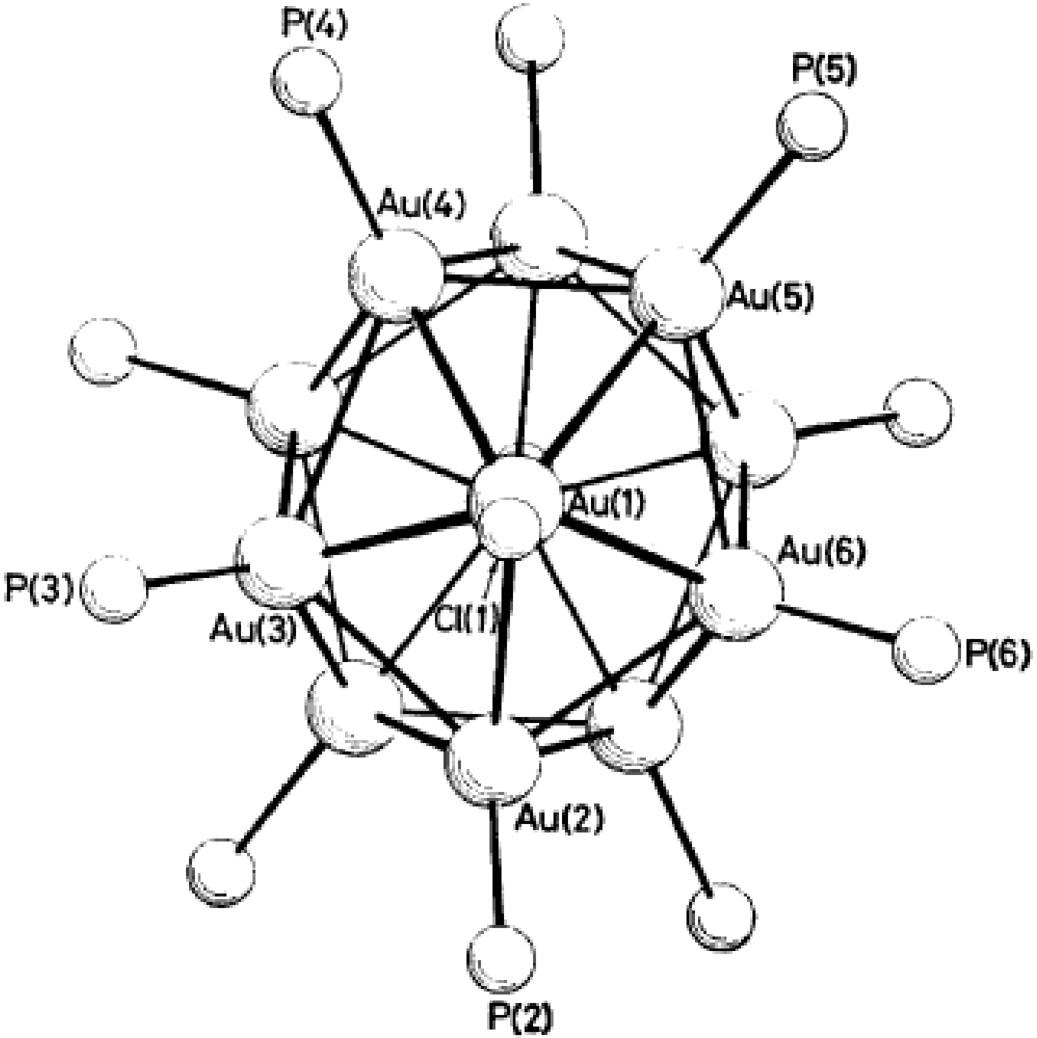

Briant, C. E.; Theobald, B. R. C.; White, J. W.; Bell, L. K.; Mingos, D. M. P.; Welch, A. J. Synthesis and x-ray structural characterization of the centered icosahedral gold cluster compound $[Au_{13}(PPhMe_2)_{10}Cl_2](PF_6)_3$; the realization of a theoretical prediction. *J. C. S. Chem. Comm*. **1981**, *5*, 201.

Gold clusters

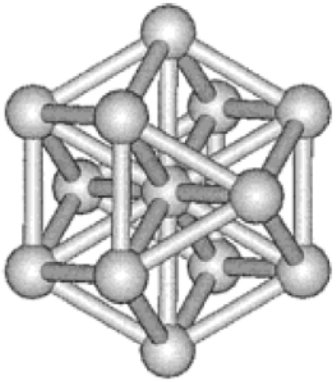

Au_{13}

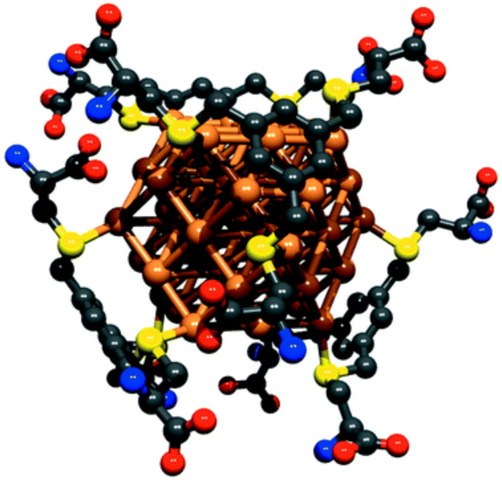

Au_{55}

- **Au_{55} $[P(C_6H_5)_3]_{12}Cl_6$ - a gold cluster of unusual size,** Schmid, G.; Pfeil, R.; Boese, R.; Brandermann, F.; Meyer, S.; Calis, G. H. M.; Van der Velden.; Jan W. A. *Chemische Berichte* **1981**, *114*, 3634.
- **Synthesis and x-ray structural characterization of the centered icosahedral gold cluster compound [Au_{13} $(PMe_2Ph)_{10}Cl_2](PF_6)_3$; the realization of a theoretical prediction,** Briant, C. E.; Theobald, B. R. C.; White, J. W.; Bell, L. K.; Mingos, D. M. P.; Welch, A. J. *Chem. Commun.* **1981**, *5*, 201.
- **Synthesis of water-soluble undecagold cluster compounds of potential importance in electron microscopic and other studies in biological systems**, Bartlett, P. A.; Bauer, B.; Singer, S. *J. Am. Chem. Soc.* **1978**, *100*, 5085.

Magic clusters

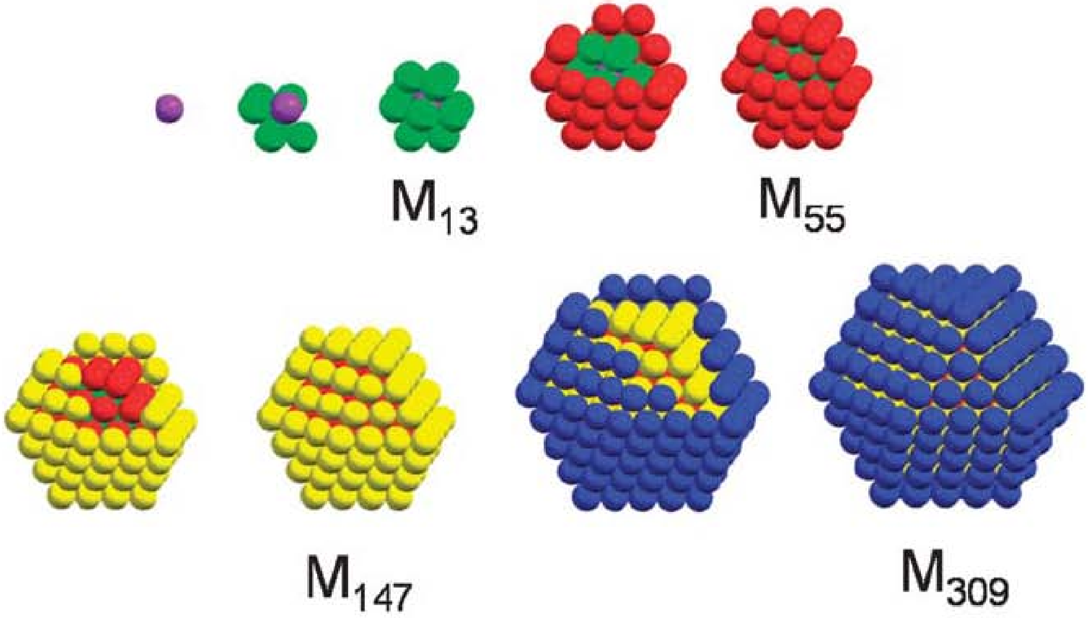

Fig. 1 Organization of full-shell clusters: a first single atom (purple) is surrounded by 12 others (green) to give a one-shell cluster M_{13}. 42 atoms (red) can be densely packed on the 12 green atoms ending with the M_{55} two-shell cluster, followed by 92 atoms (yellow) and 162 atoms (blue) to give M_{147} and M_{309}, respectively.

From Gunter Schmidt, *Chem. Soc. Rev.* **2008**, *37*, 1909–1930

Dendrimer encapsulated clusters

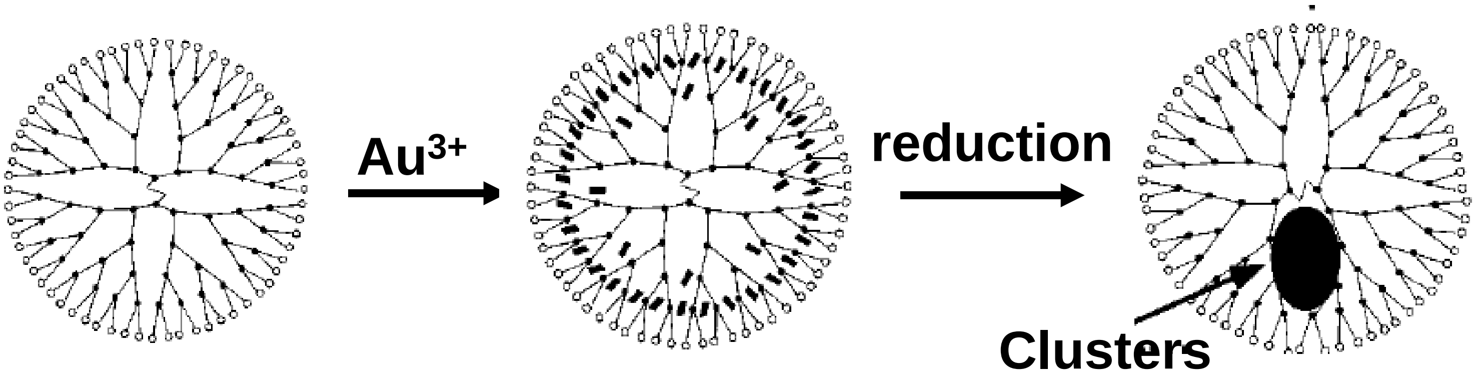

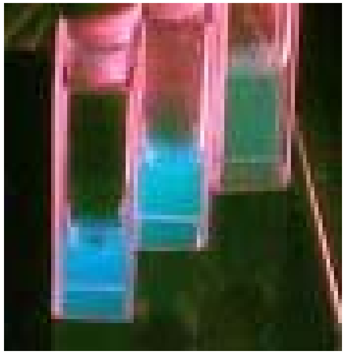

- **High quantum yield blue emission from water-soluble Au_8 nanodots**, Zheng, J.; Petty, J. T.; Dickson, R. M. *J. Am. Chem. Soc*. **2003**, *125*, 7780.
- **Highly fluorescent, water-soluble, size-tunable gold quantum dots,** Zheng, J.; Zhang, C. W.; Dickson, R. M. *Phys. Rev. Lett*. **2004**, *93*, 077402.
- **Highly fluorescent noble-metal quantum dots**, Zheng, J.; Nicovich, P. R.; Dickson, R. M. *Annu. Rev. Phys. Chem.* **2007**, *58*, 409.
- **Etching colloidal gold nanocrystals with hyperbranched and multivalent polymers: A new route to fluorescent and water-soluble atomic clusters**, Duan, H.; Nie, S. *J. Am. Chem. Soc*. **2007**, *129*, 2412.

DNA encapsulated clusters

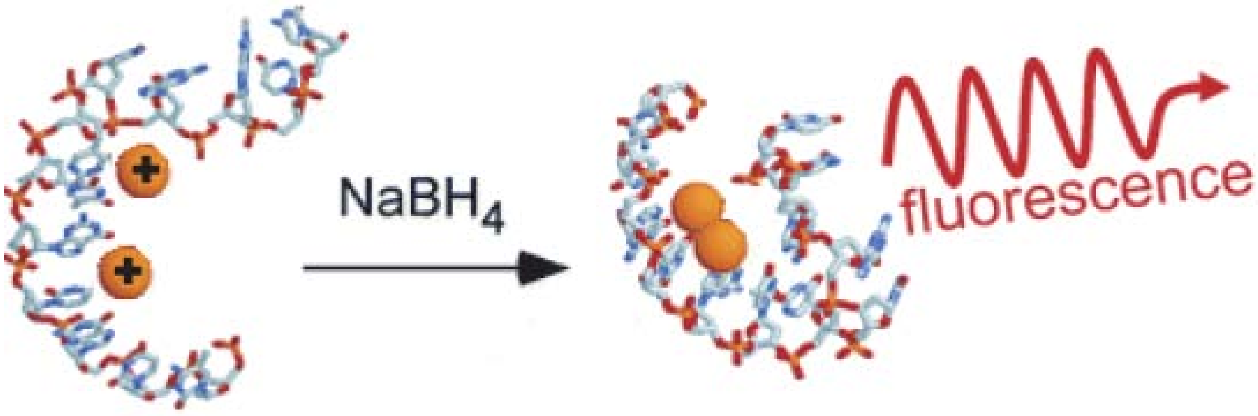

DNA-Templated Ag Nanocluster Formation, Petty, J. T.; Zheng, J.; Hud, N. V.; Dickson, R. M. *J. Am. Chem. Soc*. **2004**, *126*, 5207.

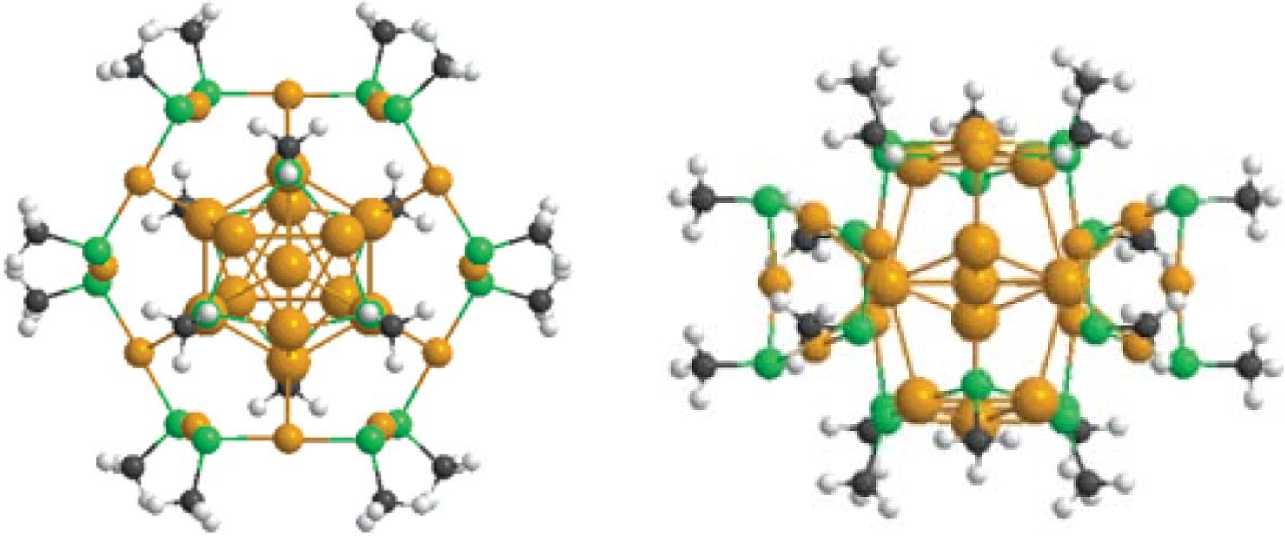

Top and side view of $[Au_{25}(SCH_3)_{18}]^+$

Theoretical Investigation of Optimized Structures of Thiolated Gold Cluster $[Au_{25}(SCH_3)_{18}]^+$, Iwasa, T.; Nobusada, K. *J. Phys. Chem. C* **2007**, *111*, 45.

Au_{102}

Au_{102}(p-MBA)$_{44}$

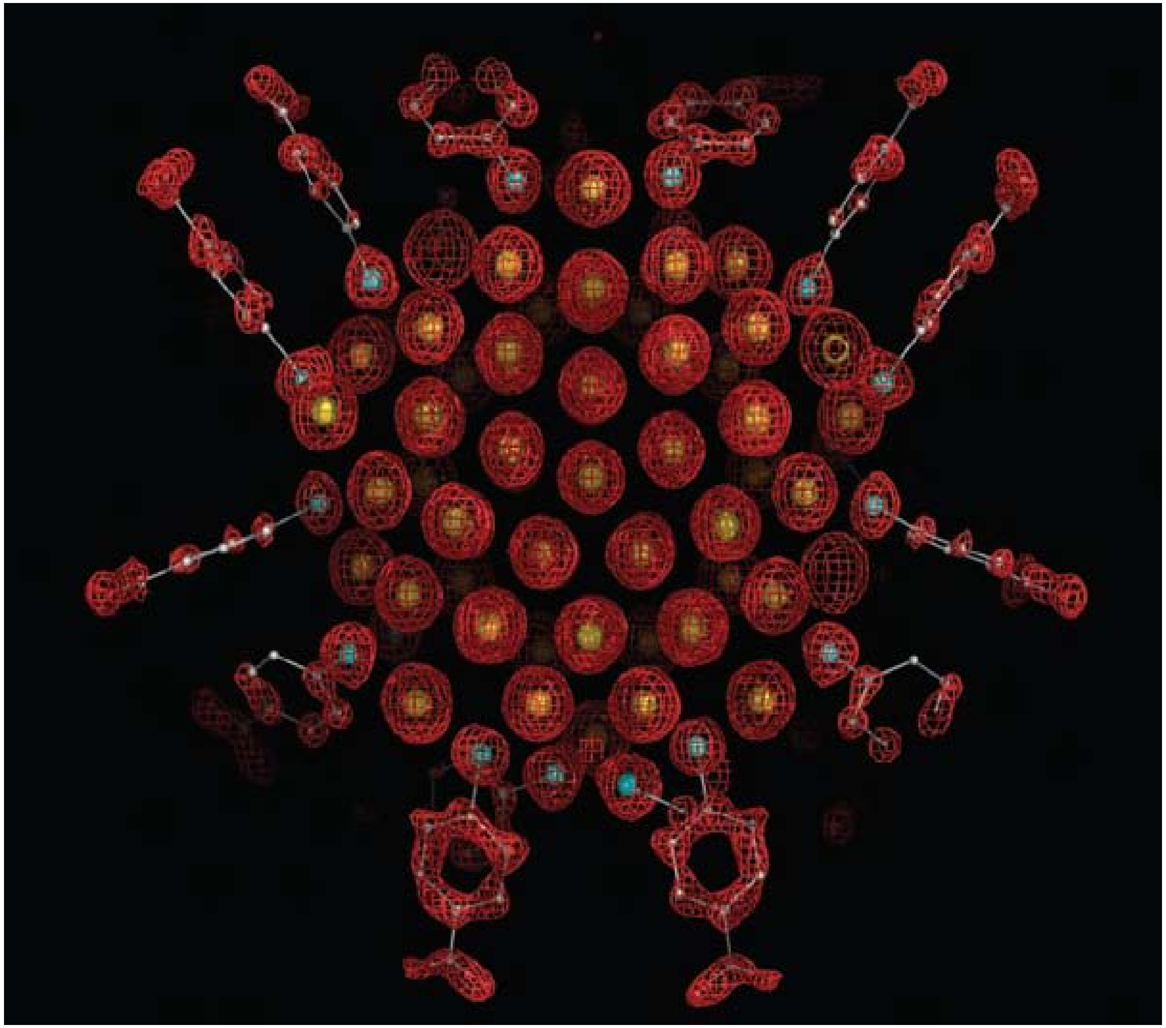

Jadzinsky, P. D.; Calero, G.; Ackerson, C. J.; Bushnell, D. A.; Kornberg, R. D. Structure of a Thiol Monolayer–Protected Gold Nanoparticle at 1.1 Å Resolution *Science* **2007**, *318*, 430.

Coulomb staircase

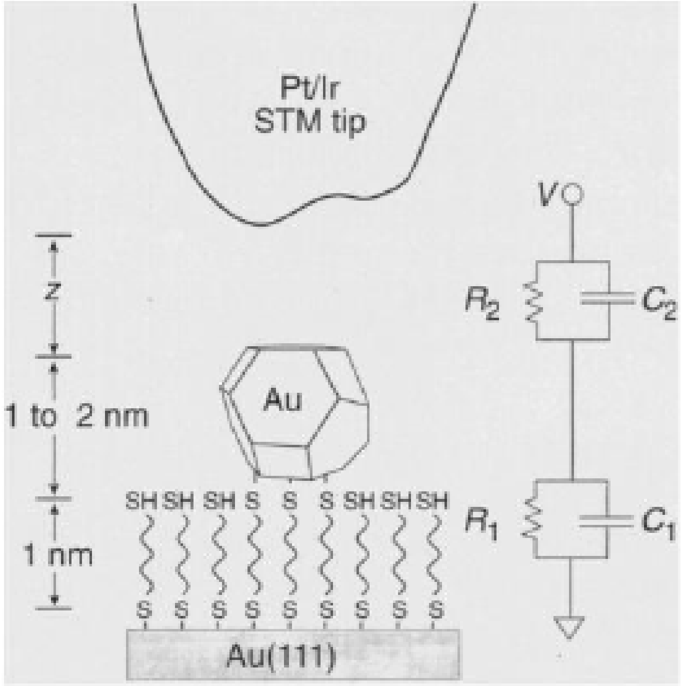

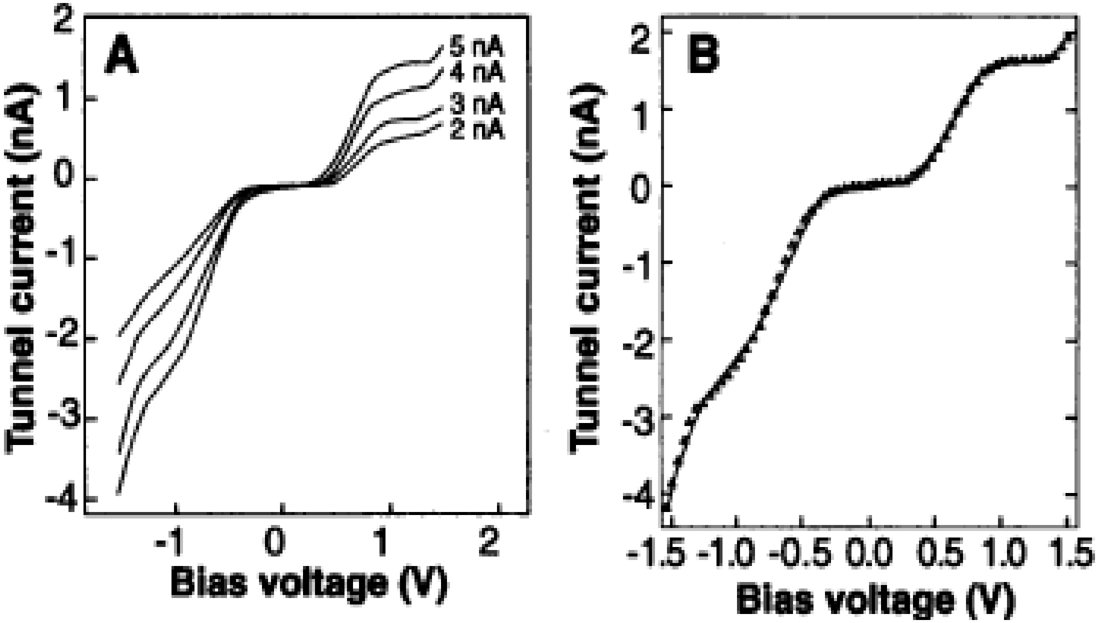

Andres, R. P. Bein, T.; Dorogi, M.; Feng, S.; Henderson, J. I.; Kubiak, C. P.; Mohoney, W.; Osifchin, R. G.; Reifenberger, O. R. Coulomb staircase at room temperature in a self-assembled molecular nanostructure. *Science* **1996**, *272*, 1323.

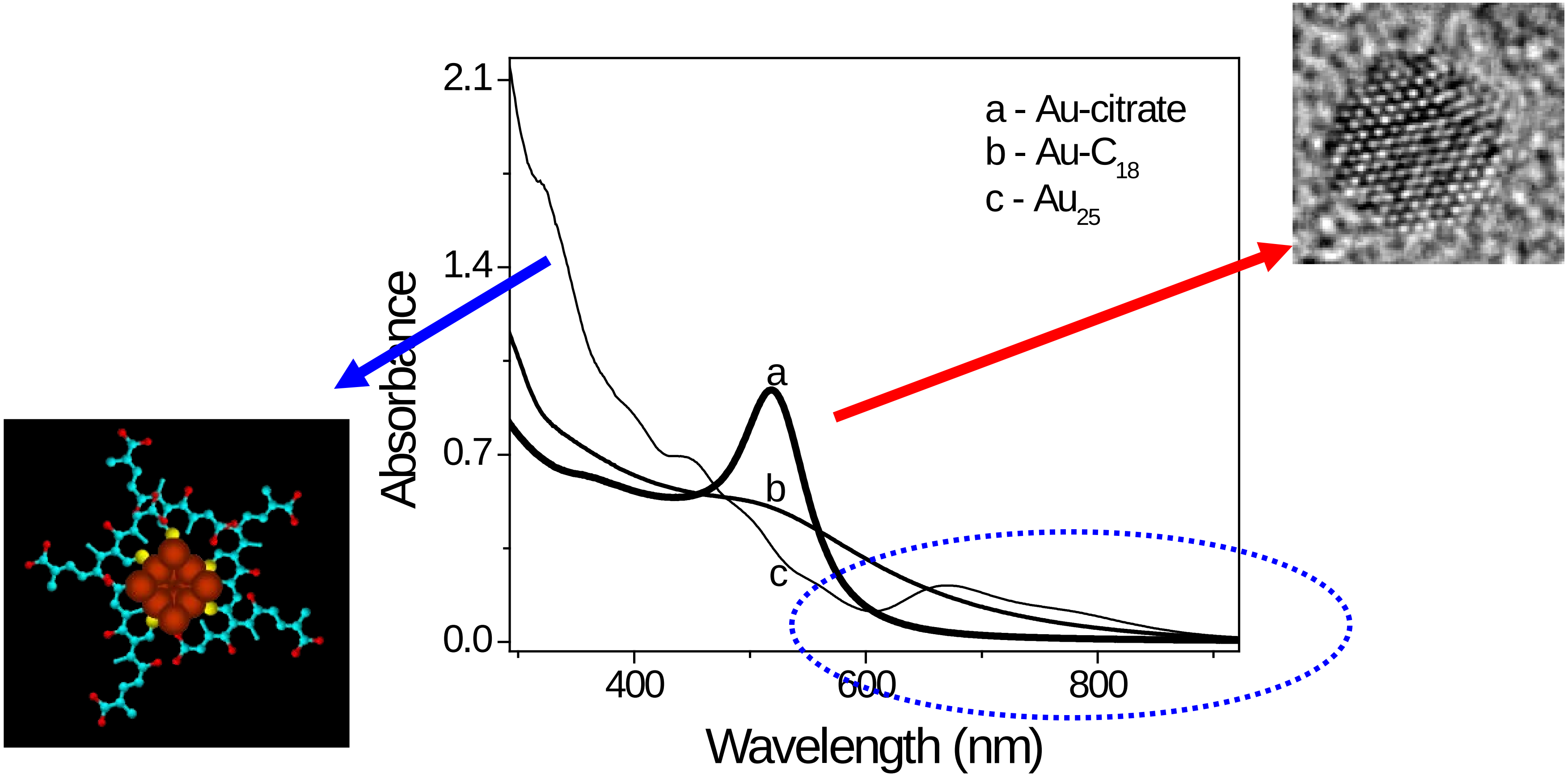

Optical absorption (extinction) spectrum of (a) 15 nm gold particles in aqueous solution (labeled Au@citrate). The spectrum of (b) 3 nm particles in toluene is also shown. See the broadening of the plasmon feature. The spectrum of (c) Au_{25} in water. In this, there is no plasmon excitation and all the features are due to molecular absorptions of the cluster.

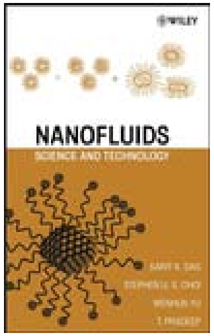

Das, Choi, Yu and Pradeep, *Nanofluids*, John Wiley, New York, 2008

Polyacrylamide gel electrophoresis (PAGE)

How to make them?

Au^{3+}

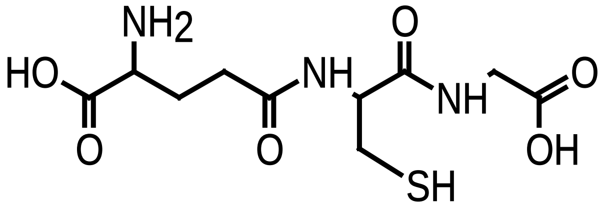

BH_4^-

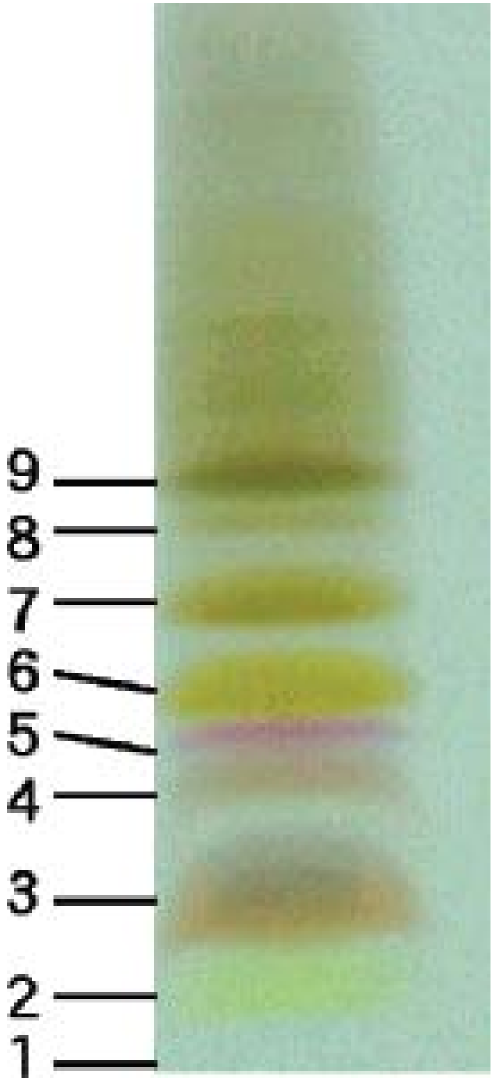

→ µg

Negishi, Y.; Nobusada, K.; and Tsukuda, T. Glutathione-Protected Gold Clusters Revisited: Bridging the Gap between Gold(I)-Thiolate Complexes and Thiolate-Protected Gold Nanocrystals. *J. Am. Chem. Soc*. 2005, *127*, 5261-70.

$Au_{25}SG_{18}$

Synthesis: Au_{25} clusters can be preferentially populated by dissociative excitation of larger precursors

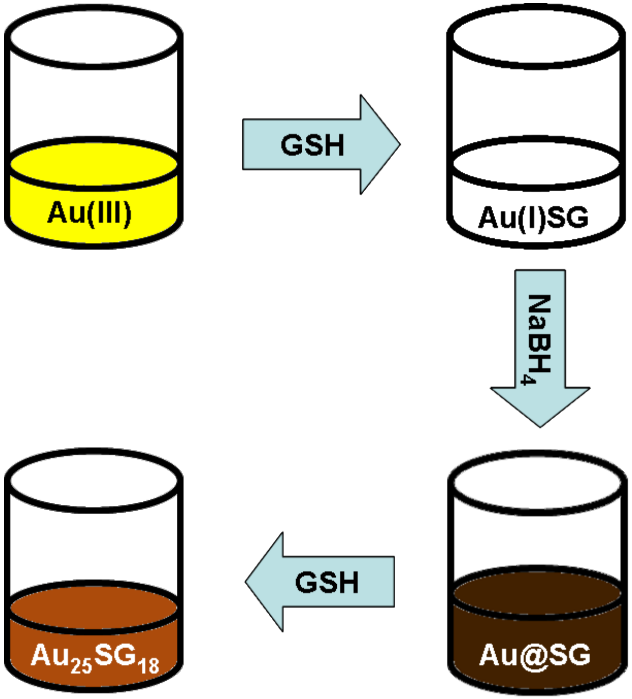

Scheme showing the synthesis of $Au_{25}SG_{18}$ clusters

Optic
absc

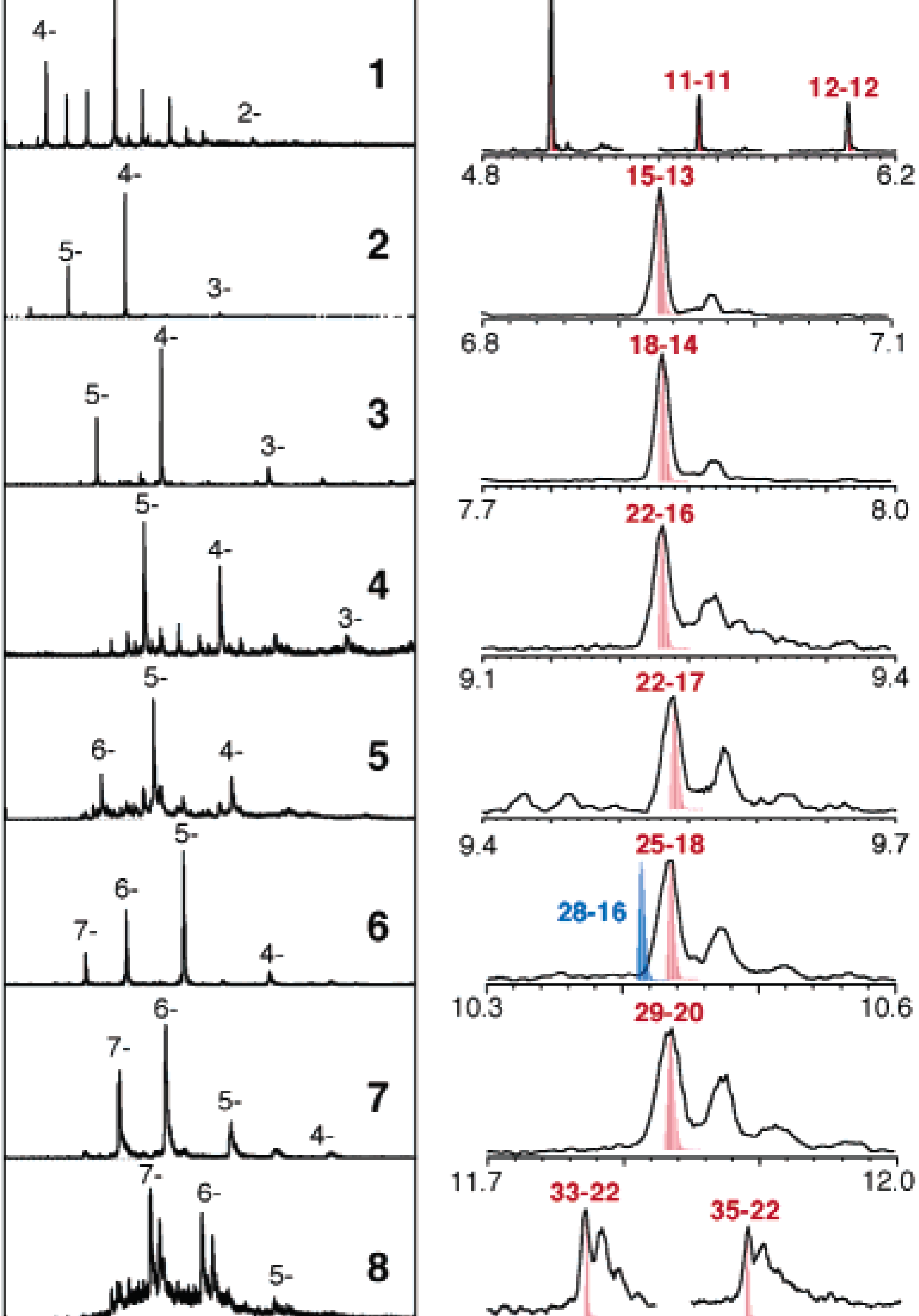

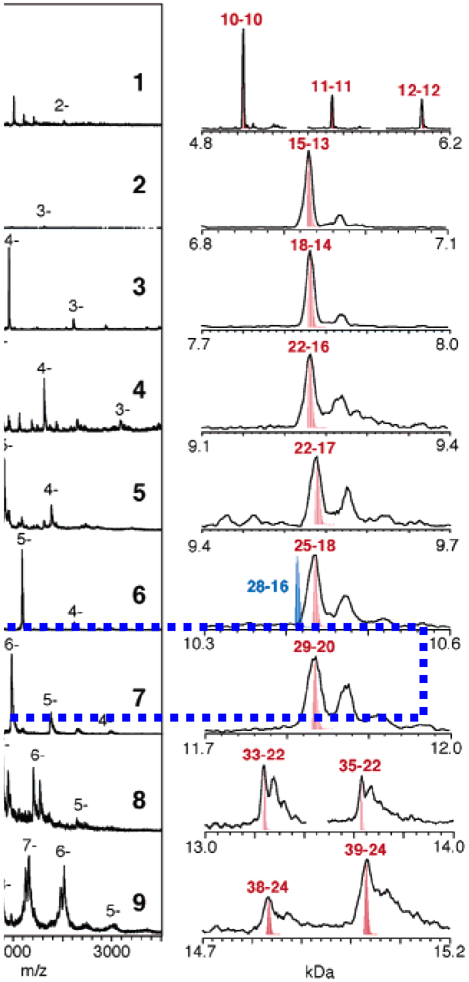

da et. al. JACS 2005

excitation
d 700 nm,

Q-Trap ESI Mass Spectrometer

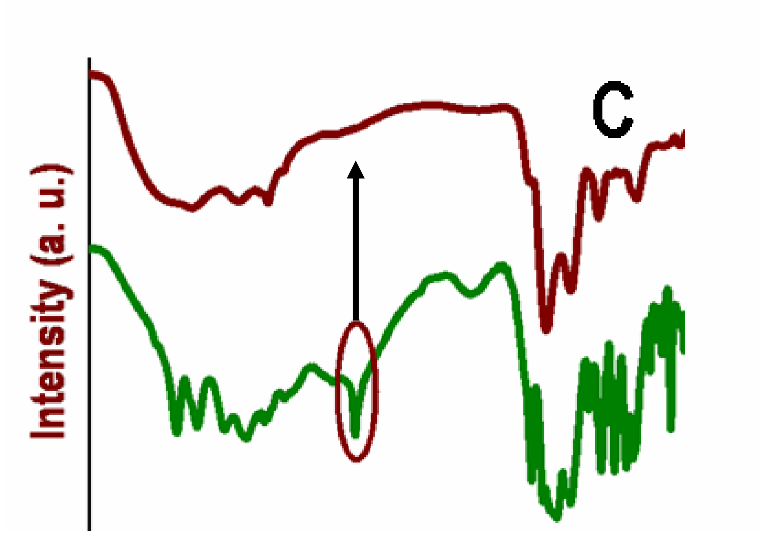

FTIR spectrum: The peak at 2526 cm^{-1} of glutathione due to –SH stretching frequency is absent in IR spectrum of Au_{25} suggesting the ligand binding on cluster surface.

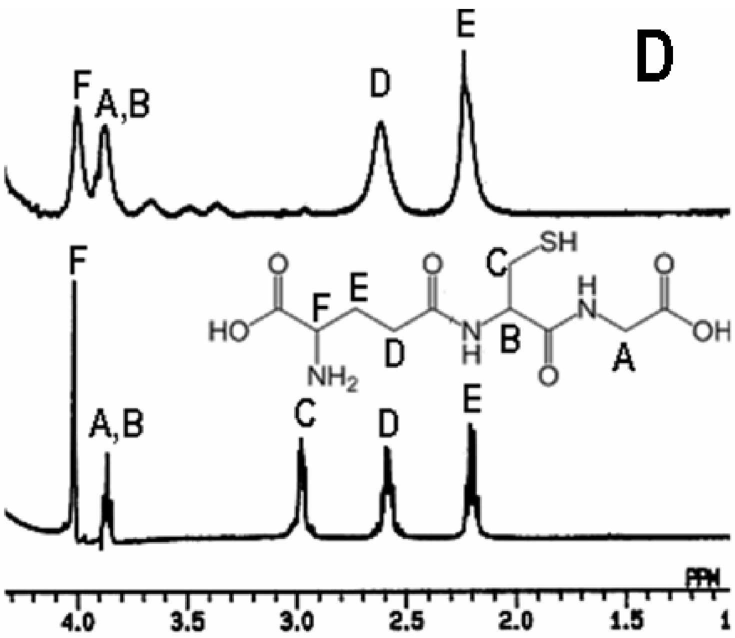

1H NMR spectrum: There is one-to-one correspondence between the two spectra, except that the **β**CH_2 resonance (labeled as C) disappears completely in the cluster which is expected as it is close to the cluster surface. All the observed resonances have been broadened in view of their faster relaxation and non-uniform distribution of ligands.

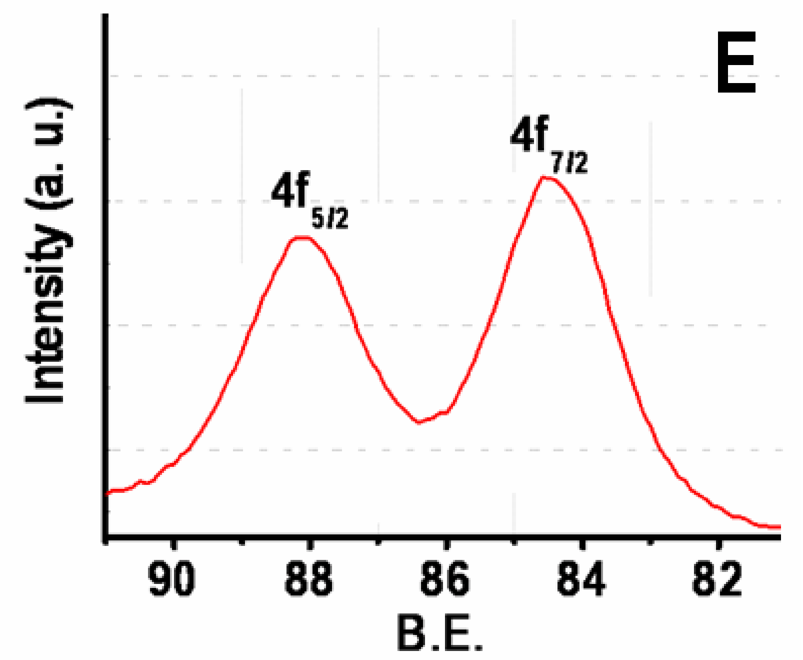

XPS spectrum

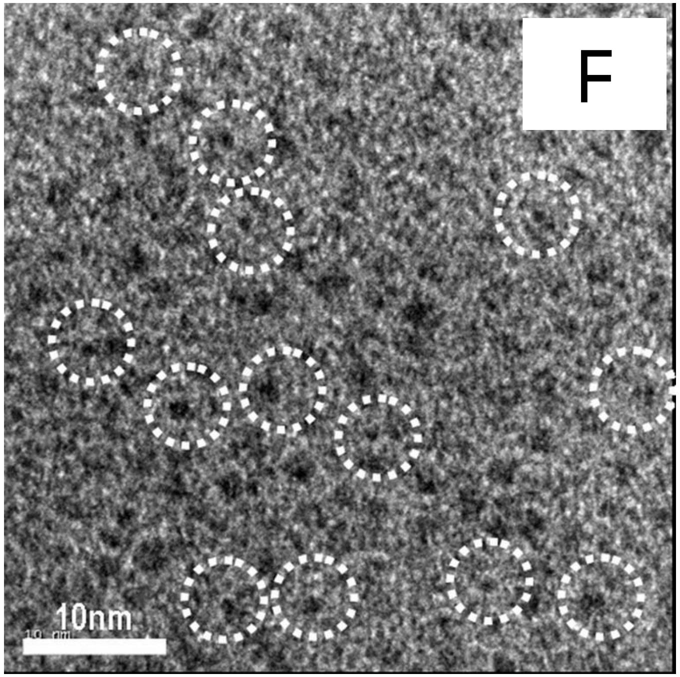

TEM image: The clusters are seen only faintly since the size is ~1 nm. Some of the individual clusters are shown by circles. There are also cluster aggregates which upon extended electron beam irradiation fuse to form bigger particles

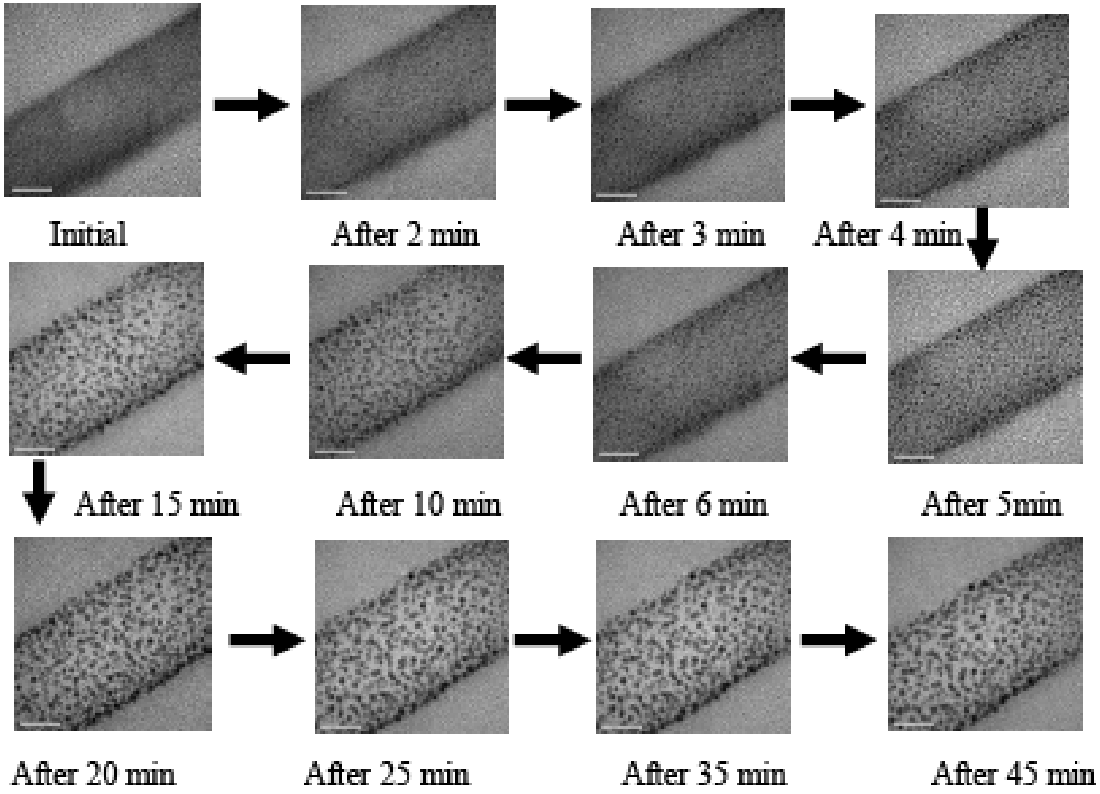

Initial

After 2 min

After 3 min

After 4 min

After 5min

After 6 min

After 10 min

After 15 min

After 20 min

After 25 min

After 35 min

After 45 min

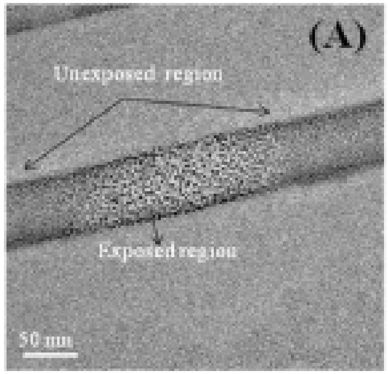

Perumal Ramasamy *et al. J. Mater. Chem.*, **2009**, *19*, 8456.

With Arindam Banerjee

Ligand exchange of Au_{25}

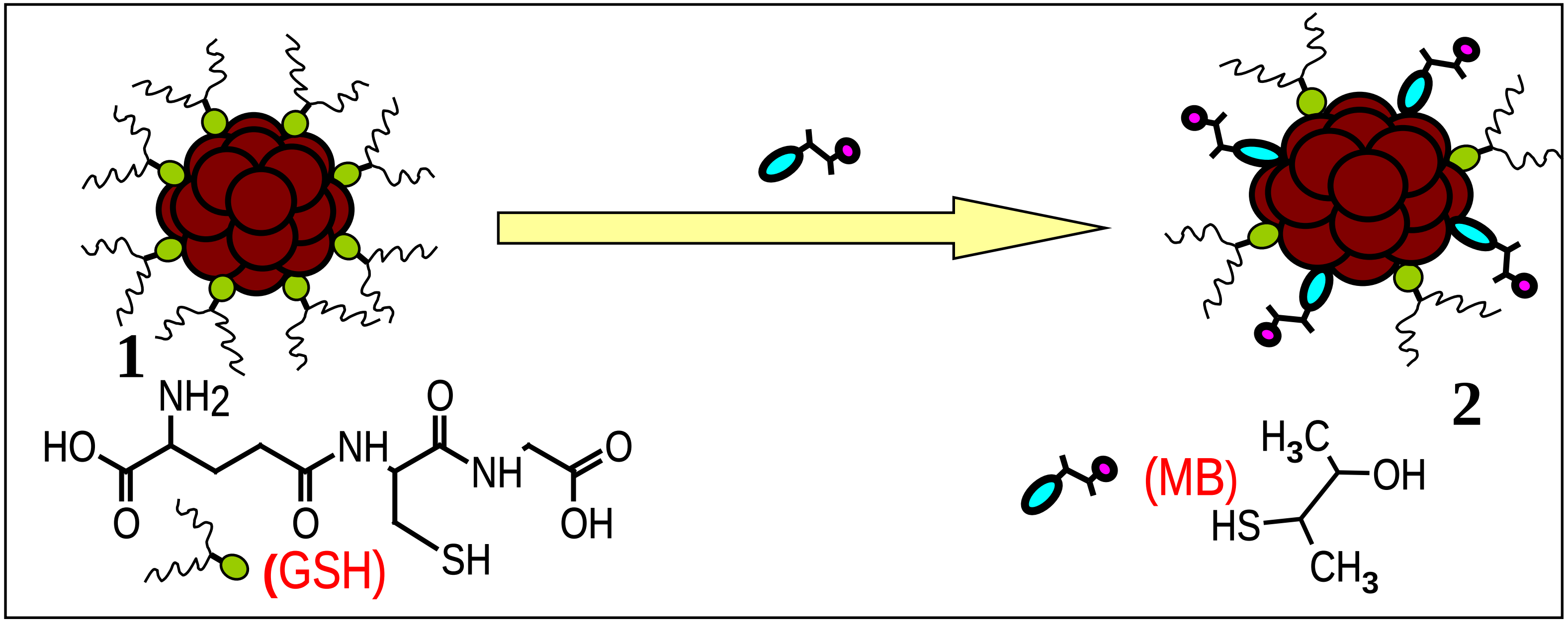

1

(GSH)

2

(MB)

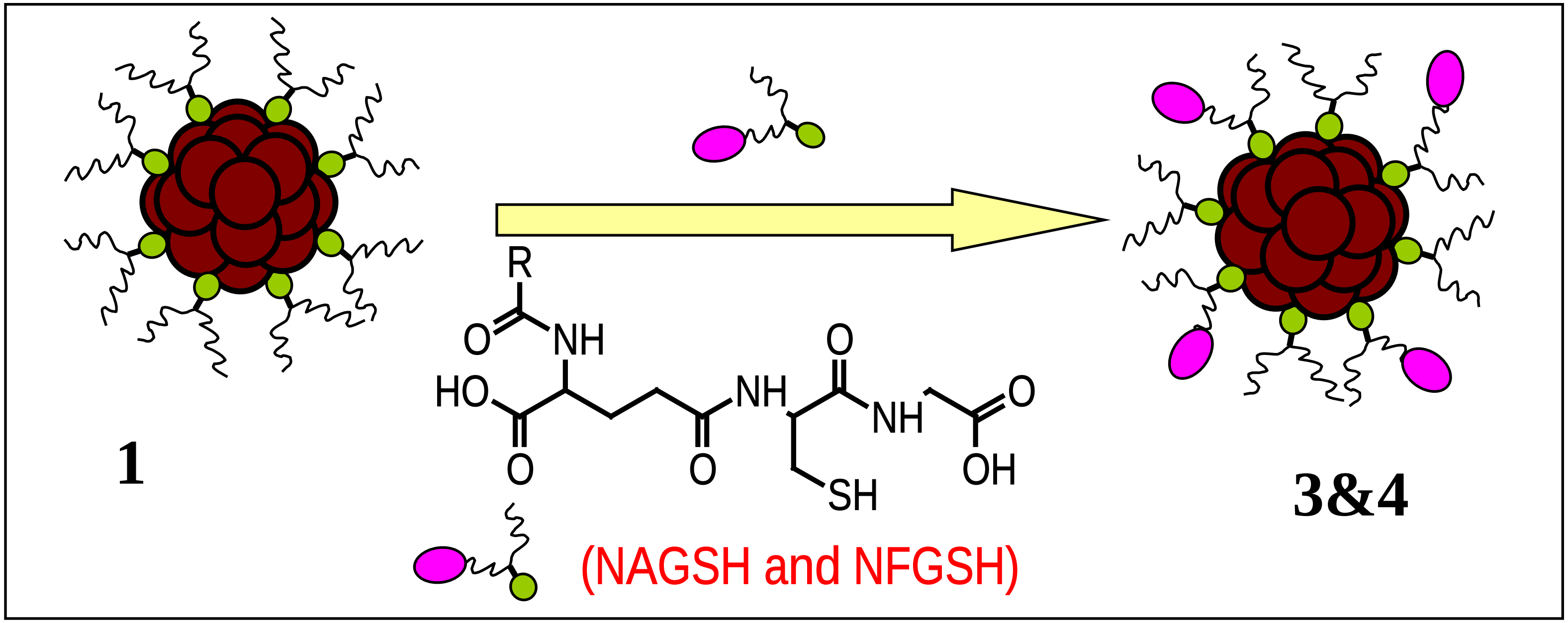

1

3&4

(NAGSH and NFGSH)

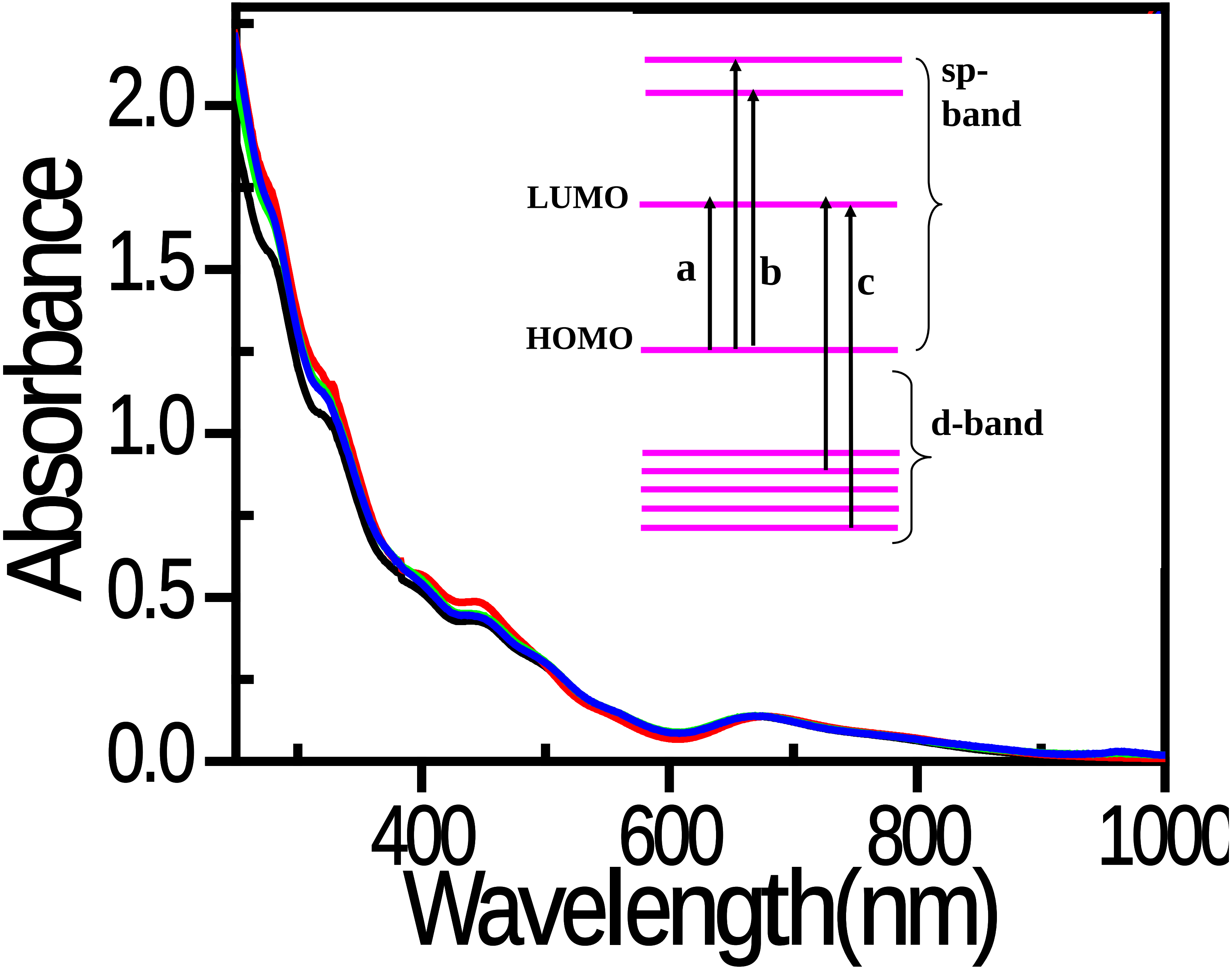

E.S. Shibu *et al. J. Phys. Chem. C* **2008**, *112*, 12168.

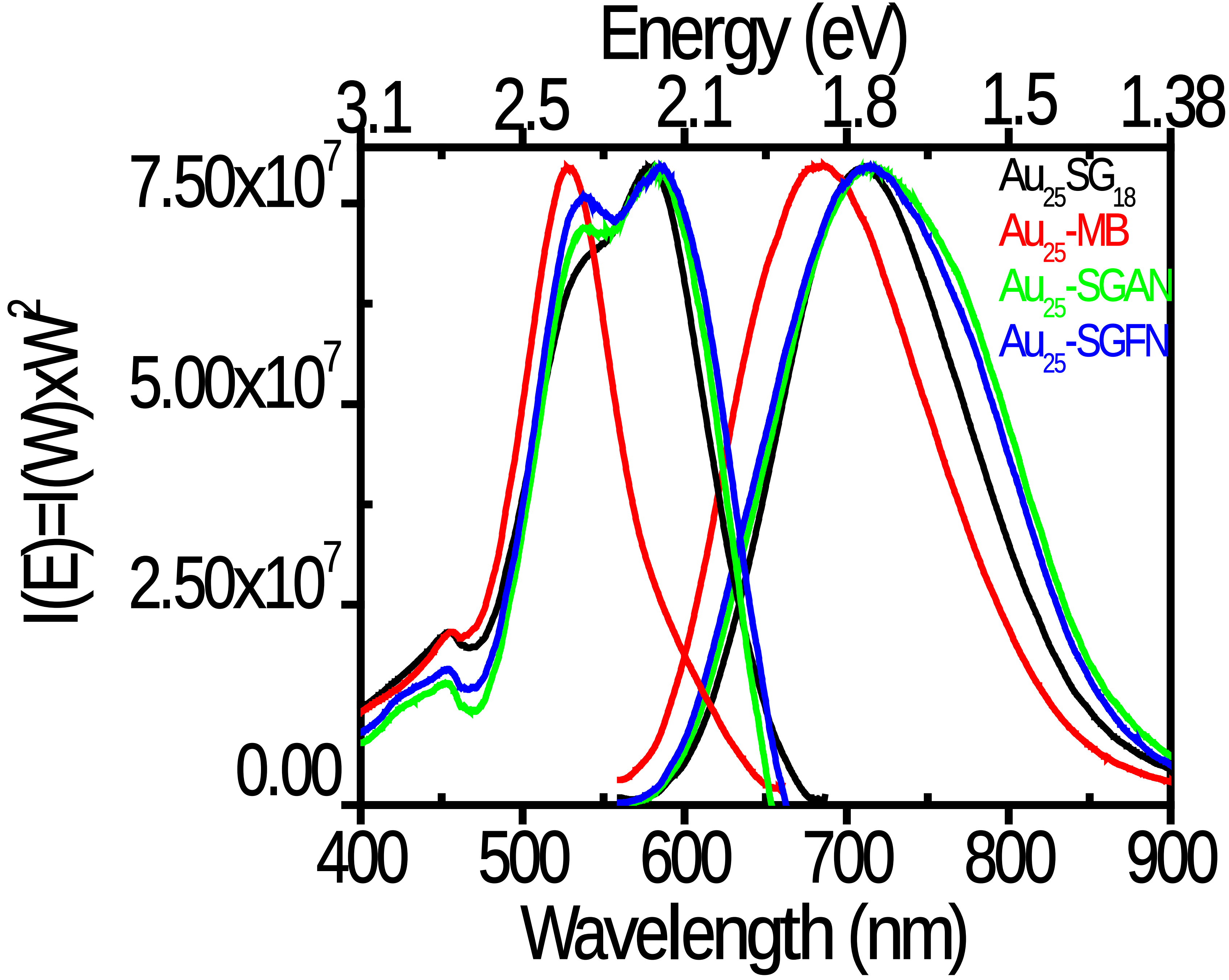
Energy (eV)
3.1
2.5
2.1
1.8
1.5
1.38
I(E)=I(W)xW^2
7.50x10^7
5.00x10^7
2.50x10^7
0.00
400
500
600
700
800
900
Wavelength (nm)
Au$_{25}$SG$_{18}$
Au$_{25}$-MB
Au$_{25}$-SGAN
Au$_{25}$-SGFN

Fluorescence : A comprehensive study between organic dye, gold atoms and molecular clusters of gold

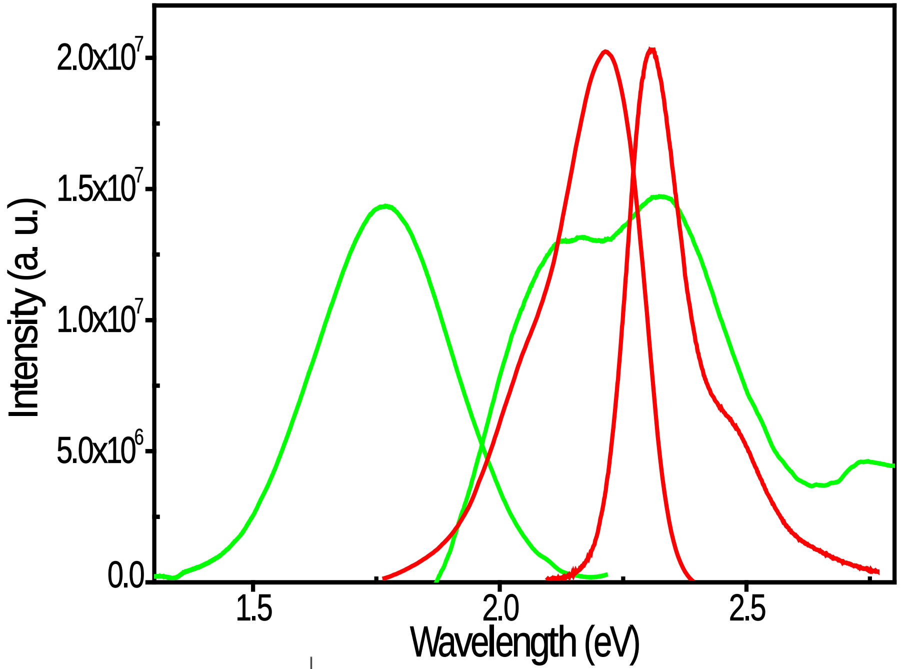

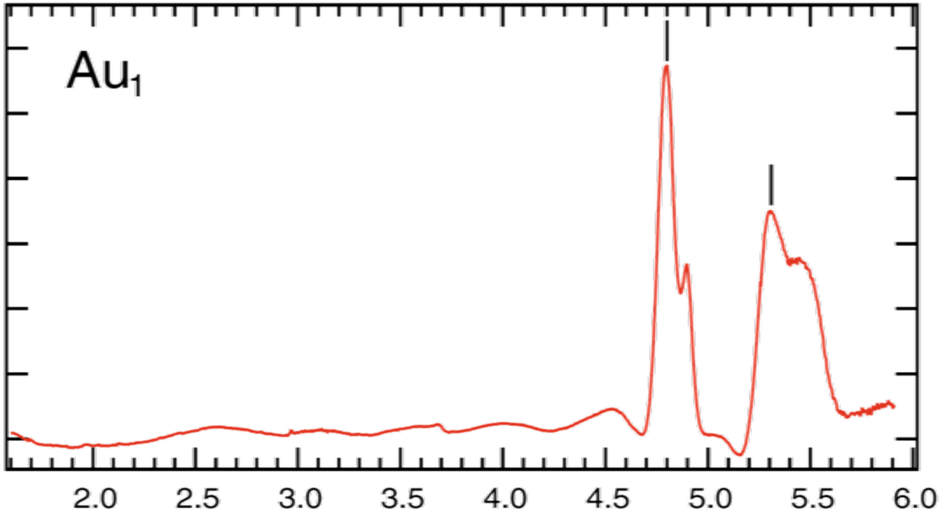

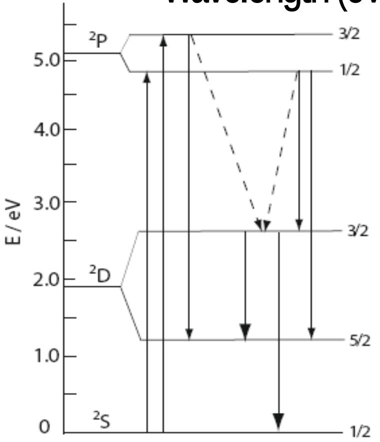

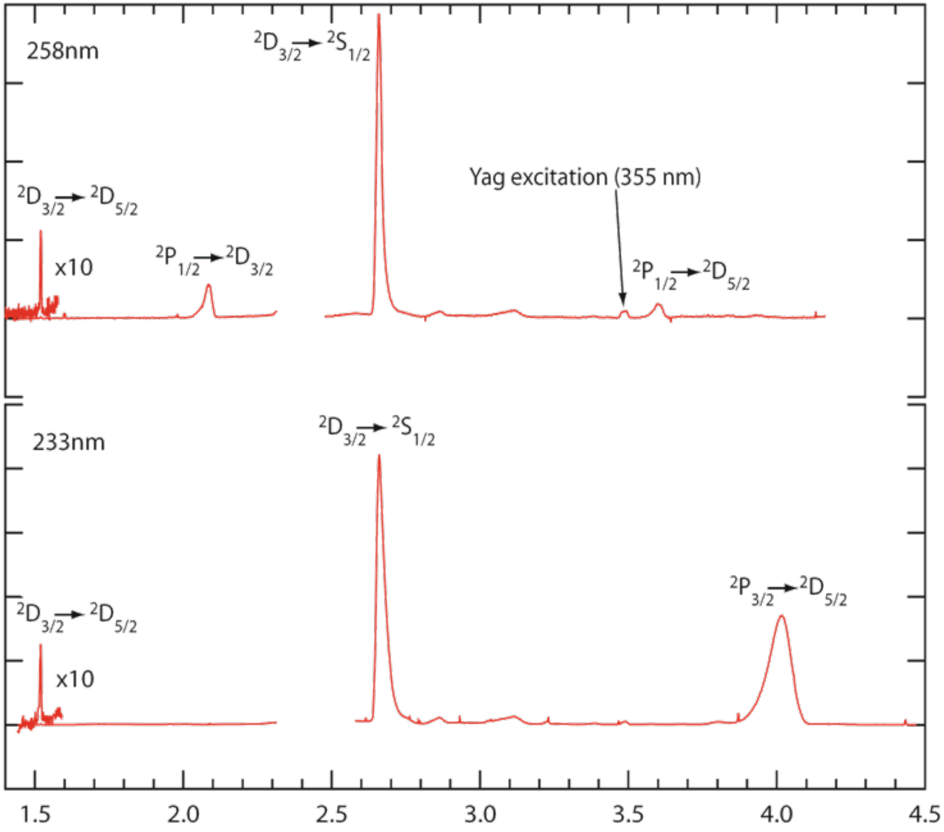

Lecoultrea, S.; Rydlo, A.; F elixb, C.; Harbich, W. *Eur. Phys. J. D*, **2009** DOI: 10.1140/epjd/e2008-00290-0

Cluster	Q.Yield
$Au_{10}(SG)_{10}$ $Au_{11}(SG)_{11}$ $Au_{11}(SG)_{11}$	$1*10^{-4}$
$Au_{15}(SG)_{13}$	$2*10^{-4}$
$Au_{18}(SG)_{14}$	$4*10^{-3}$
$Au_{22}(SG)_{16}$	$4*10^{-3}$
$Au_{22}(SG)_{17}$	$2*10^{-3}$
$Au_{25}(SG)_{18}$	$1.9*10^{-3}$
$Au_{29}(SG)_{20}$	$3*10^{-3}$
$Au_{33}(SG)_{22}$ $Au_{35}(SG)_{22}$	$2*10^{-3}$
$Au_{38}(SG)_{24}$, $Au_{39}(SG)_{24}$	$2*10^{-3}$
Gold nanoparticles	$1*10^{-10}$

Recently developed clusters using Au_{25} as precursor

Precursor

Using other ligands

Cluster	Q. Yield
Au_{22}	$4.0*10^{-2}$
Au_{23}	$1.3*10^{-2}$
Au_{31}	$1.0*10^{-2}$
$Au_8(SG)_8$	$1.5*10^{-1}$

1. Nano Res., 1(2008) 333-340.
2. Chemistry A European Journal. (In Press).
3. ACS Applied Materials and Interfaces (in press)

Negishi, Y.; Nobusada, K.; Tsukuda, T. *J. Am. Chem. Soc.* **2005**, *127*, 5261.

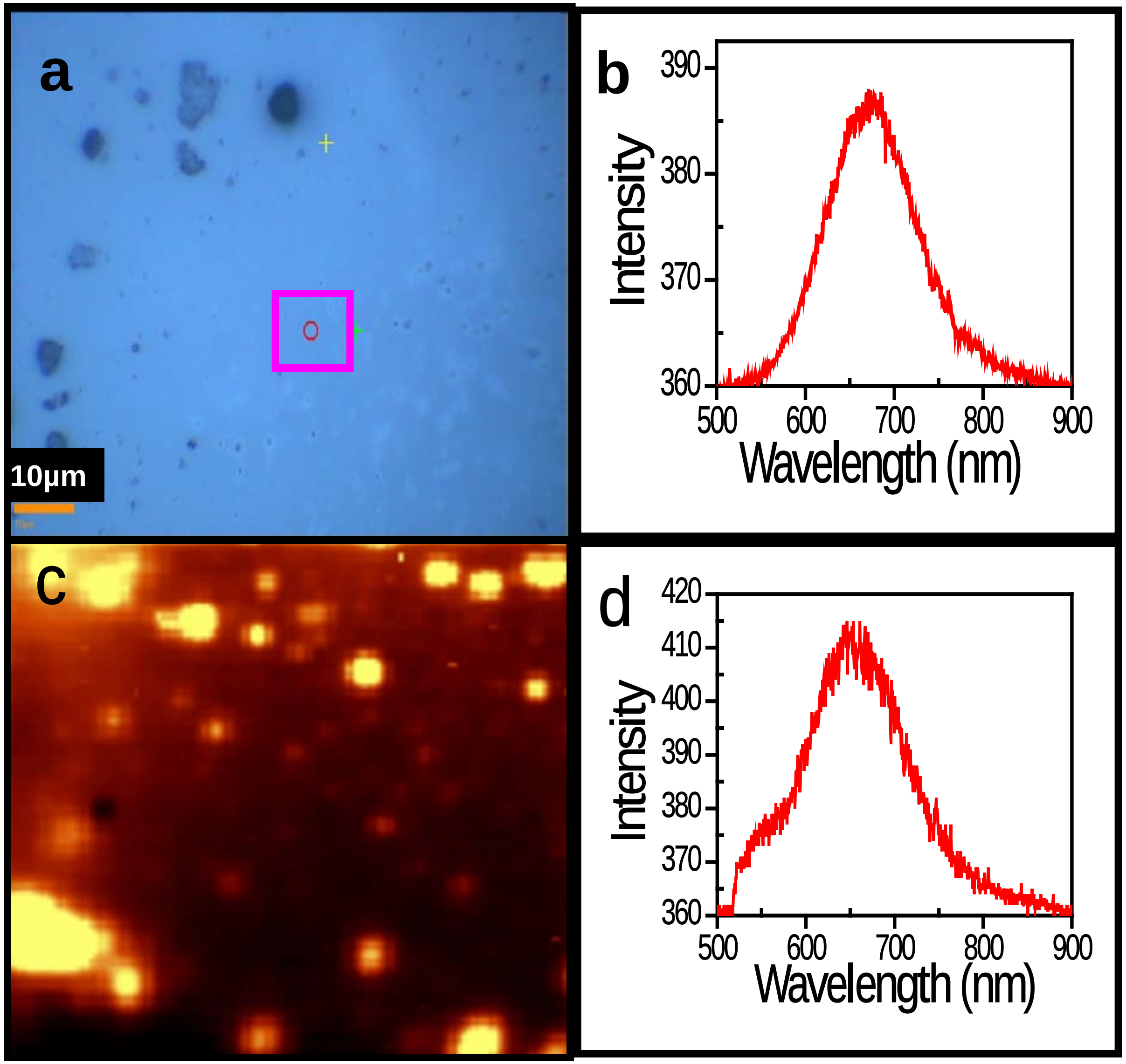
a
10µm
b
390
380
370
360
Intensity
500
600
700
800
900
Wavelength (nm)
c
d
420
410
400
390
380
370
360
Intensity
500
600
700
800
900
Wavelength (nm)

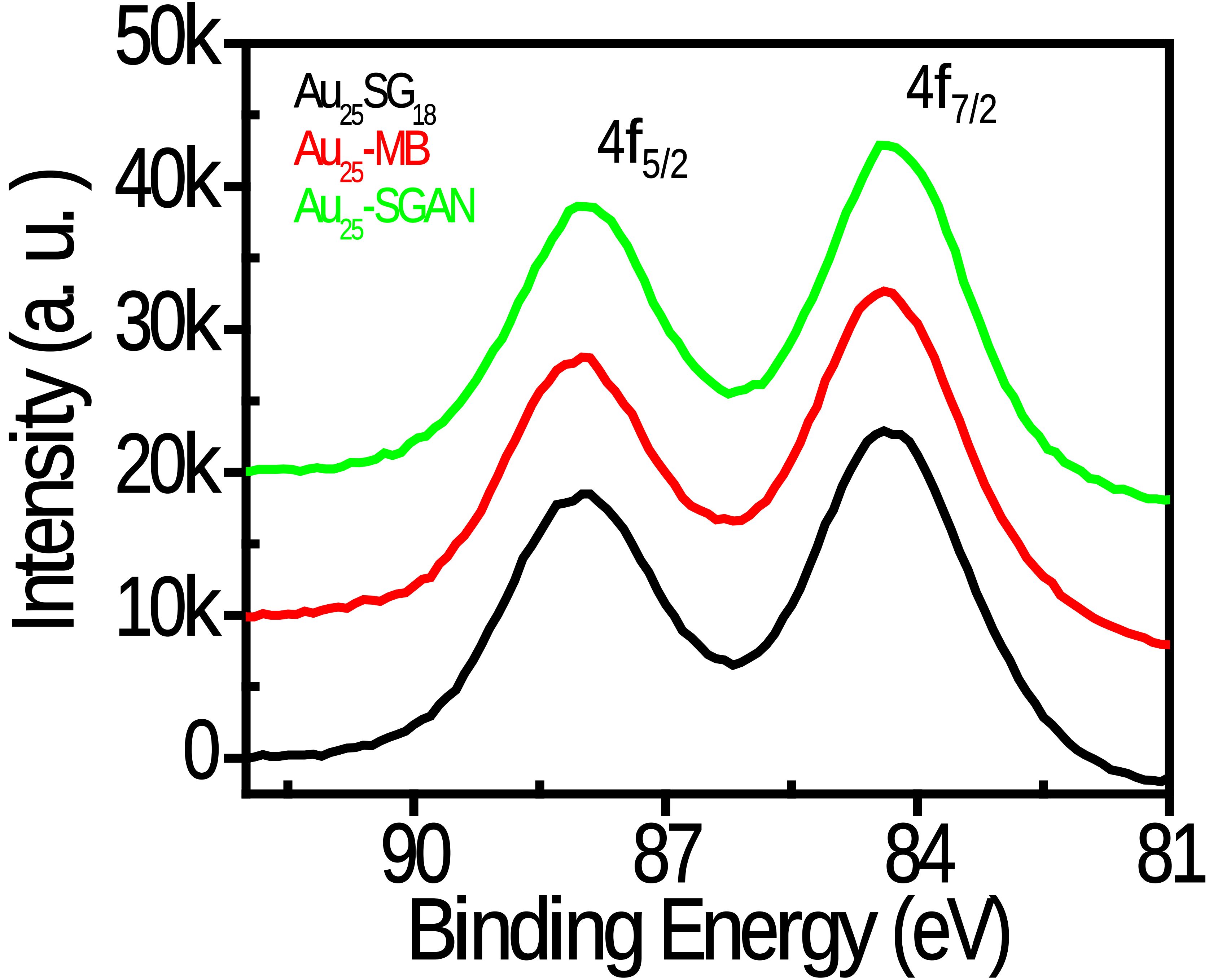
Au25SG18
Au25-MB
Au25-SGAN
4f5/2
4f7/2
Intensity (a. u.)
50k
40k
30k
20k
10k
0
90
87
84
81
Binding Energy (eV)

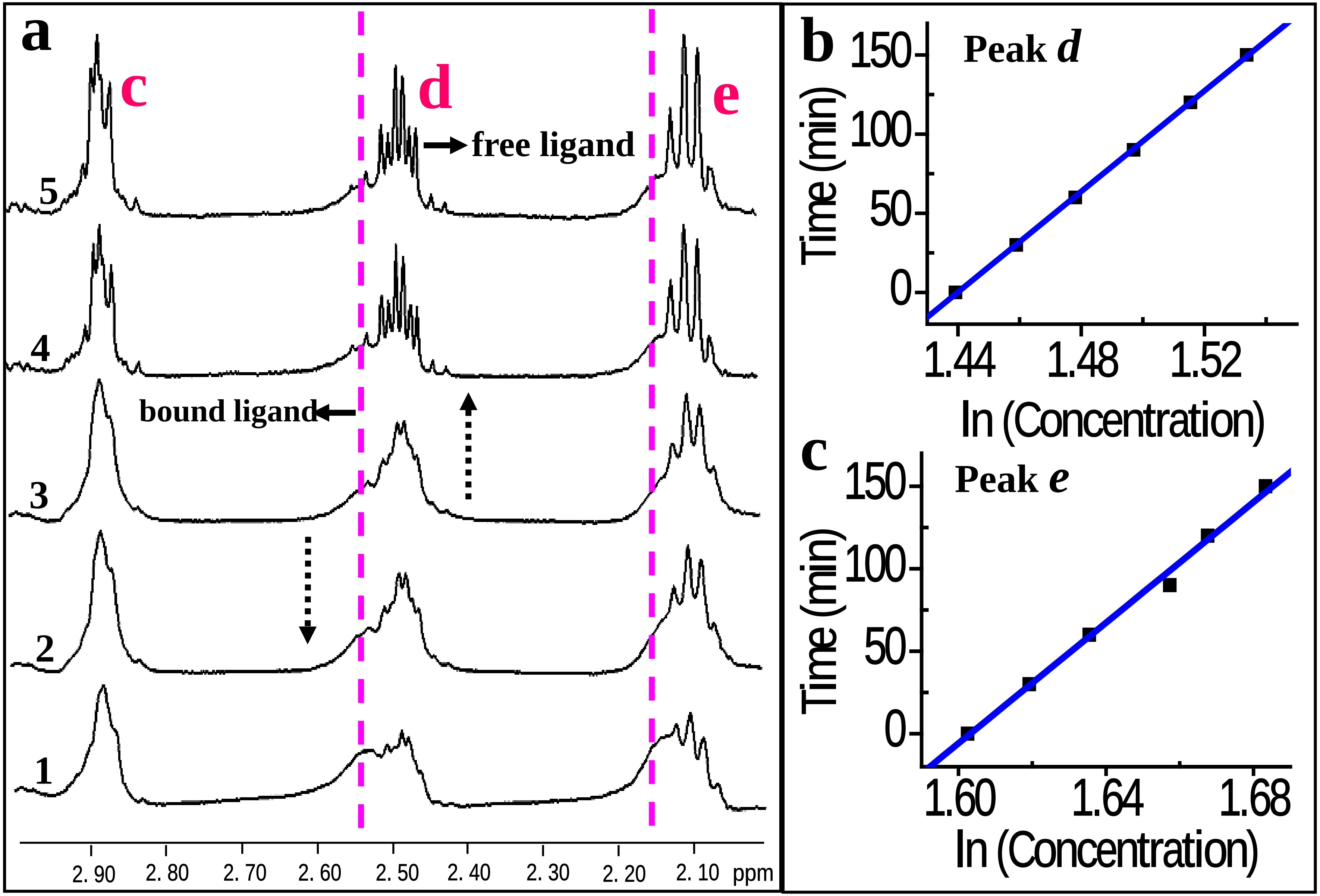
a
c
d
e
free ligand
bound ligand
5
4
3
2
1
2. 90
2. 80
2. 70
2. 60
2. 50
2. 40
2. 30
2. 20
2. 10
ppm
b
Peak d
Time (min)
150
100
50
0
1.44
1.48
1.52
ln (Concentration)
c
Peak e
Time (min)
150
100
50
0
1.60
1.64
1.68
ln (Concentration)

Au_8SG_8

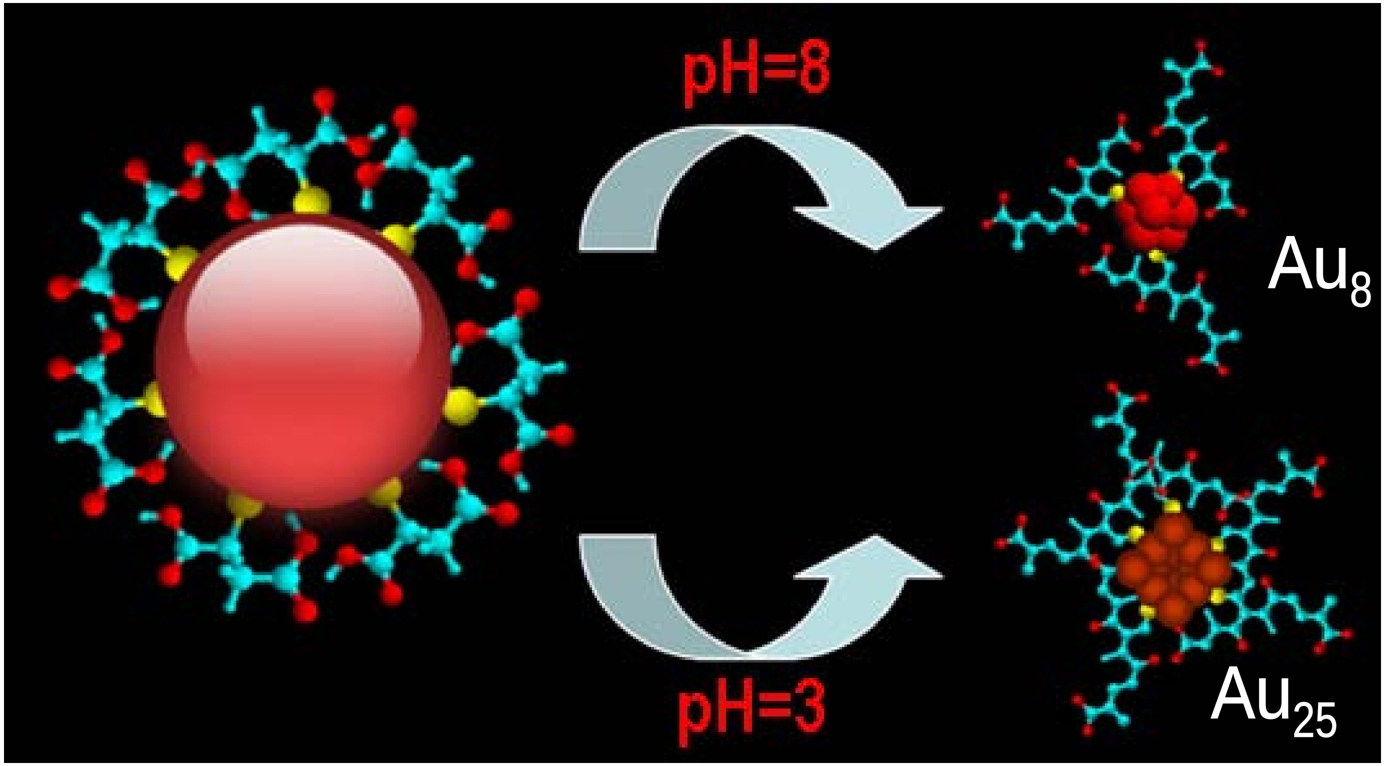

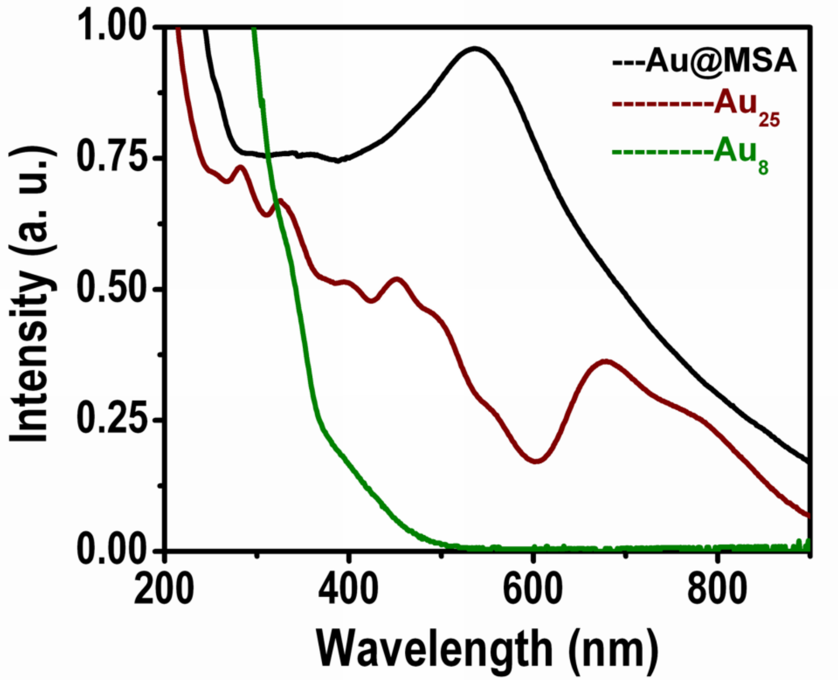

Comparison of the optical absorption profiles of Au@MSA, Au_{25} and Au_8.

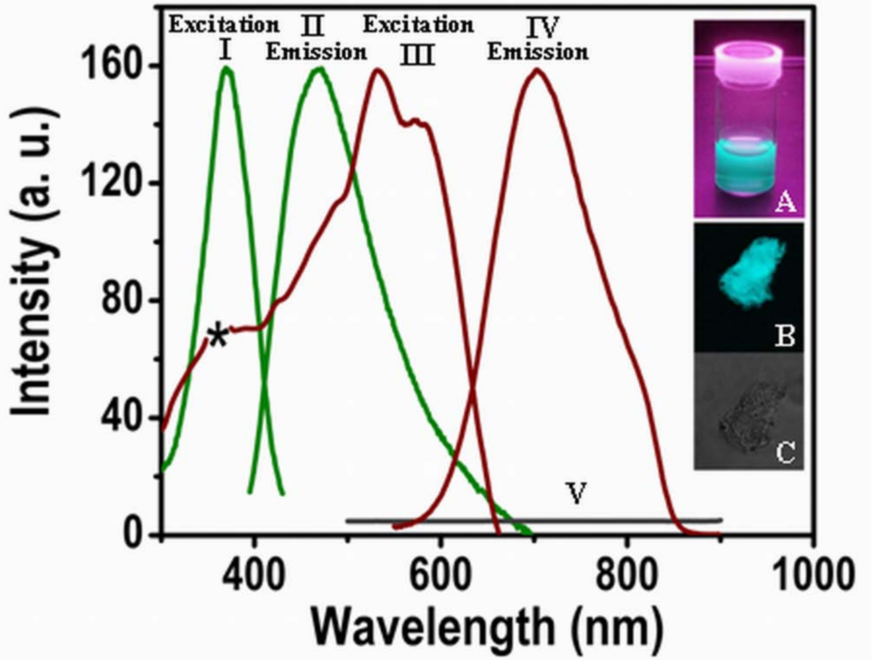

Comparison of the photoluminescence profiles of the clusters with Au@MSA. Traces I and II are the excitation and emission spectra of Au_8, respectively. Traces III and IV are the excitation and emission spectra of Au_{25}, respectively and trace V is the emission spectrum of Au@MSA.

Habeeb Muhammed *et al. Nano Res.* ***2008***, *1, 333.*

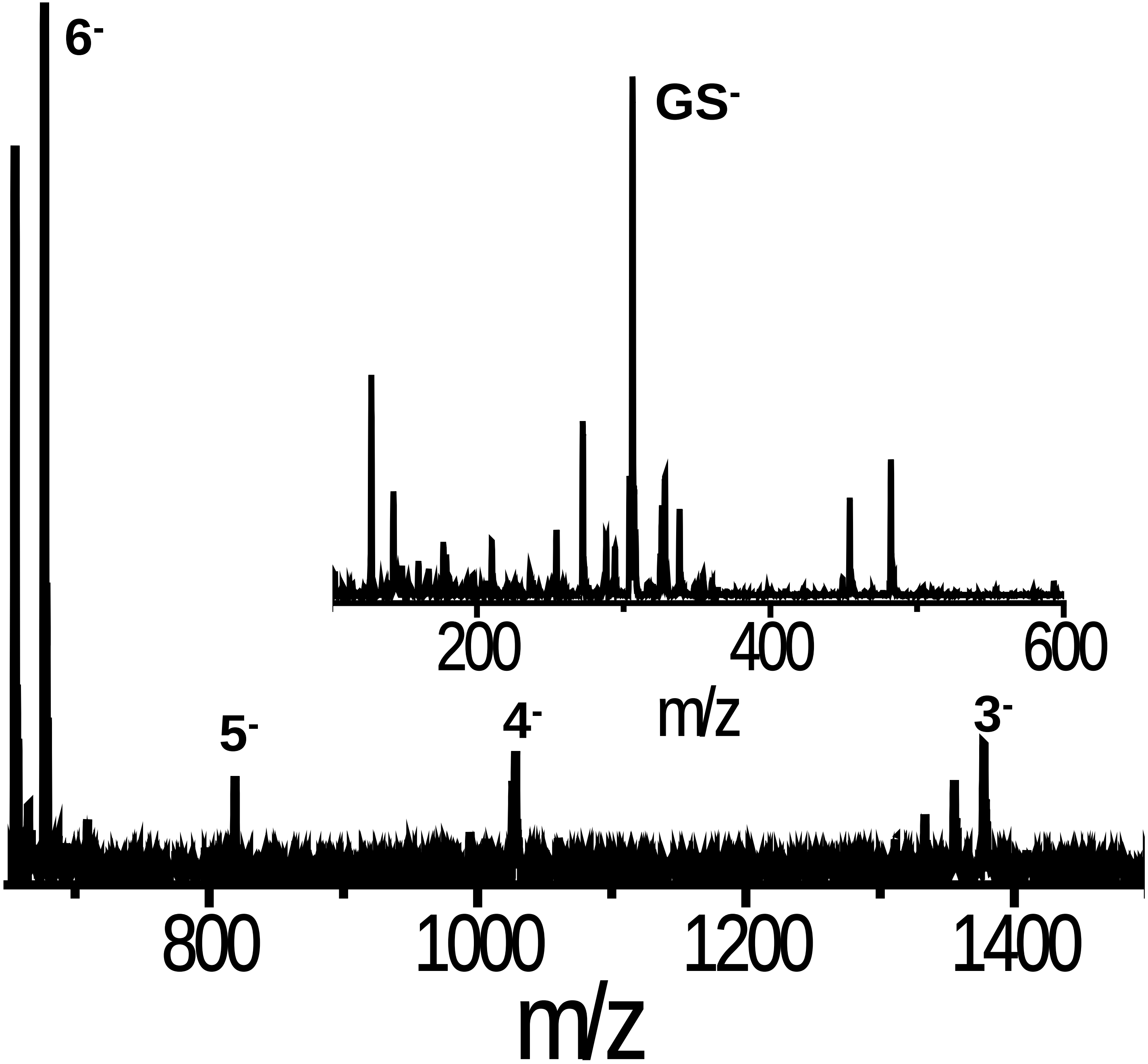

Habeeb Muhammed *et al*. Unpublished

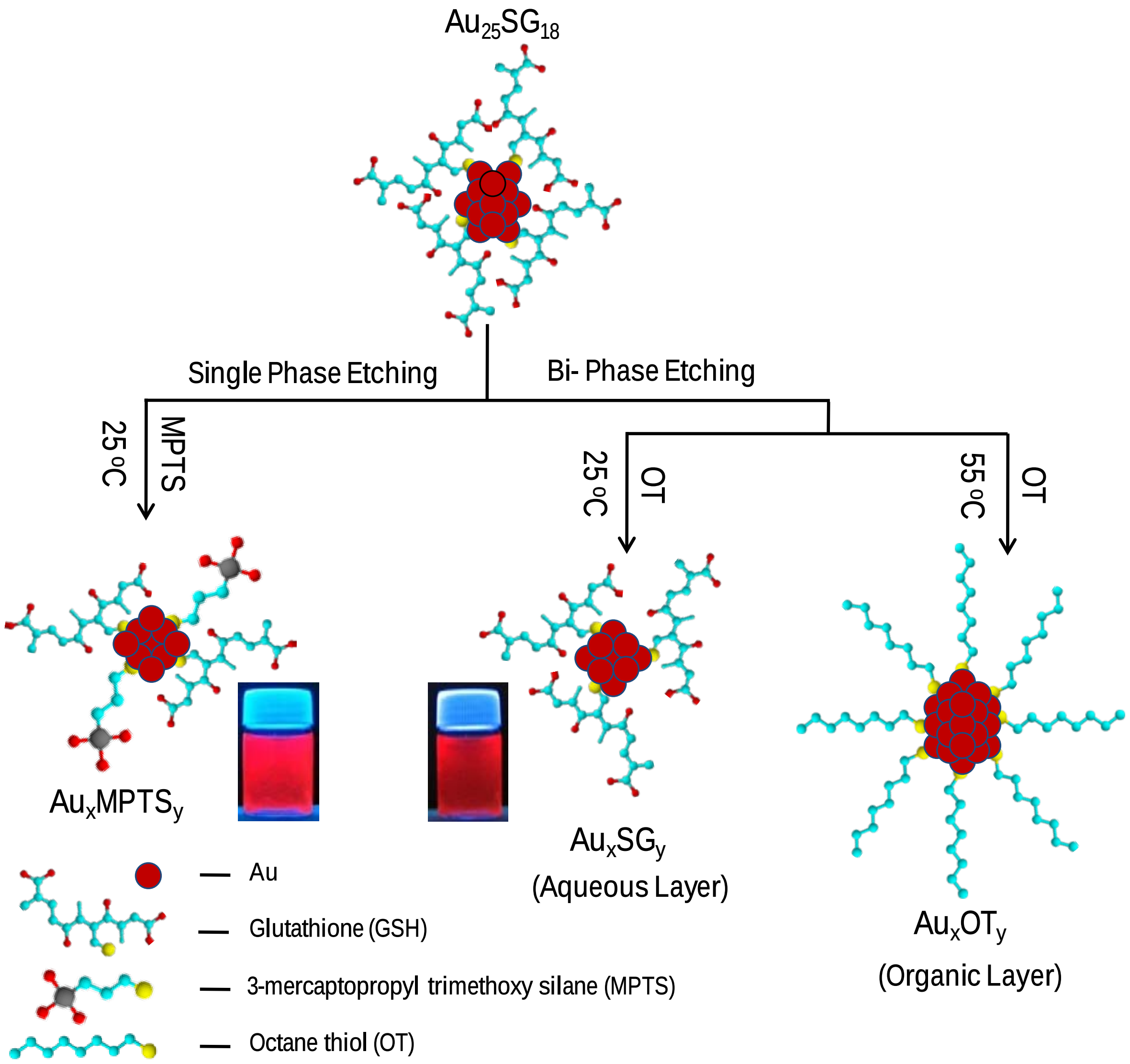

Scheme 1. Formation of the three sub-nanoclusters from $Au_{25}SG_{18}$ by core etching by two routes. Photographs of the cluster aqueous solutions under UV light are also given.

Habeeb Muhammed *et al. Chem. Euro. J.* **2009**, *15*, 10110.

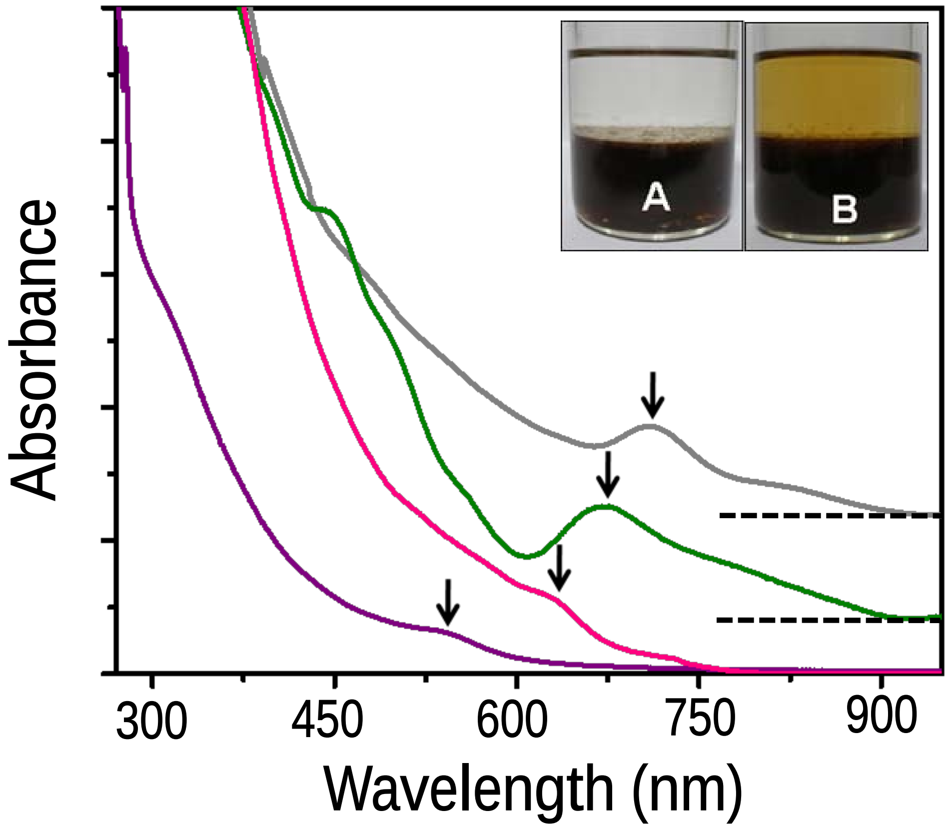

Comparison of the optical absorption features of $Au_{25}SG_{18}$ (green trace) with Au_xOT_y (grey trace), Au_xSG_y (pink trace) and Au_xMPTS_y (purple trace). The arrows show the absorption peaks of the clusters due to intra band transitions. The spectra are shifted vertically for clarity. Dotted lines indicate the threshold of absorption. Inset shows the photographs (under white light) of the water-toluene bi-phasic mixture before (A) and after (B) reaction at 55 ºC (interfacial etching) for 1 h.

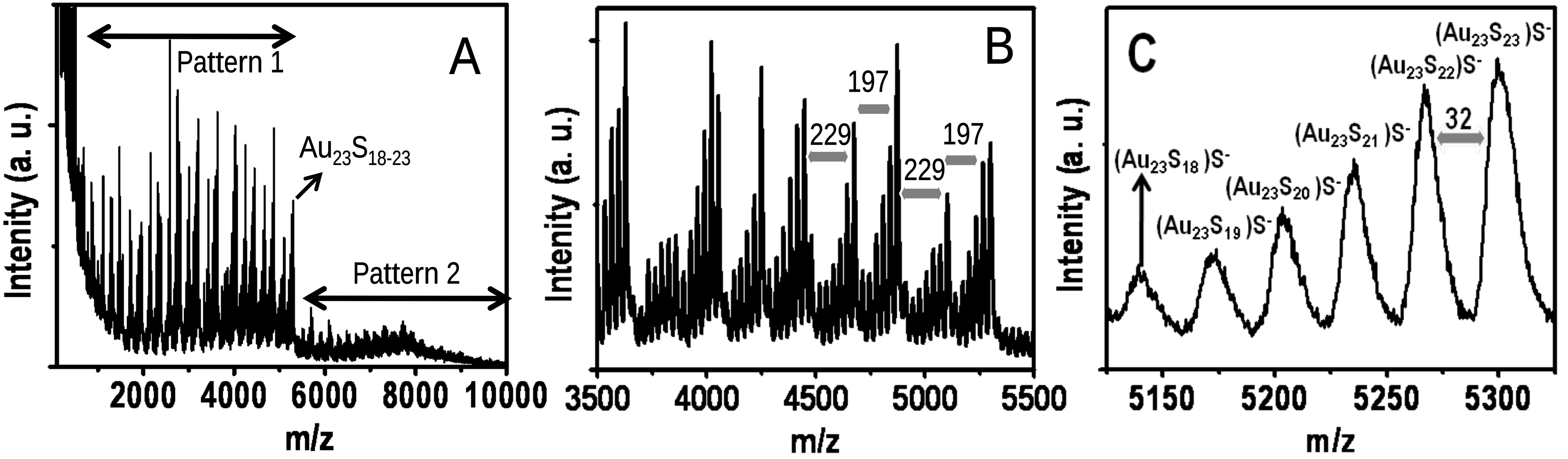

Figure 2. A) MALDI-MS of Au_xSG_y which shows bunch of peaks due to Au_mS_n clusters. B) A group of peaks with m/z spacing of 197 or 229 between the major peaks of the adjacent group of peaks. C) Expanded view of peaks due to $Au_{23}S_{18-23}$.

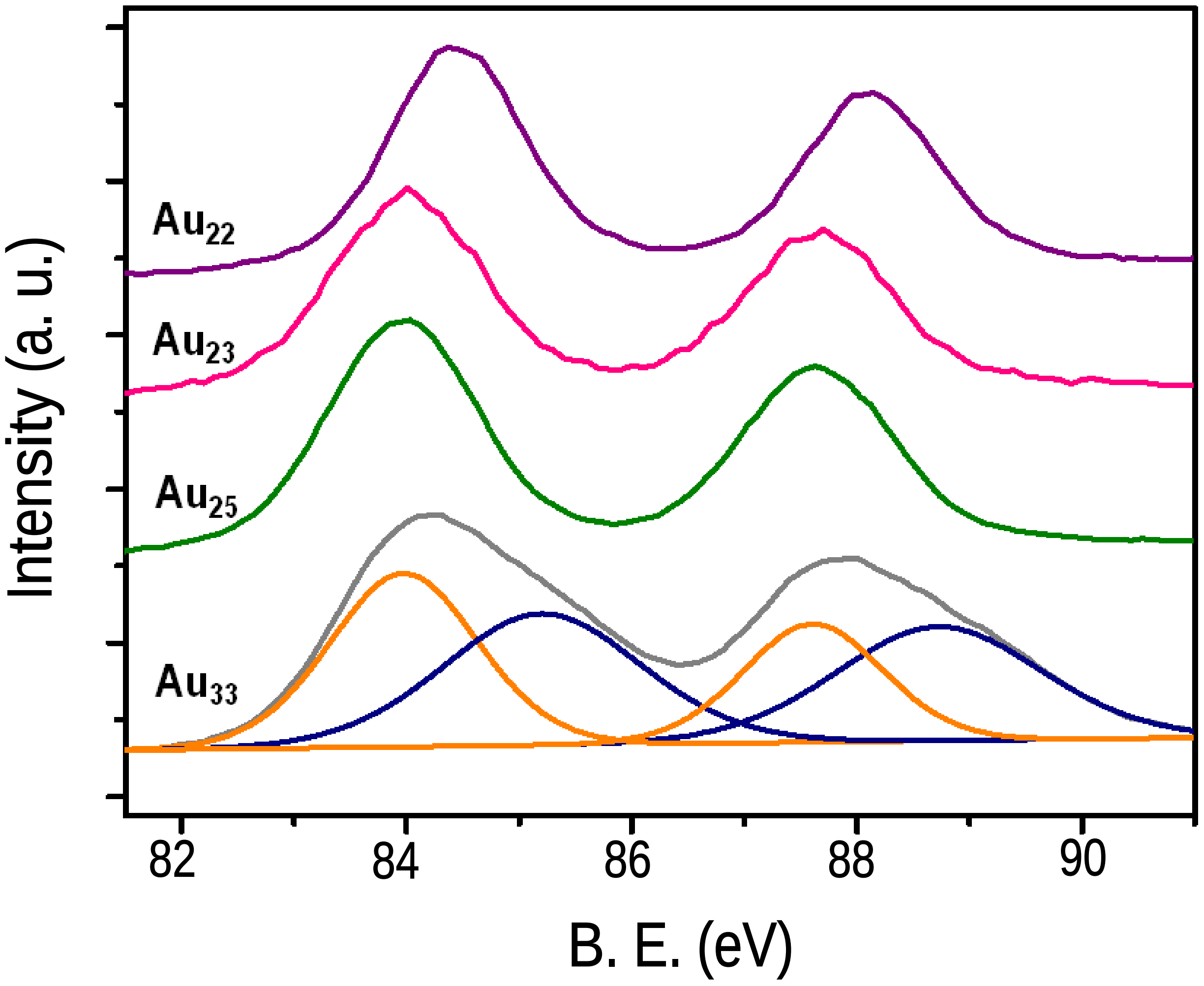

Comparison of the Au(4f) XPS spectra of Au_{22}, Au_{23} and Au_{33} along with parent Au_{25}.

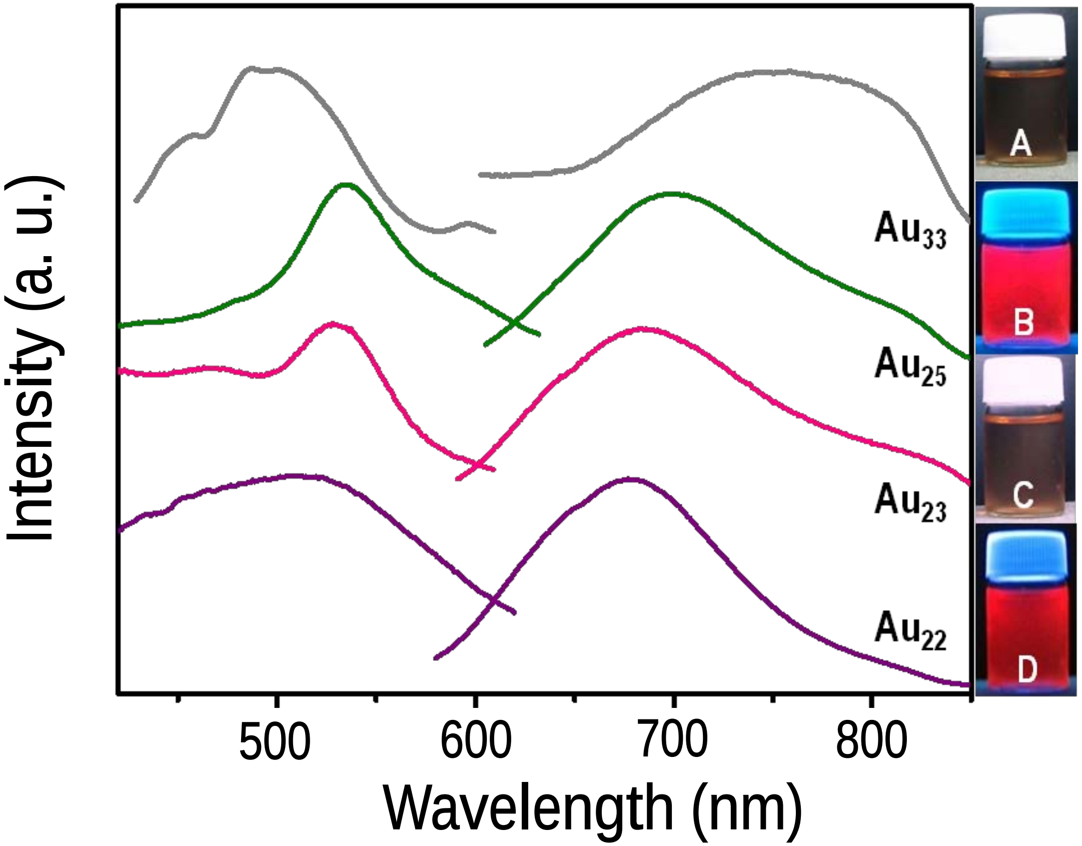

Comparison of the photoluminescence profiles of Au_{22}, Au_{23} and Au_{33} along with parent Au_{25}. Photographs of the aqueous solutions of Au_{22} and Au_{23} under white light (A and C, respectively) and UV light (B and D, respectively) are also given.

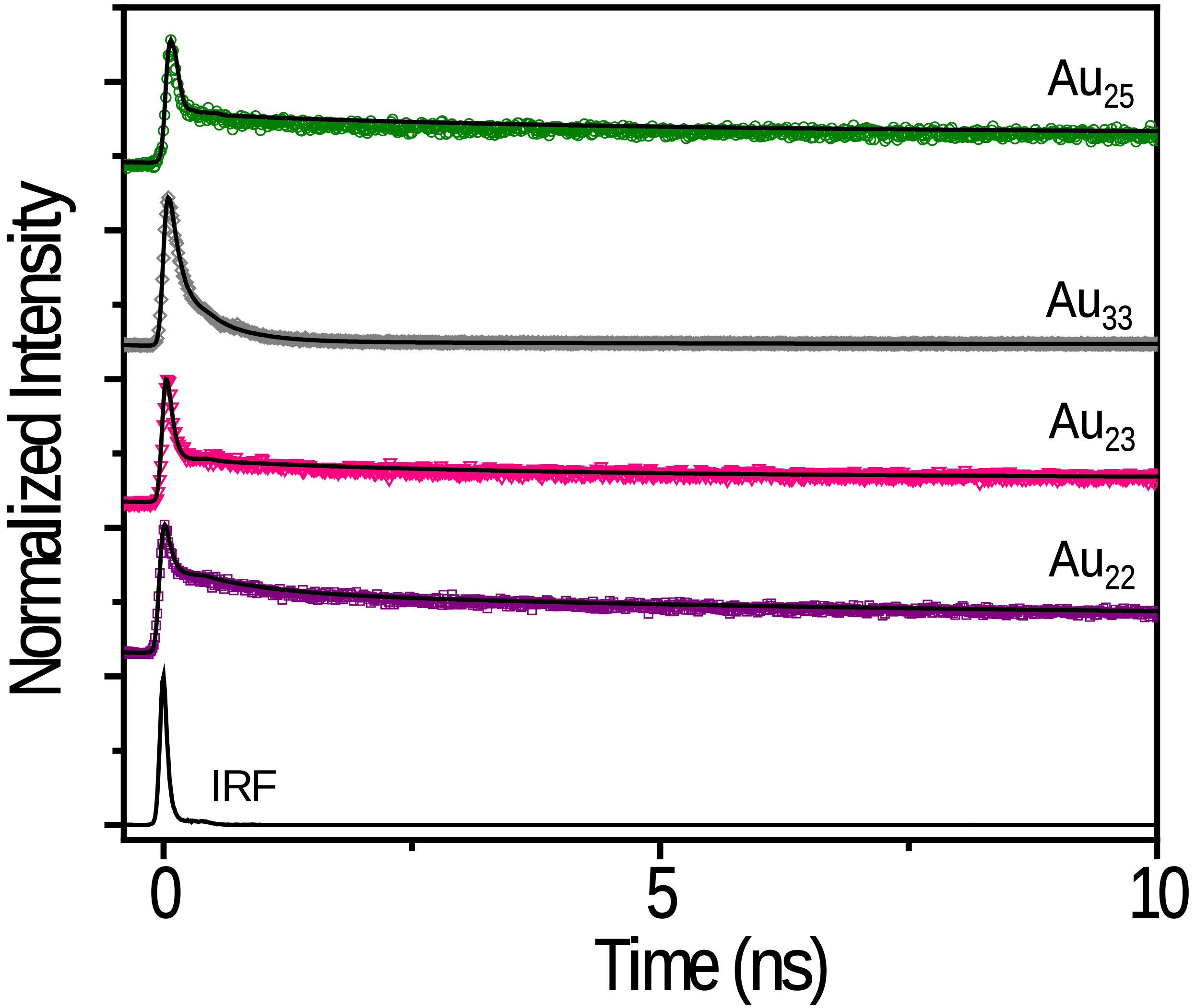

Fluorescence decay pattern of Au_{25}, Au_{33}, Au_{23}, and Au_{22} collected at 630 nm.

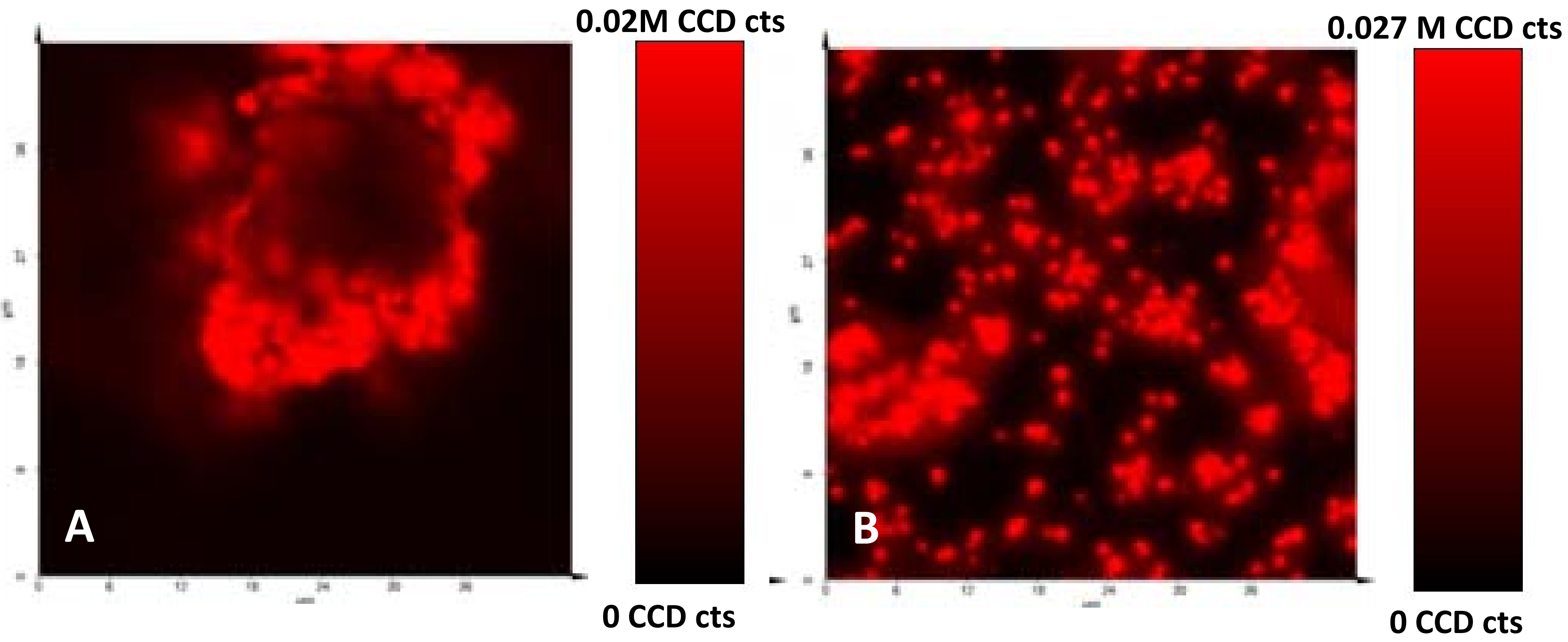

Inherent fluorescence image of Au$_{22}$ (A) and Au$_{23}$ (B) collected by the spectroscopic mapping at an excitation wavelength of 532 nm. Regions coded red represents the pixels where the signal (used for mapping) is a maximum, the minima being represented with black colors. The scan area was 40 µM x 40 µM.

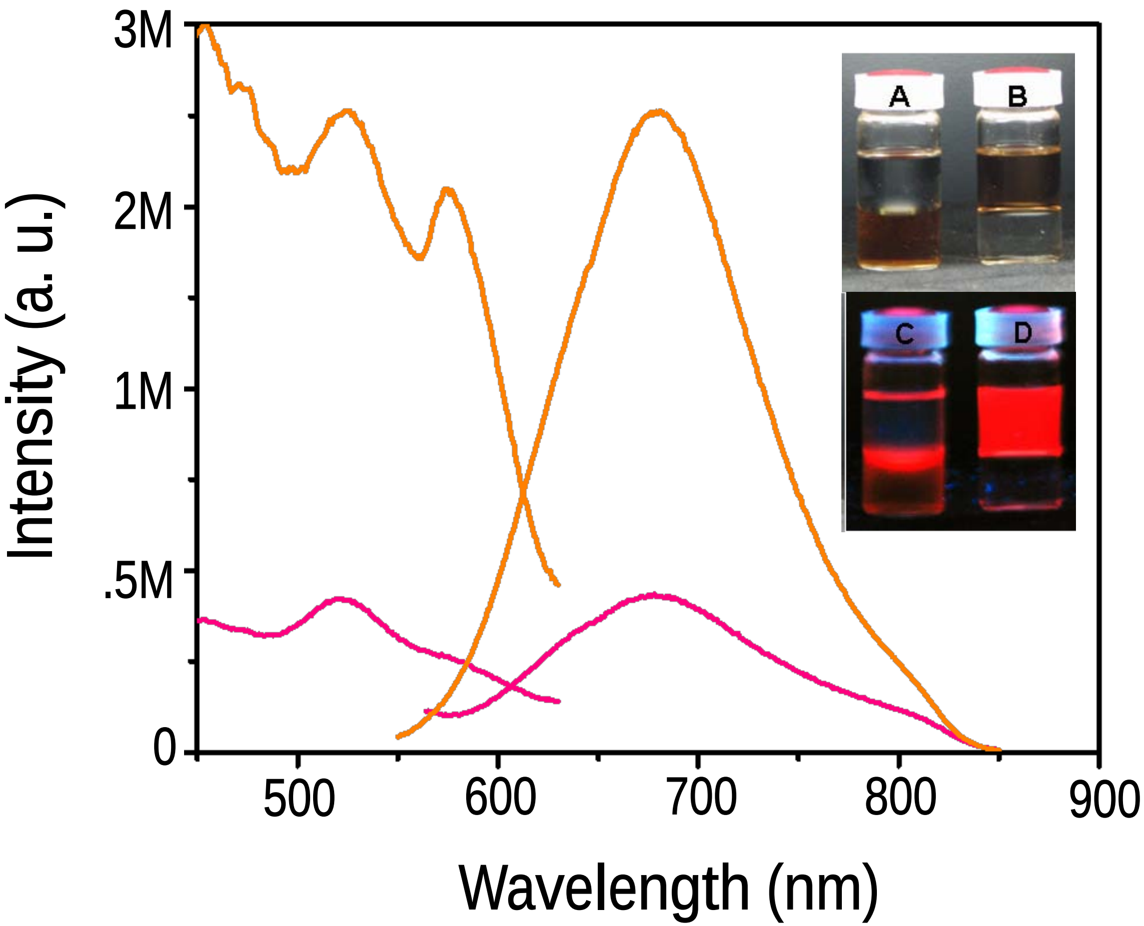

Photoluminescene profile of Au_{23} cluster before (pink trace) and after (orange trace) phase transfer. Emission of the cluster enhances considerably after the phase transfer. Photographs of the aqueous-toluene mixture containing the cluster before and after phase transfer under white light (A and B, respectively) and UV light (C and D, respectively). In C, only the interface is illuminated as the UV is attenuated as the sample was irradiated from the top

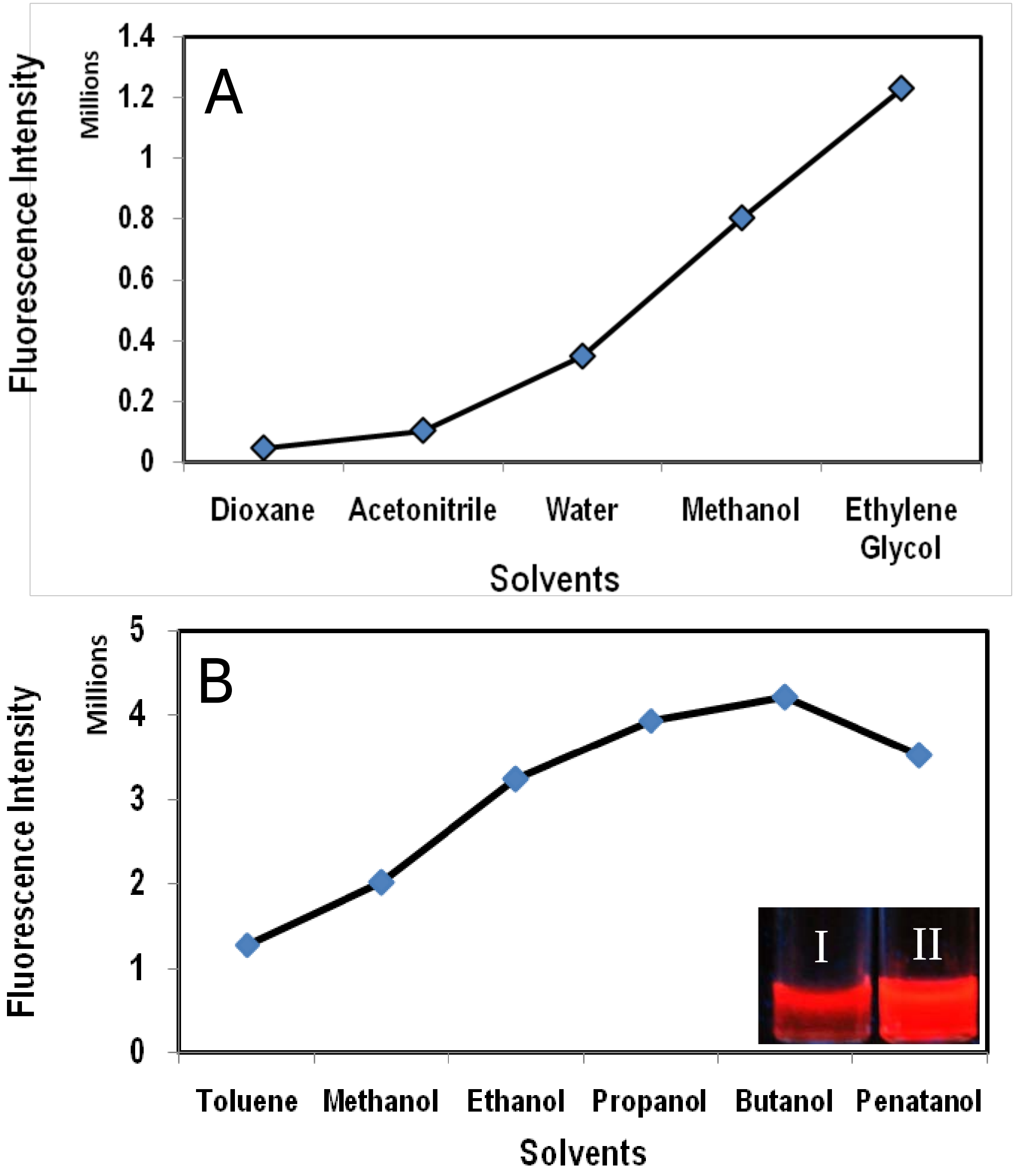

A) Solvent dependent fluorescence of 50 μM Au$_{23}$ in ethylene glycol, methanol, water, acetonitrile and dioxane before phase transfer. B) Solvent dependent fluorescence of Au$_{23}$ in methanol, ethanol, propanol, butanol and pentanol after phase transfer. Inset of B shows the photograph of phase transferred Au$_{23}$ in toluene (I) and butanol (II) under UV light irradiation

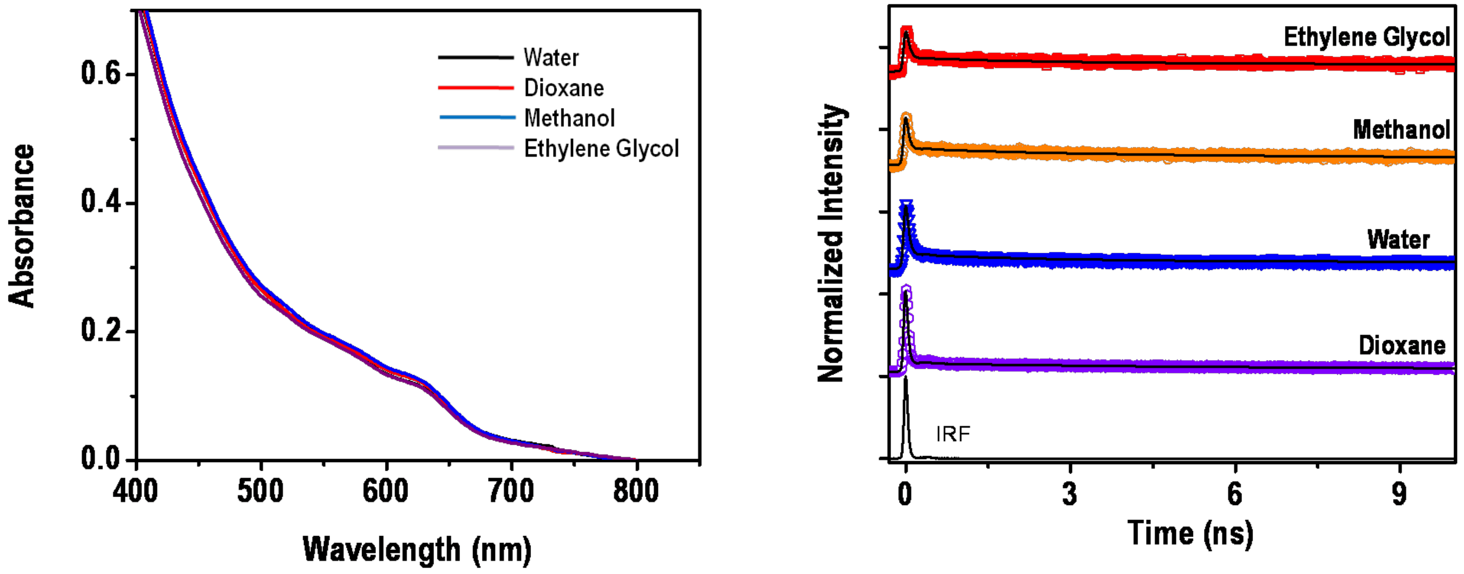

Solvent	τ_1(ps)	%	τ_2 (ns)	%	τ_3 (ns)	%
Ethylene Glycol	47	86.5	2.67	5.5	70.06	7.9
Methanol	36	87.6	3.27	5.8	62.91	6.6
Water	39	92.4	2.41	3.6	68.55	3.9
Dioxane	16	98.0	5.07	1.1	31.63	0.9

A) Optical absorption spectra of Au_{23} in dioxane, water, methanol and ethylene glycol. B) Fluorescence decay of Au collected at 630 nm in various solvents. Table tabulates the life time of the cluster in various solvents.

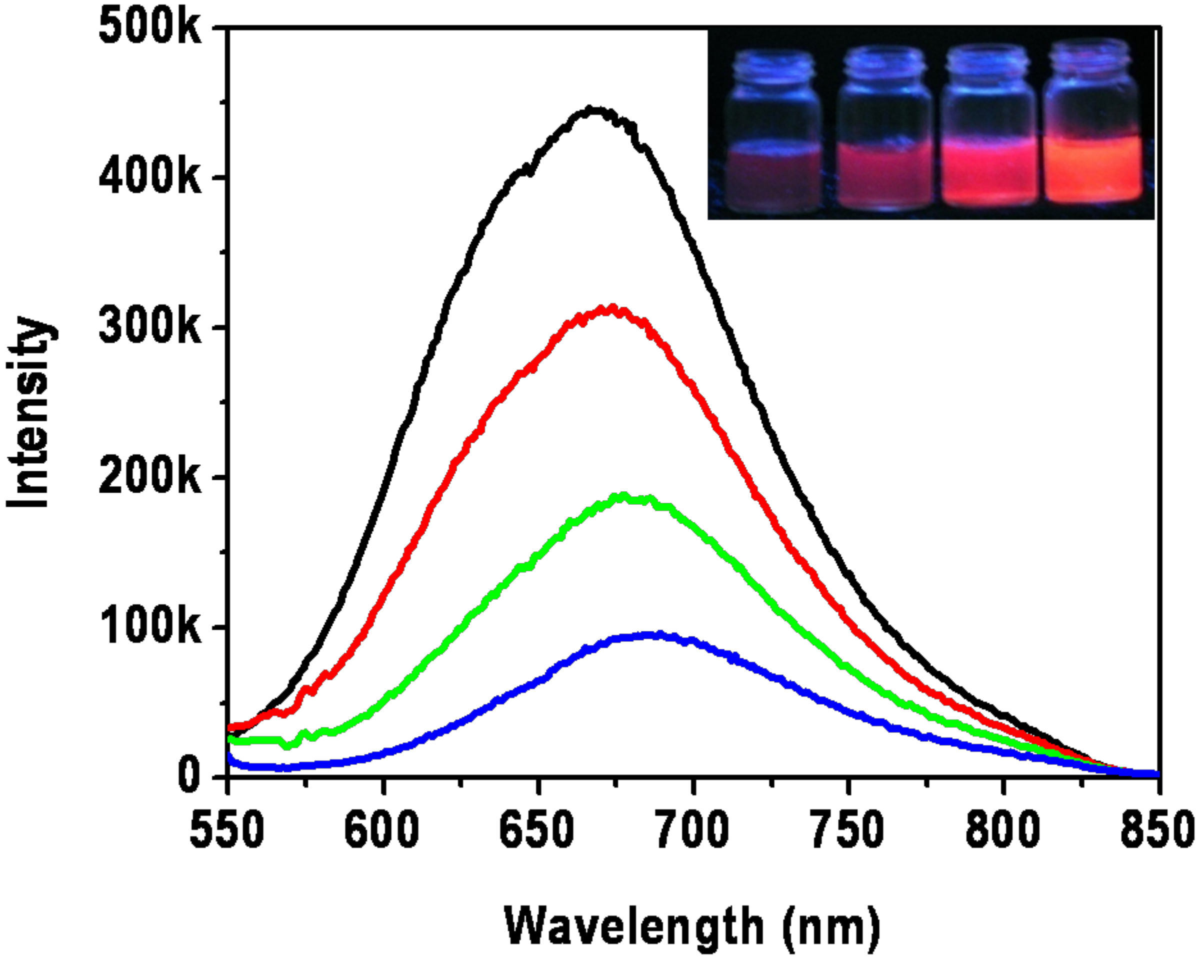

Plot of fluorescence intensity of Au_{23} cluster in water-DMSO mixture starting from pure water (blue line) to 1:1 (green line), 1:2 (red line) and 1:3 (black trace) water-DMSO mixtures. Inset shows the photographs of the corresponding solutions under UV light irradiation

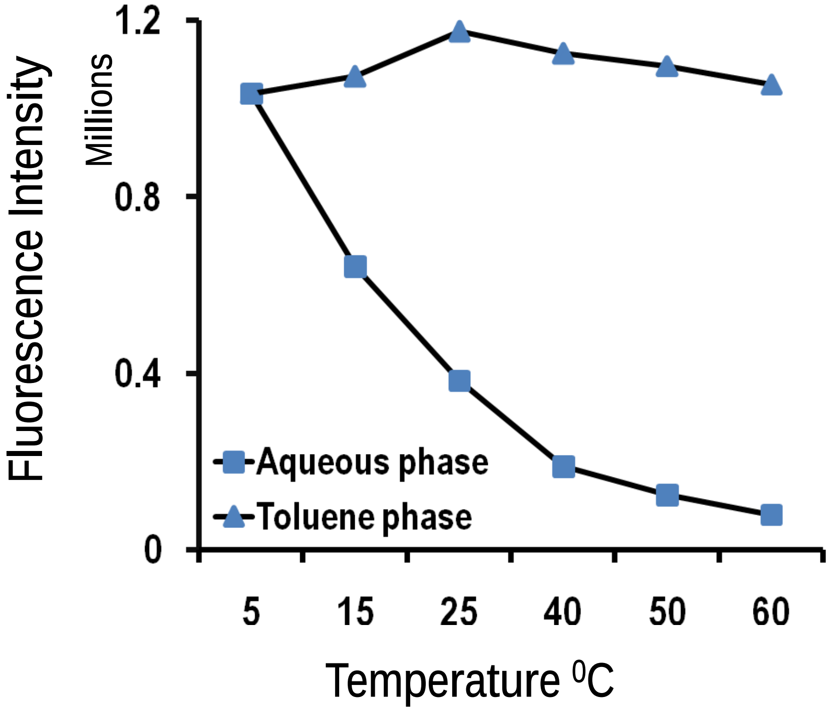

Plot of temperature *vs* fluorescence intensity of the cluster in the aqueous and toluene layers. While the intensity of emission of aqueous solution of Au_{23} decreases with increase in temperature, the emission intensity remains unaltered for phase transferred Au_{23}.

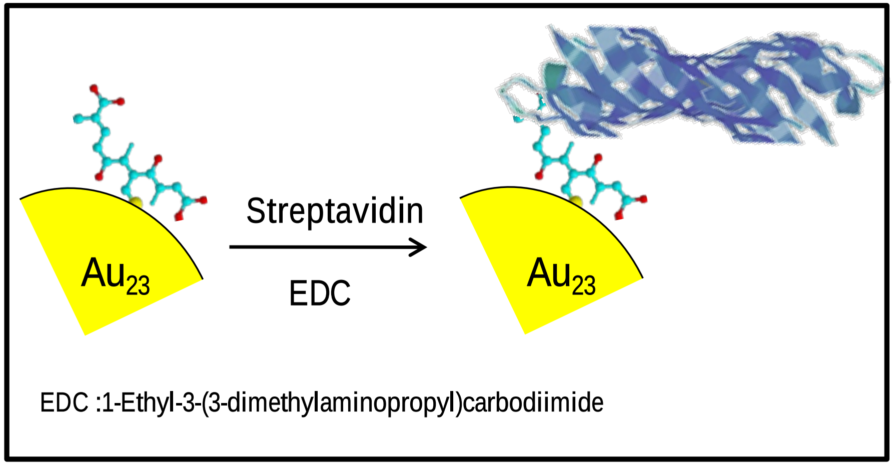

Schematic representation of the conjugation of streptavidin on Au$_{23}$SG$_{18}$ by EDC coupling.

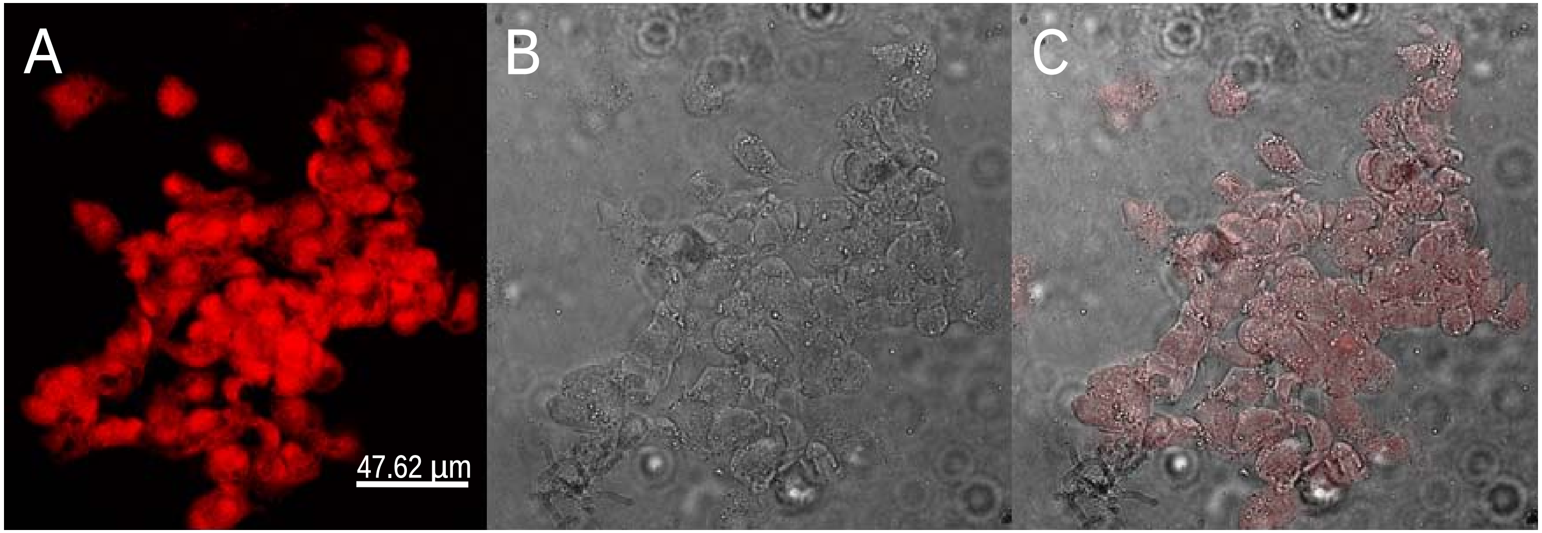

Fluorescence (A), bright field (B) and overlay of fluorescent and bright field images (C) of human hepatoma (HepG2) cells stained with streptavidin conjugated Au$_{23}$.

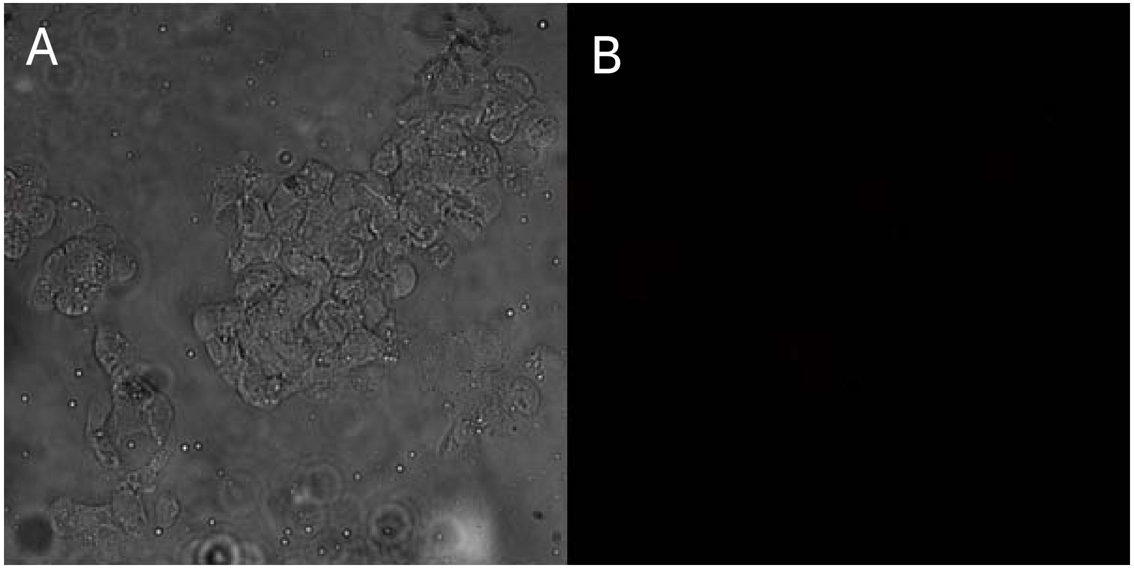

Bright field (A) and fluorescence (B) images of HepG2 cells stained with unconjugated Au_{23} clusters. No fluorescence was observed from the cells after washing

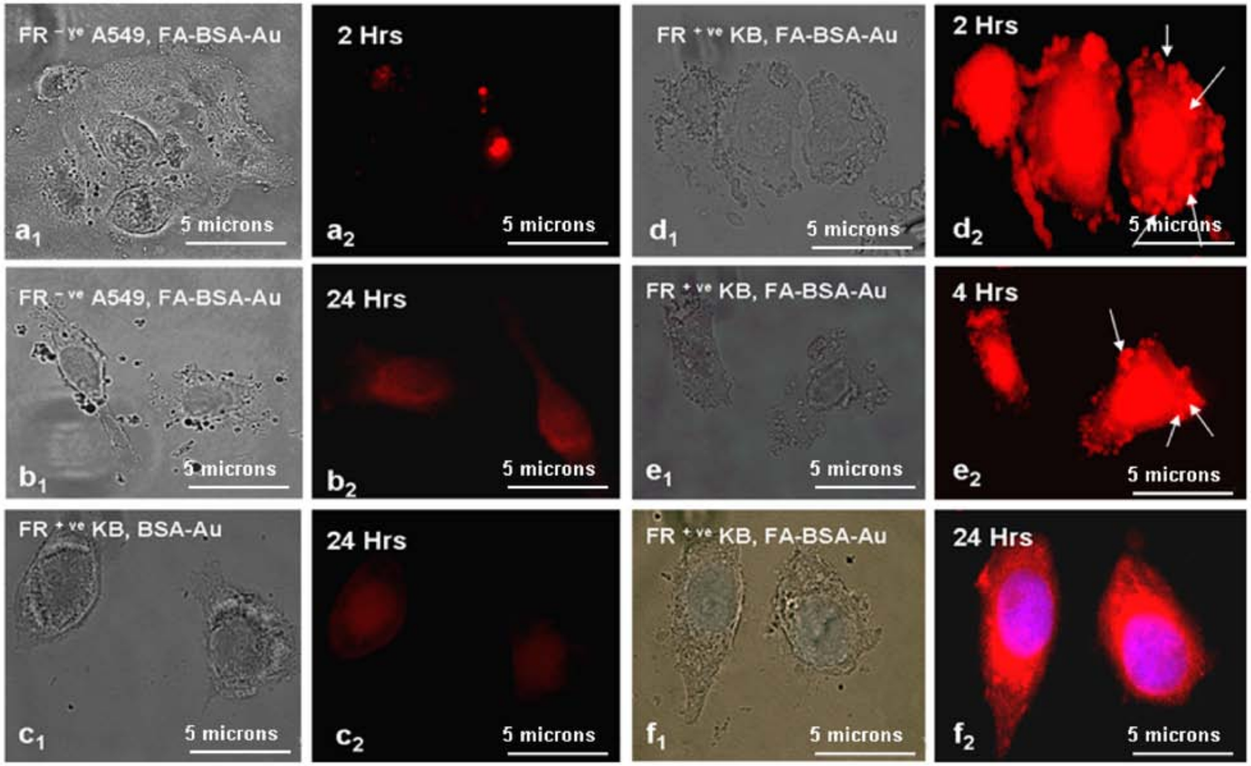

Fluorescent microscopic images showing interaction of Au-BSA-FA NCs with different types of cell lines: a1-a2) FR-ve lung carcinoma A549 after 2 hours of incubation, b1-b2) FR-ve lung carcinoma A549 after 24 hours of incubation, c1-c2) FR+ve KB cells with unconjugated Au clusters, d1-d2) FR+ve KB cells with FA conjugated Au clusters at 2 hrs, e1-e2) 4 hrs and f1-f 2) 24 hrs of incubation [Archana R, Sonali S, Deepthy M et al (2009) Molecular Receptor Specific, Non-toxic, Near-infrared Emitting Au Cluster-Protein Nanoconjugates for Targeted Cancer Imaging. Nanotechnology (in press)]

.

Clusters for metal ion detection

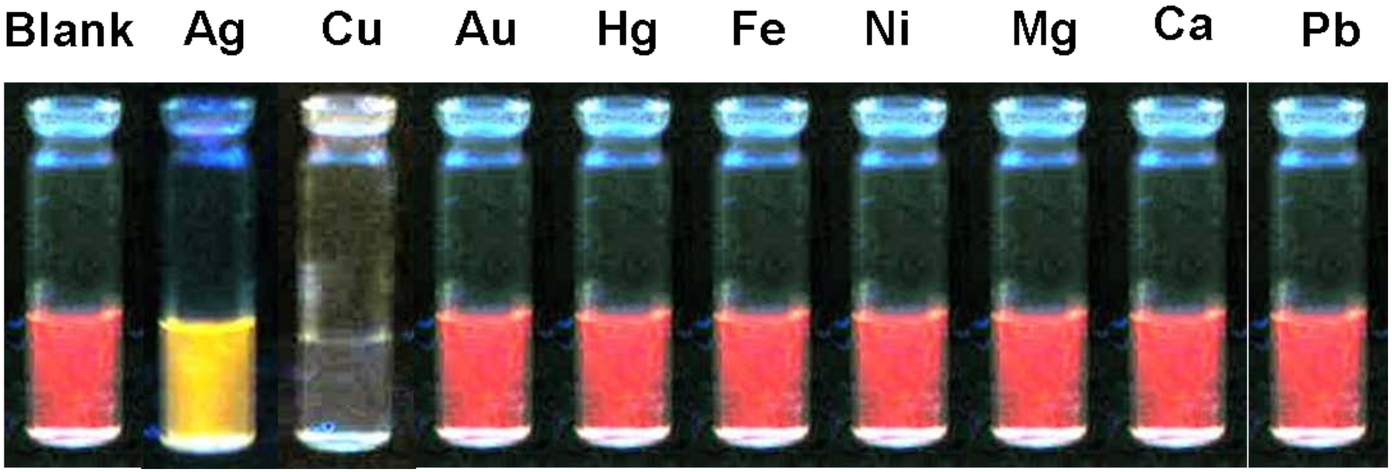

Water soluble red emitting clusters where treated with various metal ions with a final Concentration of 25 ppm. The emission was shifted to lower wavelength in case of silver ions and quenched completely in case of copper ions. The emission was an altered in case of other ions.

Habeeb Muhammed *et al. Chem. Euro. J.* **2009**, *15,* 10110.

FRET between Au_{25} and Dansyl Chromophore

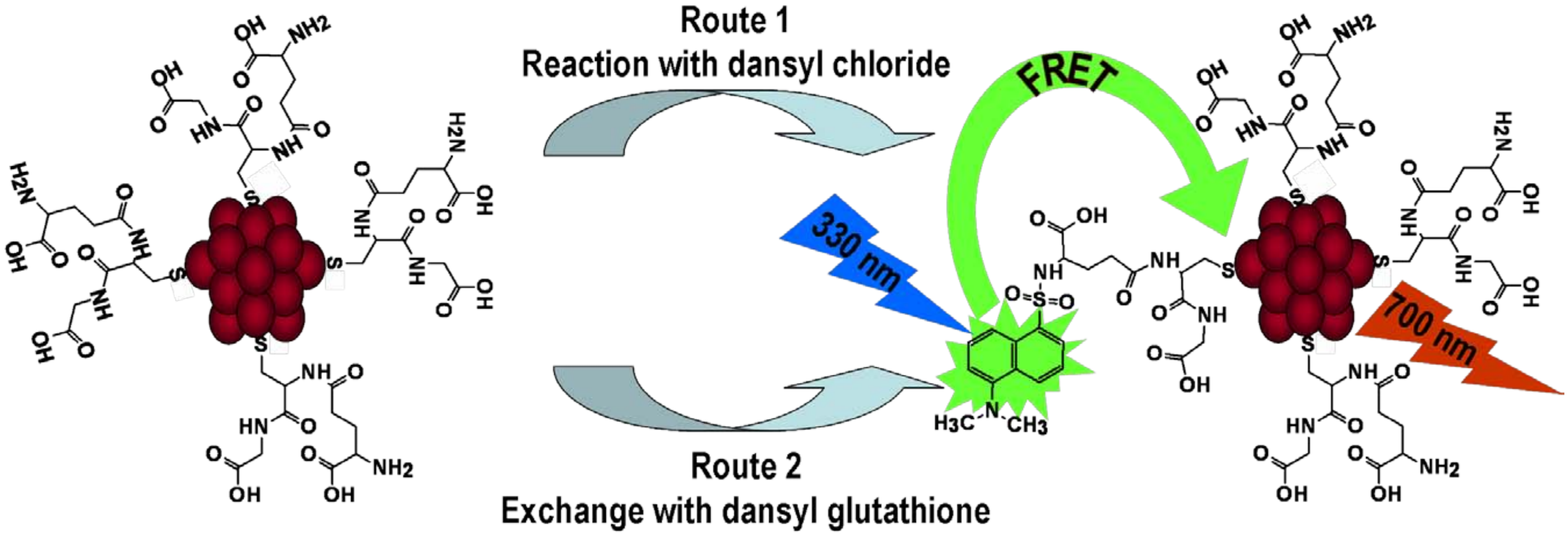

Approaches Used for the Functionalization of Dansyl Chromophore on the Au_{25} Cluster.

Habeeb Muhammmed *et al. J. Phys. Chem. C* **2008**, *112*, 14324.

Cluster based patterns

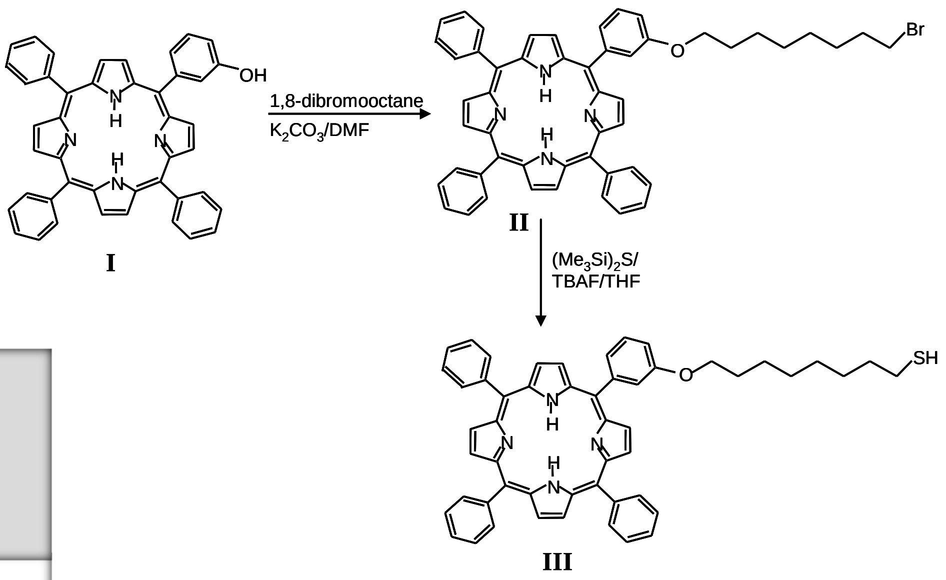

I

II

III

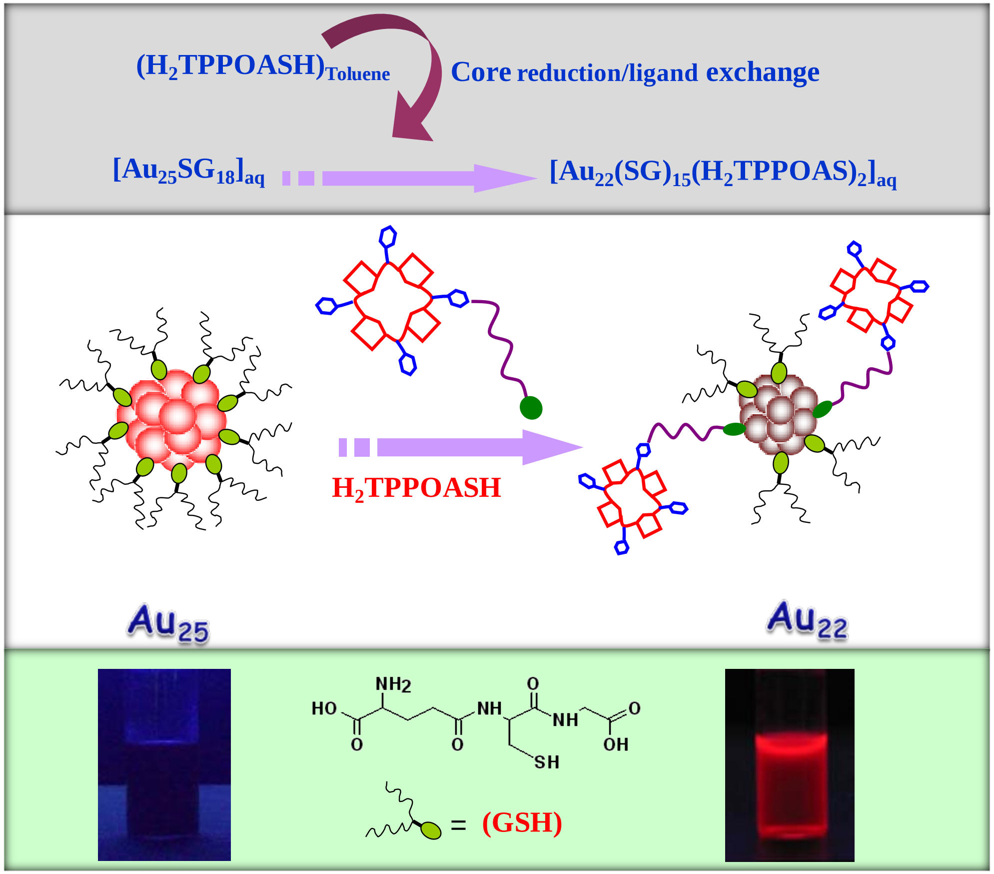

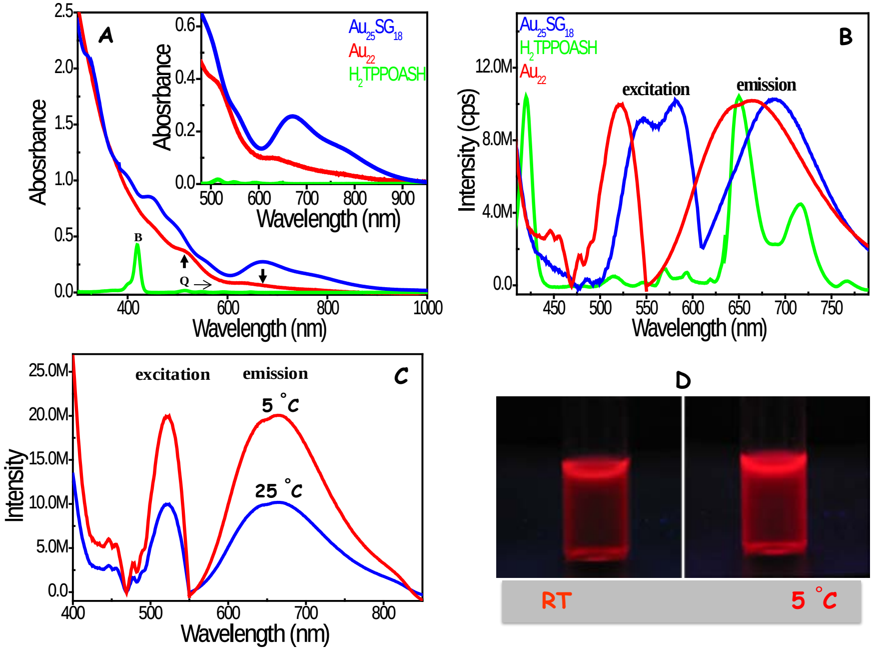

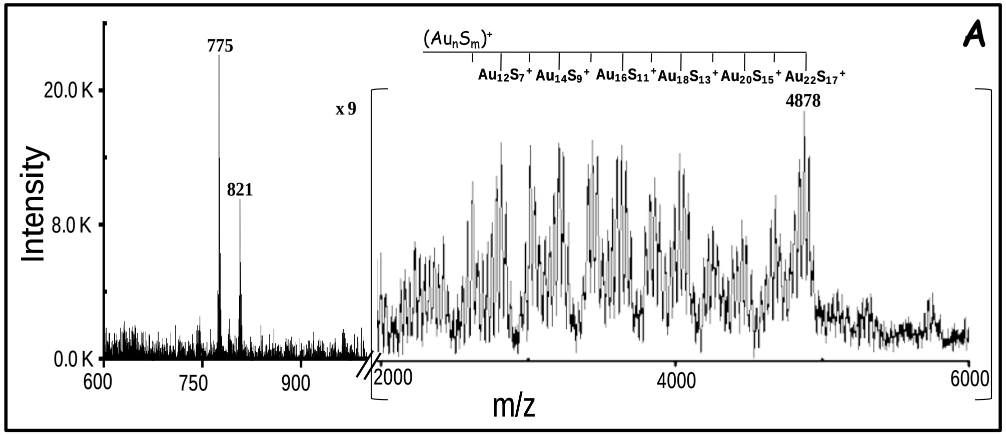

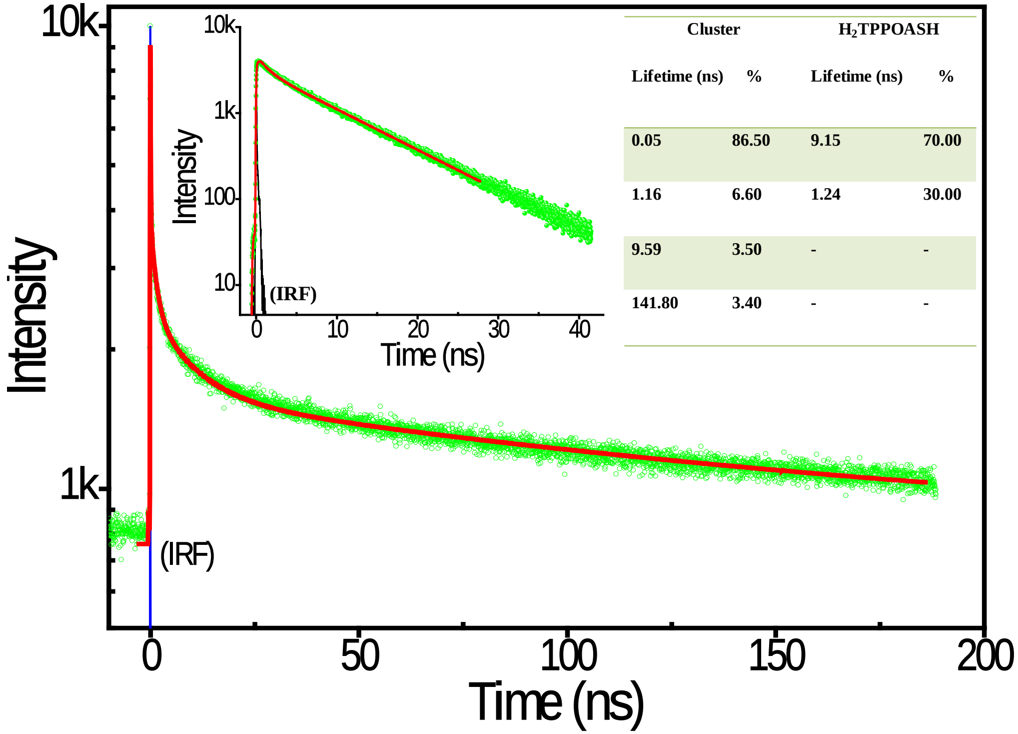

Cluster		H$_2$TPPOASH	
Lifetime (ns)	**%**	**Lifetime (ns)**	**%**
0.05	86.50	9.15	70.00
1.16	6.60	1.24	30.00
9.59	3.50	-	-
141.80	3.40	-	-

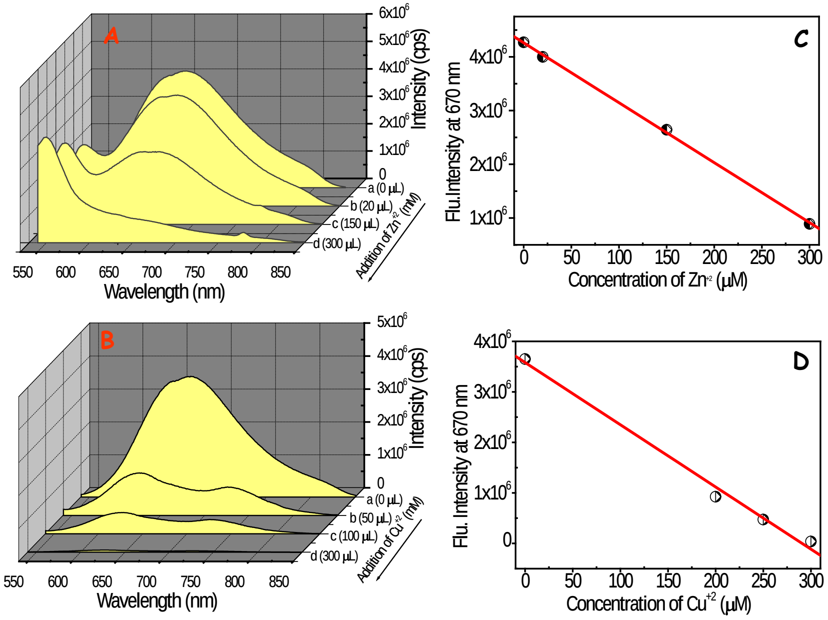

With G. U. Kulkarni

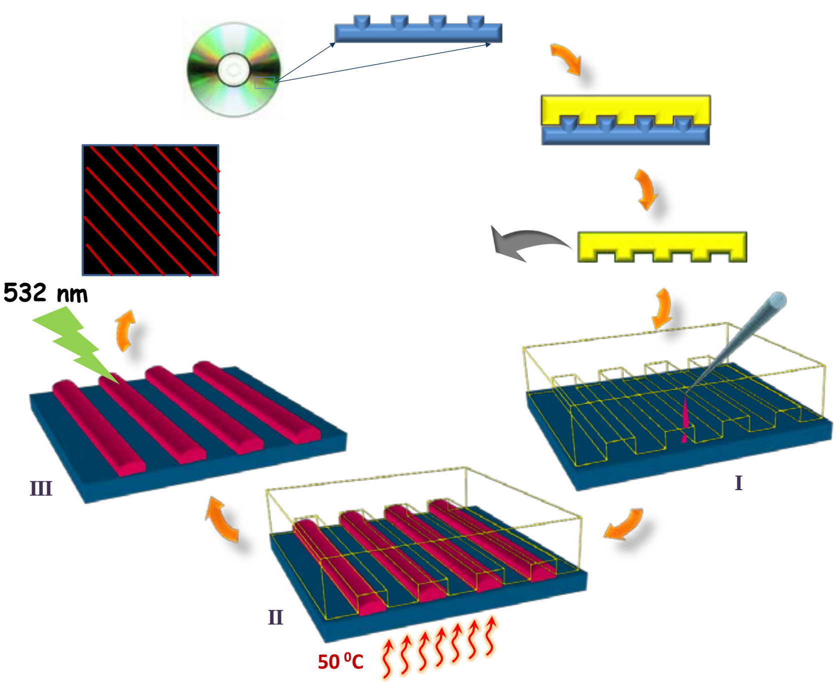

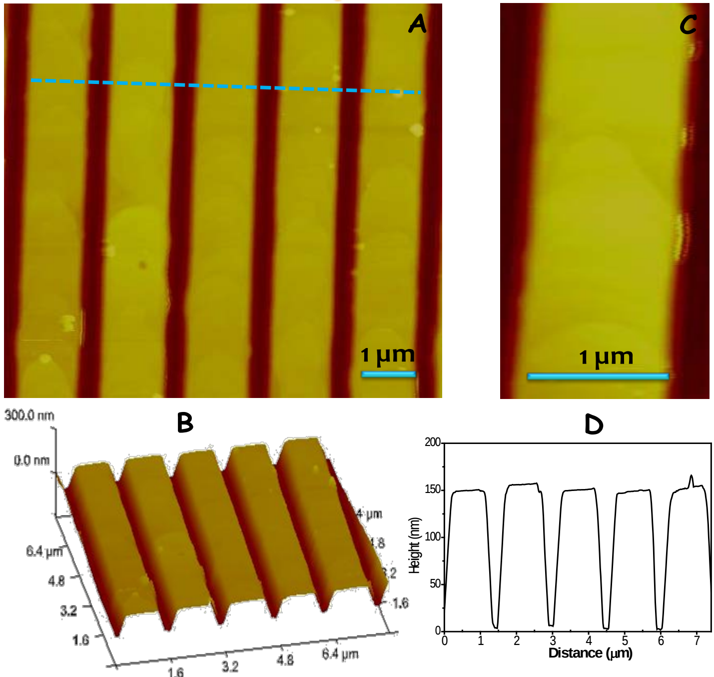

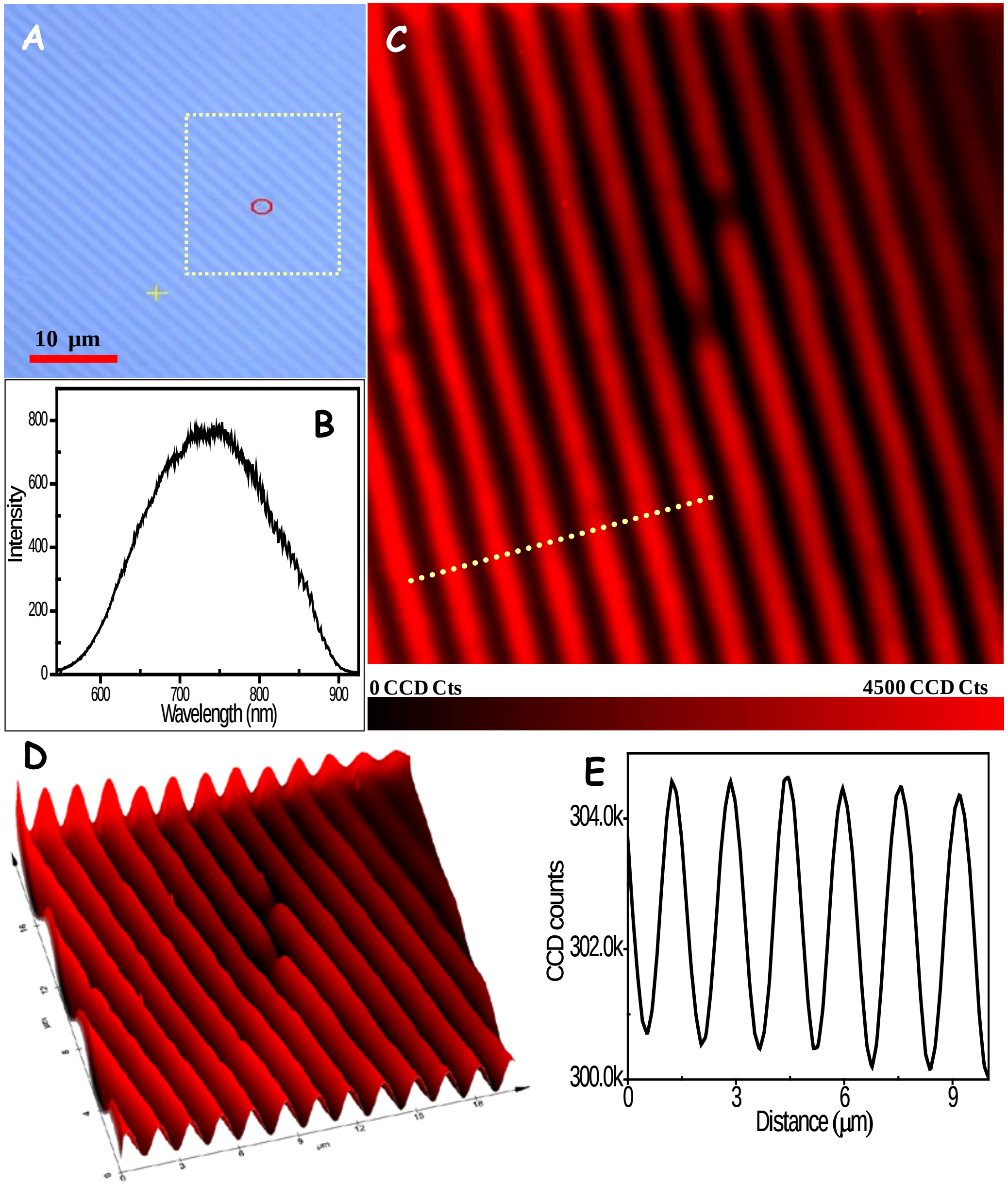

E. S. Shibu *et al.* *ACS Appl. Mater.* **2009**, *1*, 2199.

Au@SG – glutathione (GSH) protected gold nanoparticle

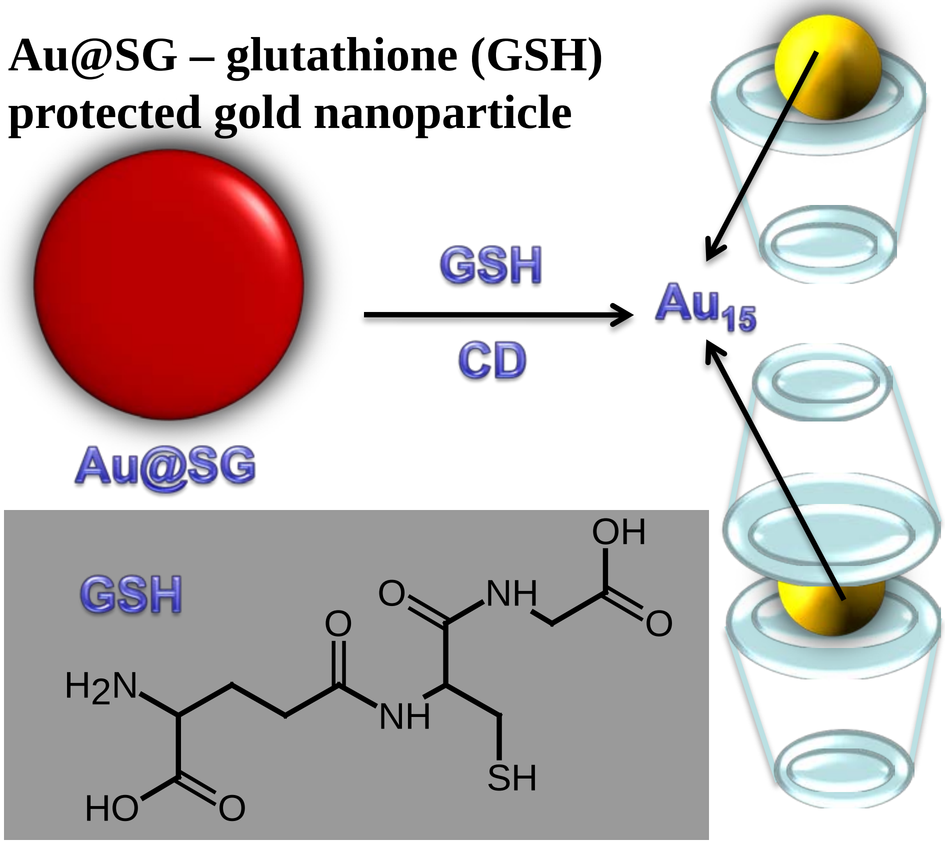

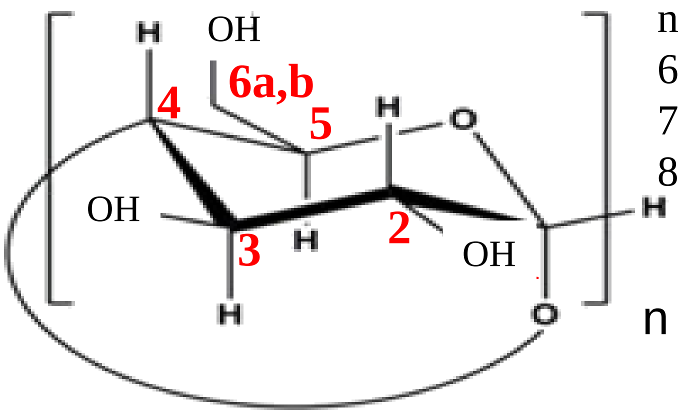

n= 6, 7, 8
6---alpha CD
7---beta CD
8---gamma CD

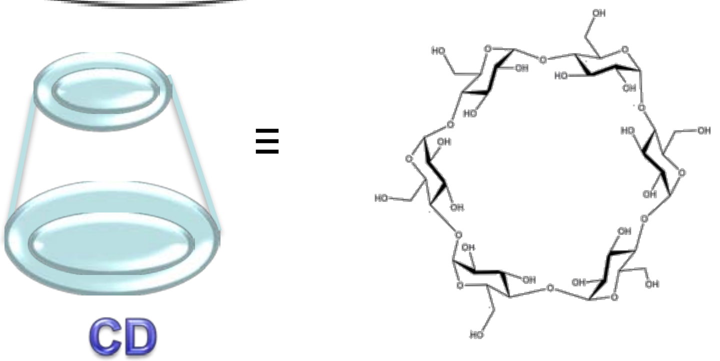

Basic unit of CD is 6 membered glucose

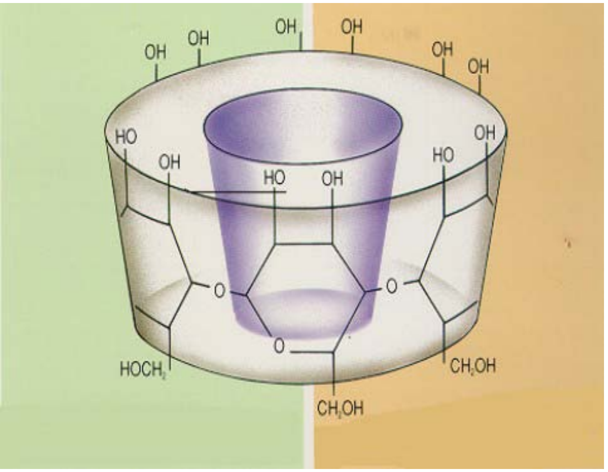

3D image of CD showing the nanometer cavity

Scheme: Au_{15} was synthesized inside the cyclodextrin (CD) cavity (*in situ*). Note: CD and GSH are the abbreviations of cyclodextrin and glutathione, respectively. For our synthesis we have used all 3 CDs (alpha, beta and gamma)

E. S. Shibu and T. Pradeep. Unpublished

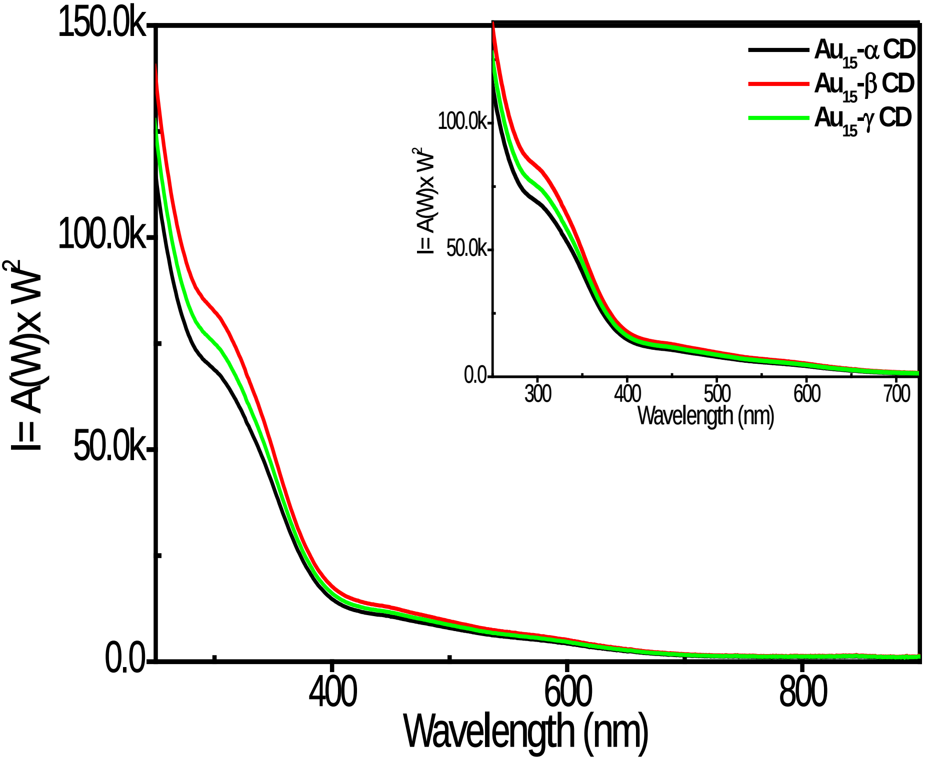

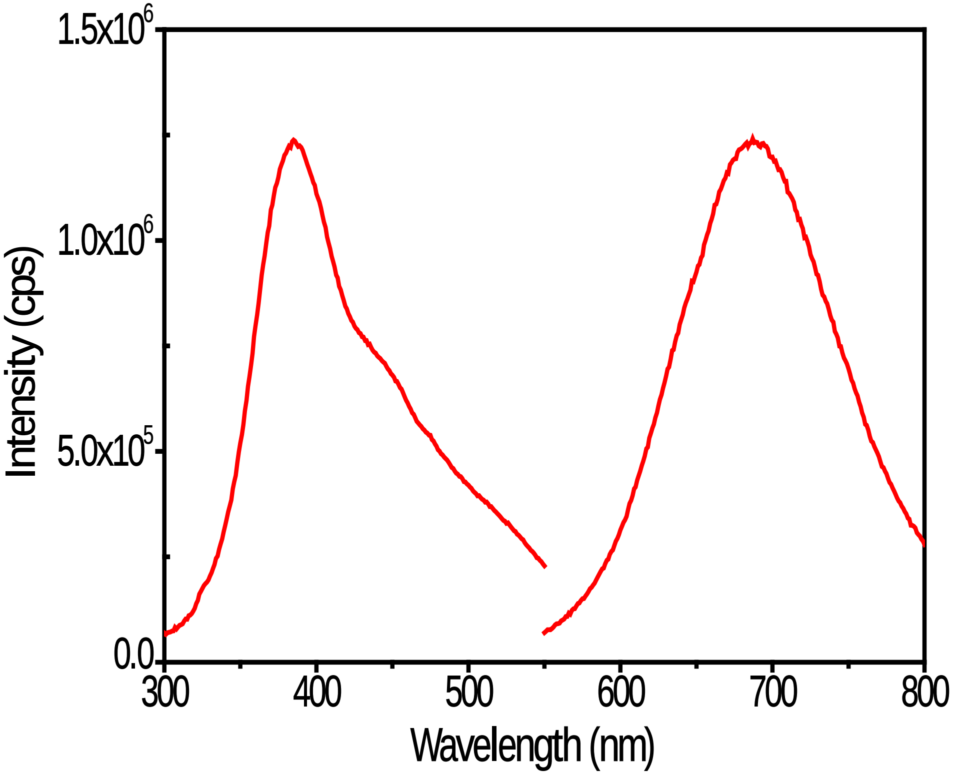

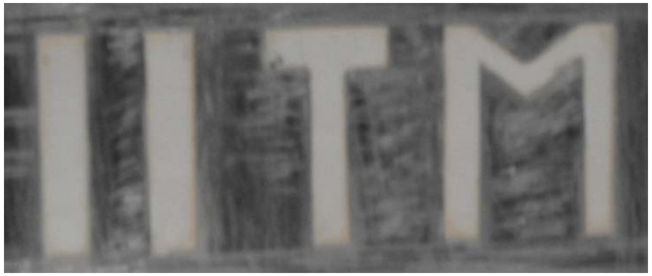

E. S. Shibu and T. Pradeep. Unpublished

Glass coating and fluorescence

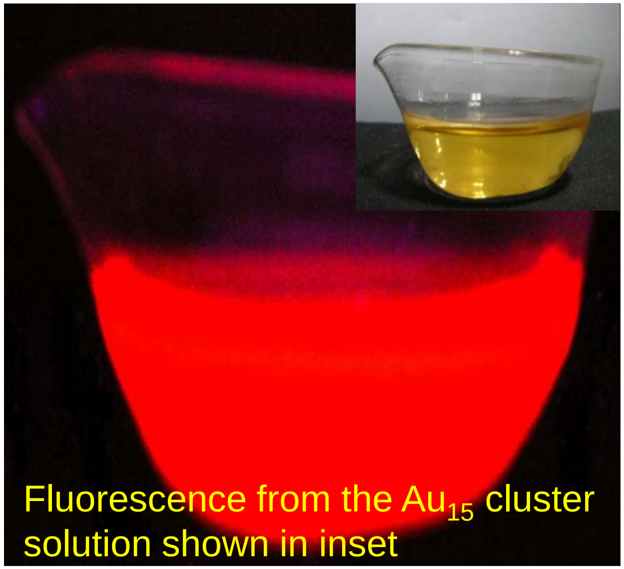

Fluorescence from the Au_{15} cluster solution shown in inset

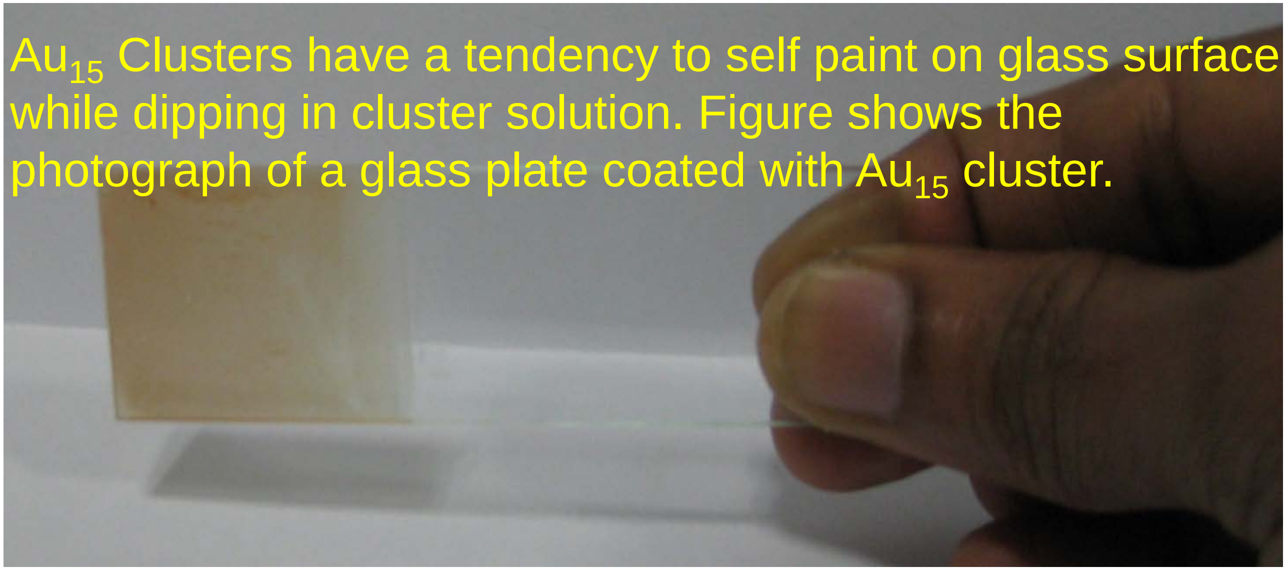

Au_{15} Clusters have a tendency to self paint on glass surface while dipping in cluster solution. Figure shows the photograph of a glass plate coated with Au_{15} cluster.

The red fluorescence coming from glass after decanting the cluster solution

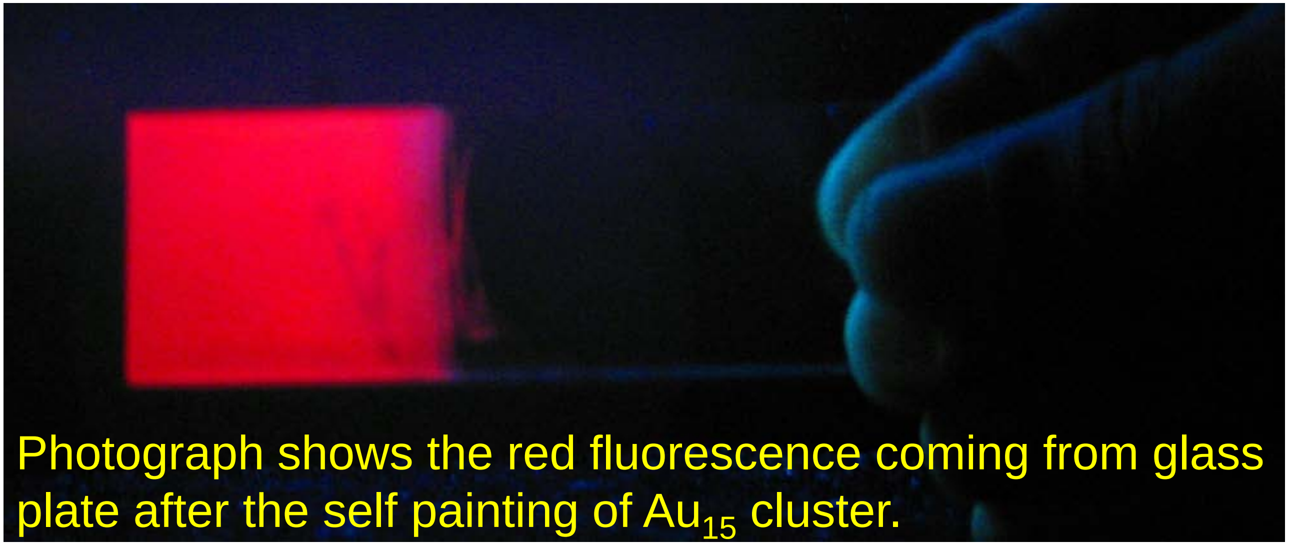

Photograph shows the red fluorescence coming from glass plate after the self painting of Au_{15} cluster.

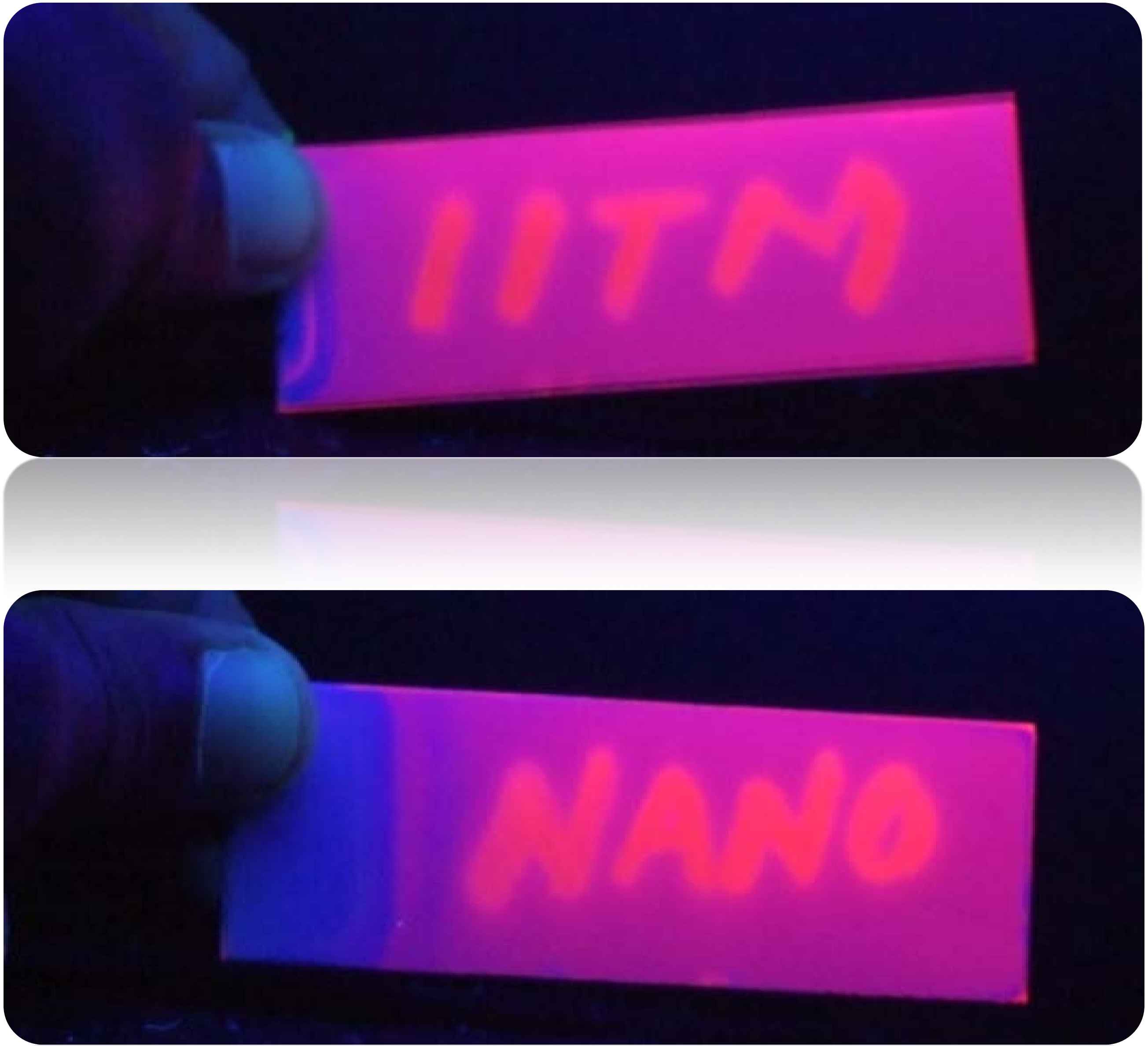

E. S. Shibu and T. Pradeep. Unpublished

Magnetism in Au_{15} cluster

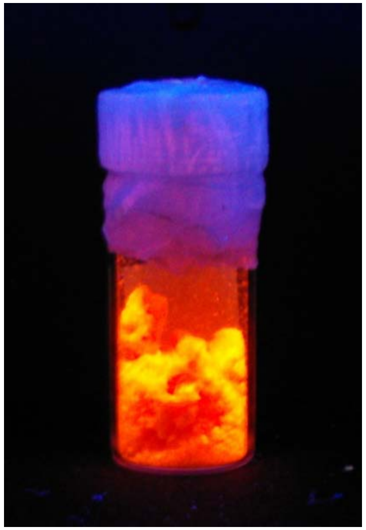

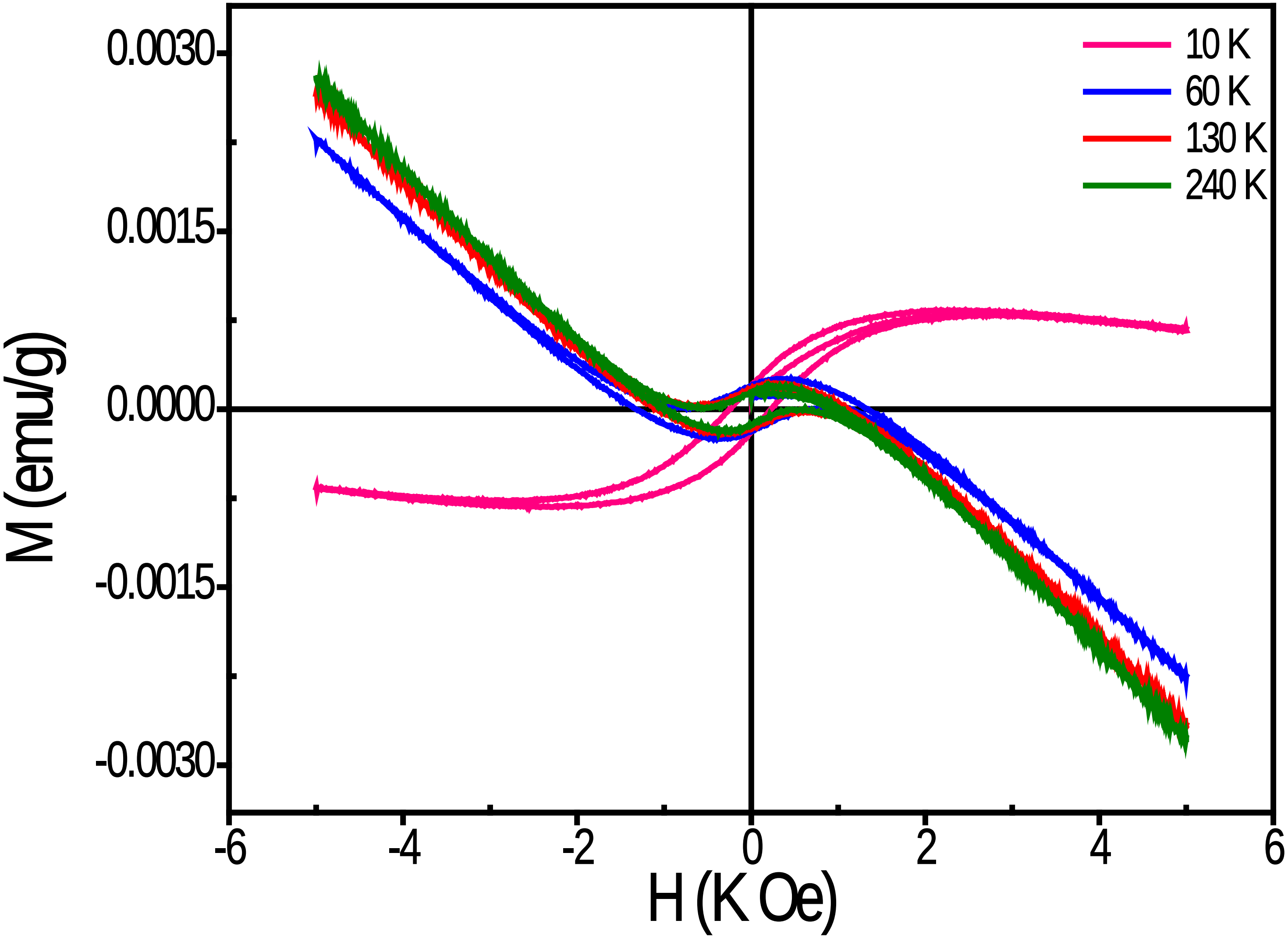

E. S. Shibu and T. Pradeep. Unpublished

Size selected metal clusters

- The Optical Absorption Spectra of Small Silver Clusters (5-11) Embedded in Argon Matrices. Harbich, W.; Fedrigo, S.; Buttet, J. *Chem. Phys. Lett.* **1992,** *195,* 613

- Soft Landing and Fragmentation of Small Clusters Deposited in Noble-Gas Films. Harbich, W.; Fedrigo, S.; Buttet, J**.** *Phys. Rev. B* **1998,** *58*, 7428

- CO combustion on supported gold clusters. Arenz M, Landman U, Heiz U. *Chemphyschem* **2006,** *7*, 1871.

- Low-temperature cluster catalysis. Judai, K.; Abbet, S.; Worz, A. S.; Heiz U.; Henry, C. R. *J Am. Chem. Soc.* **2004,** *126*, 2732.

- The Reactivity of Gold and Platinum metals in their cluster phase. Heiz, U.; Sanchez,A.; Abbet, S. *Eur. Phys. J. D* **1999,** *9*,35.

- When gold is not noble: Nanoscale gold catalysts. Sanchez A, Abbet S, Heiz U *J. Phys. Chem.* A. **1999,** *103*, 9573.

Silver clusters

Interfacial etching

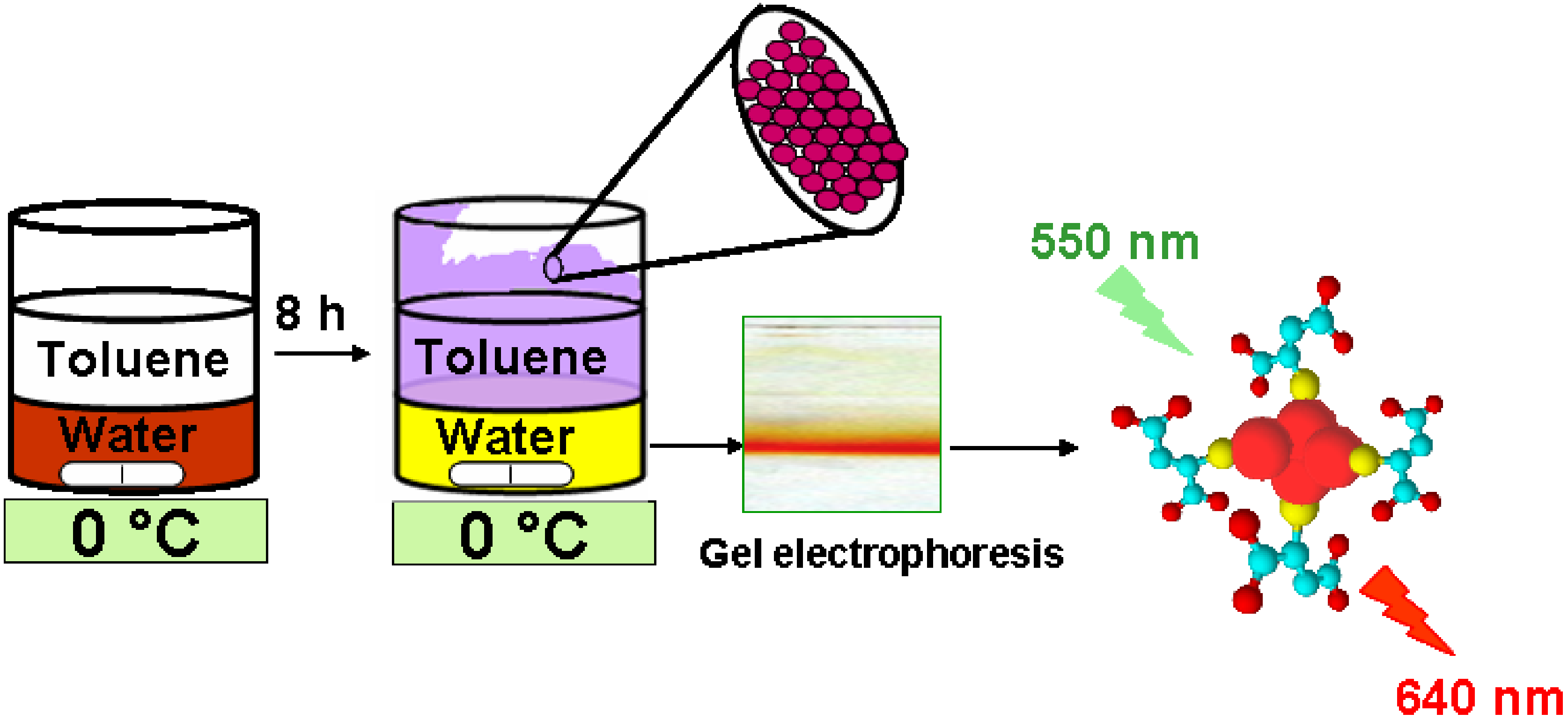

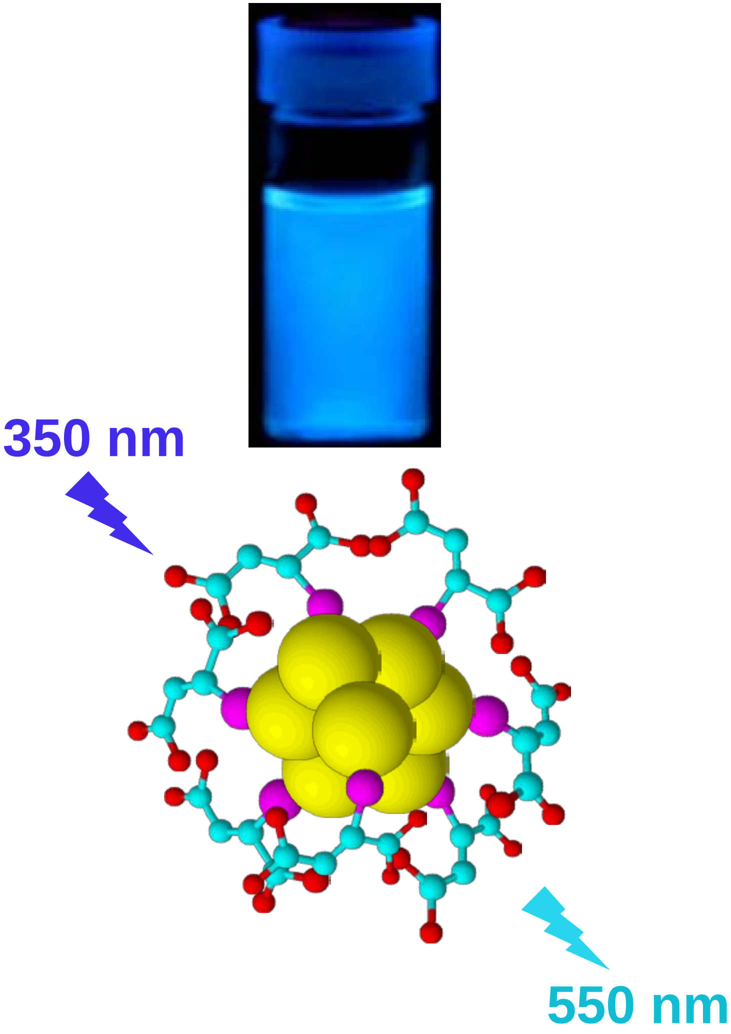
350 nm
550 nm

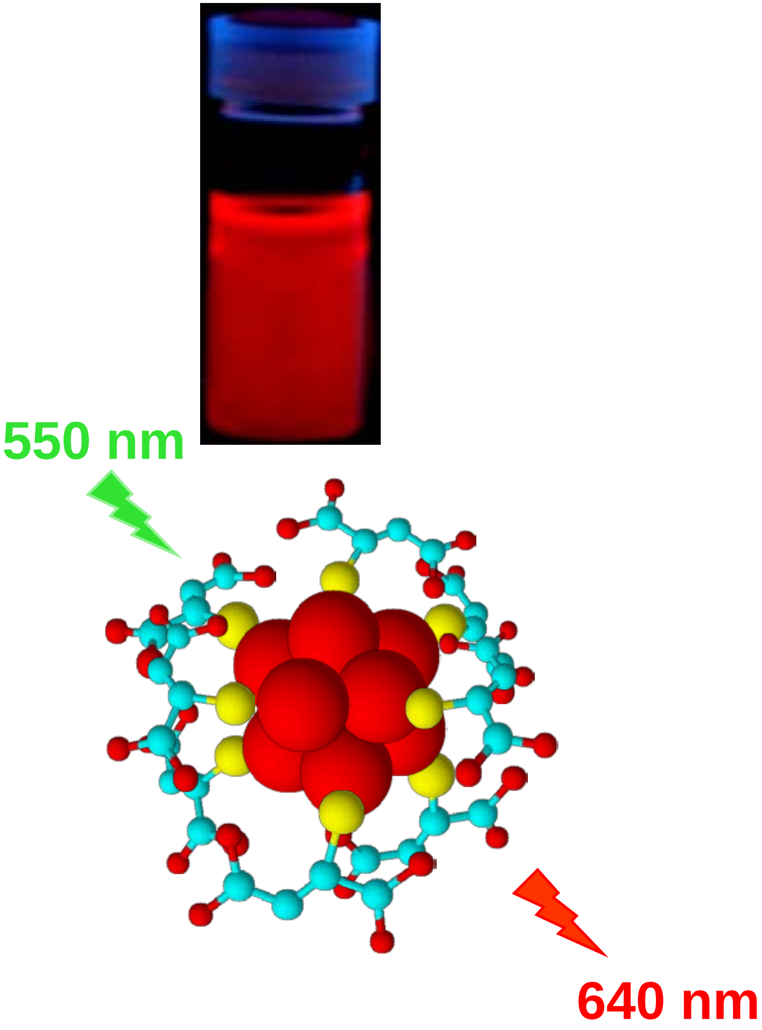
550 nm
640 nm

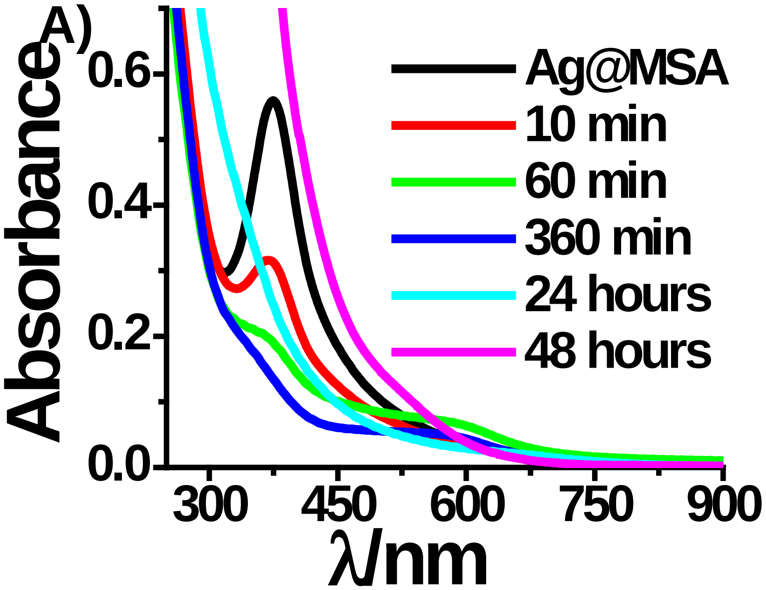

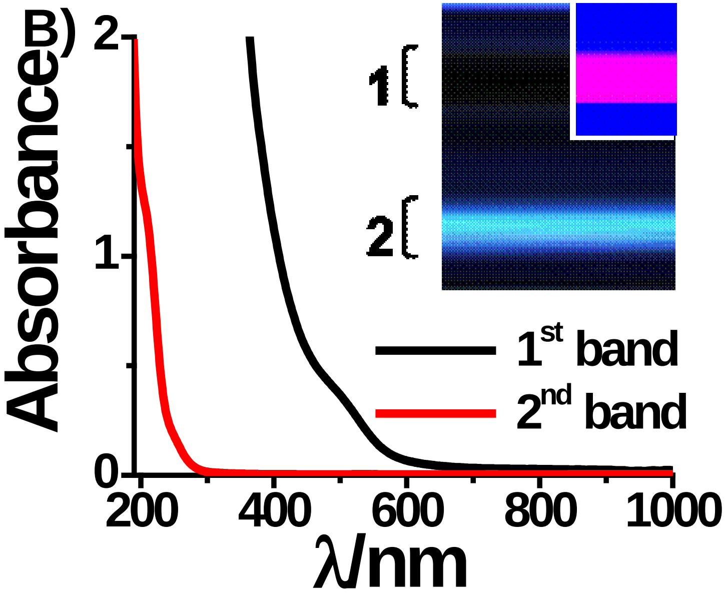

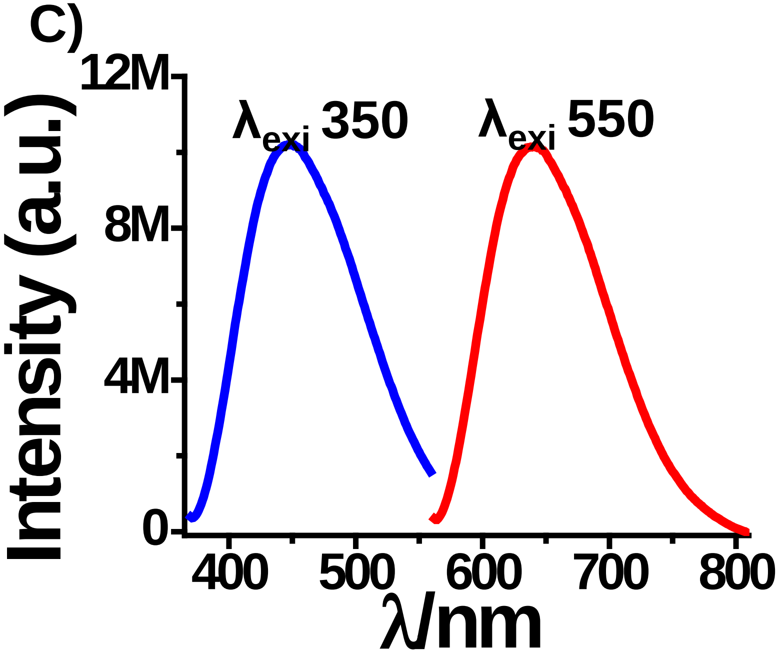

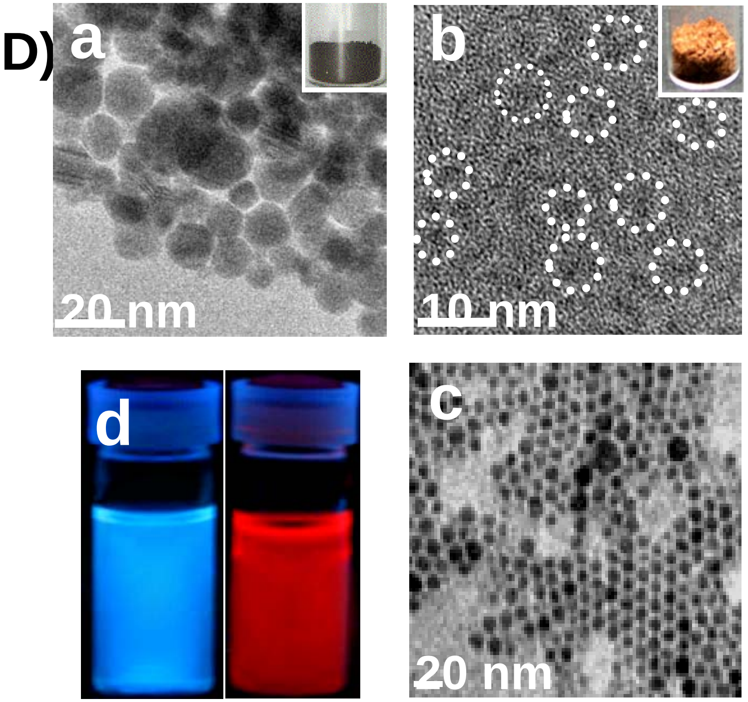

Udaybhaskar Rao and Pradeep, Submitted

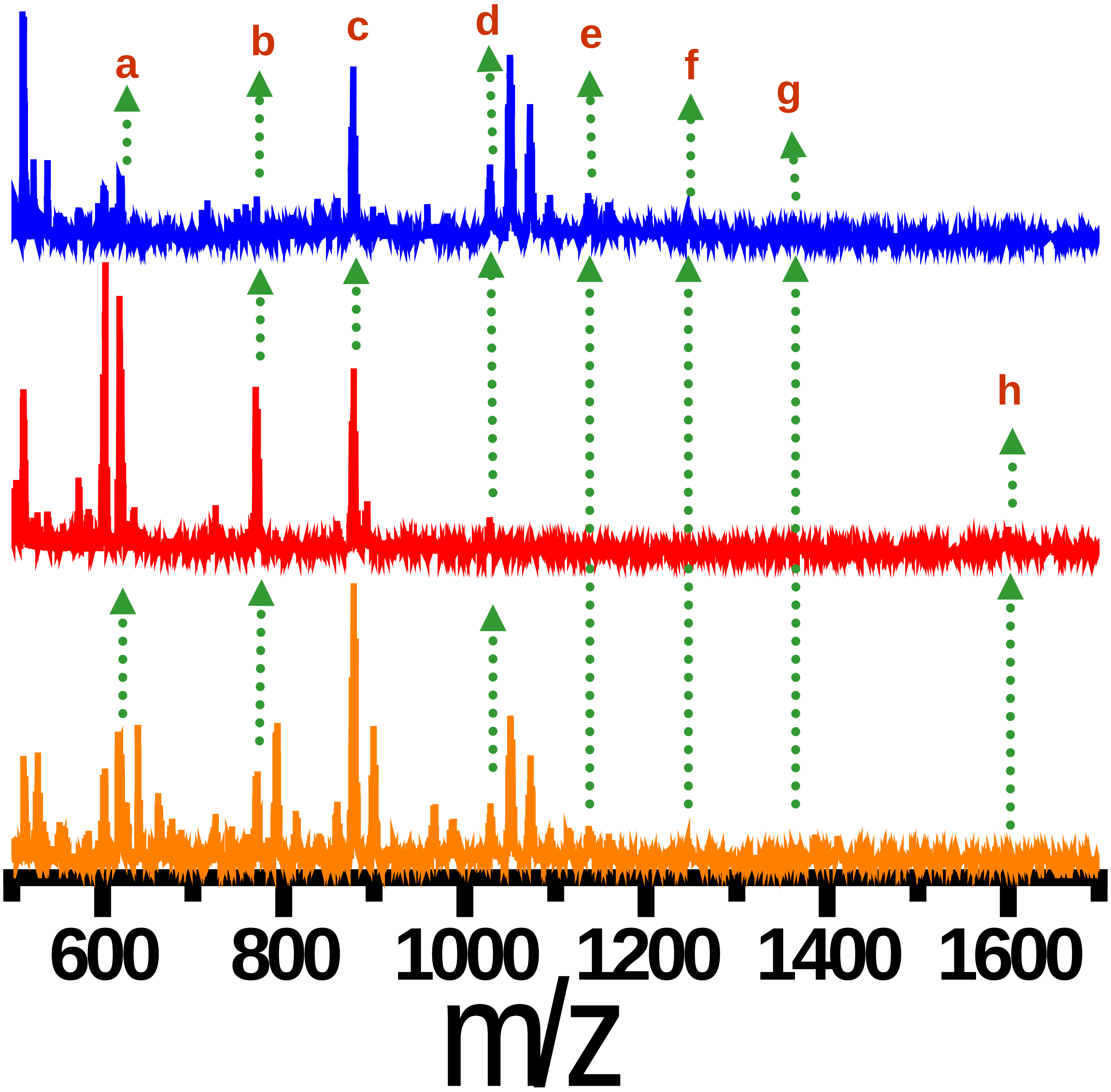
a
b
c
d
e
f
g
h
600
800
1000
1200
1400
1600
m/z

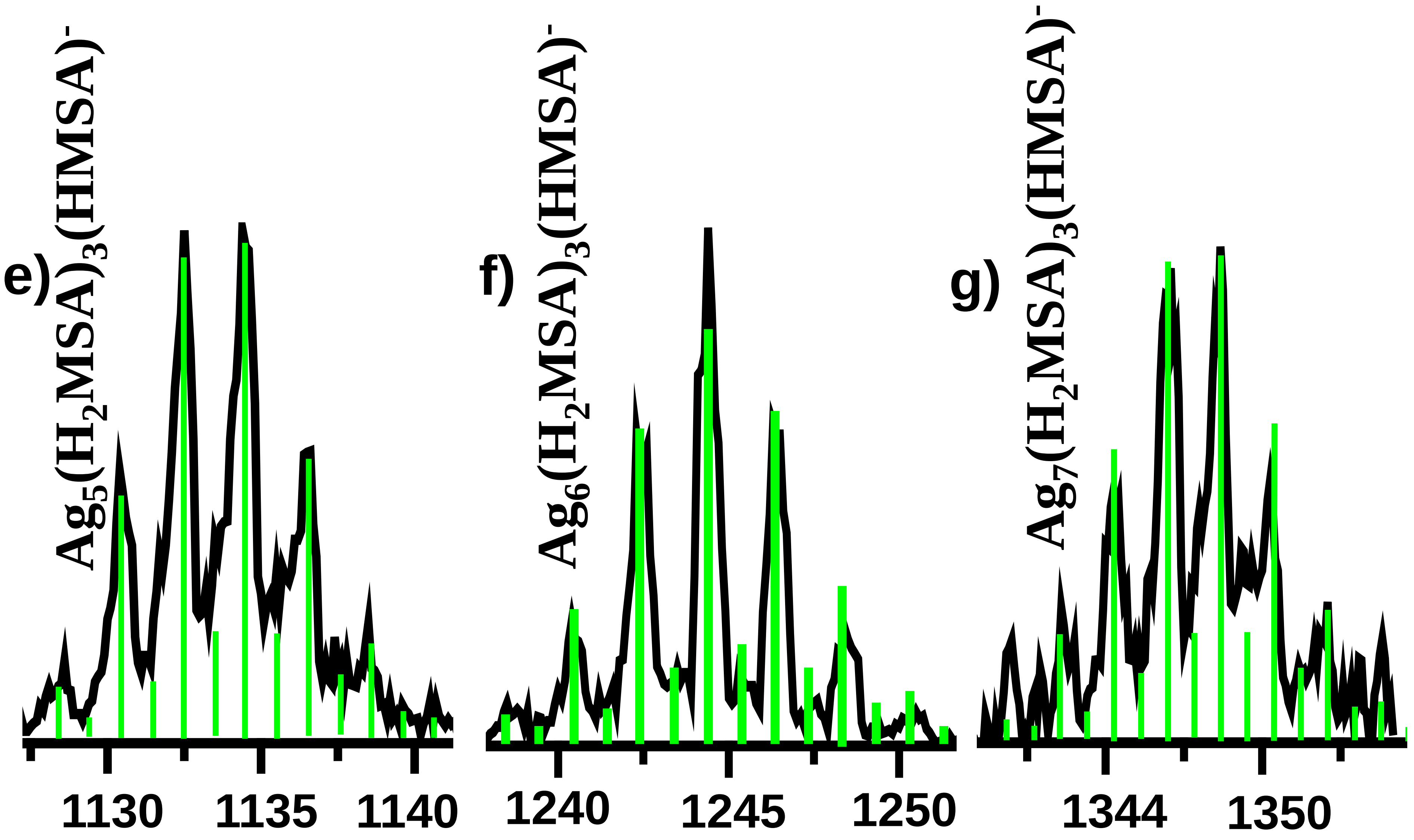
e)
$Ag_5(H_2MSA)_3(HMSA)^-$
1130
1135
1140
f)
$Ag_6(H_2MSA)_3(HMSA)^-$
1240
1245
1250
g)
$Ag_7(H_2MSA)_3(HMSA)^-$
1344
1350

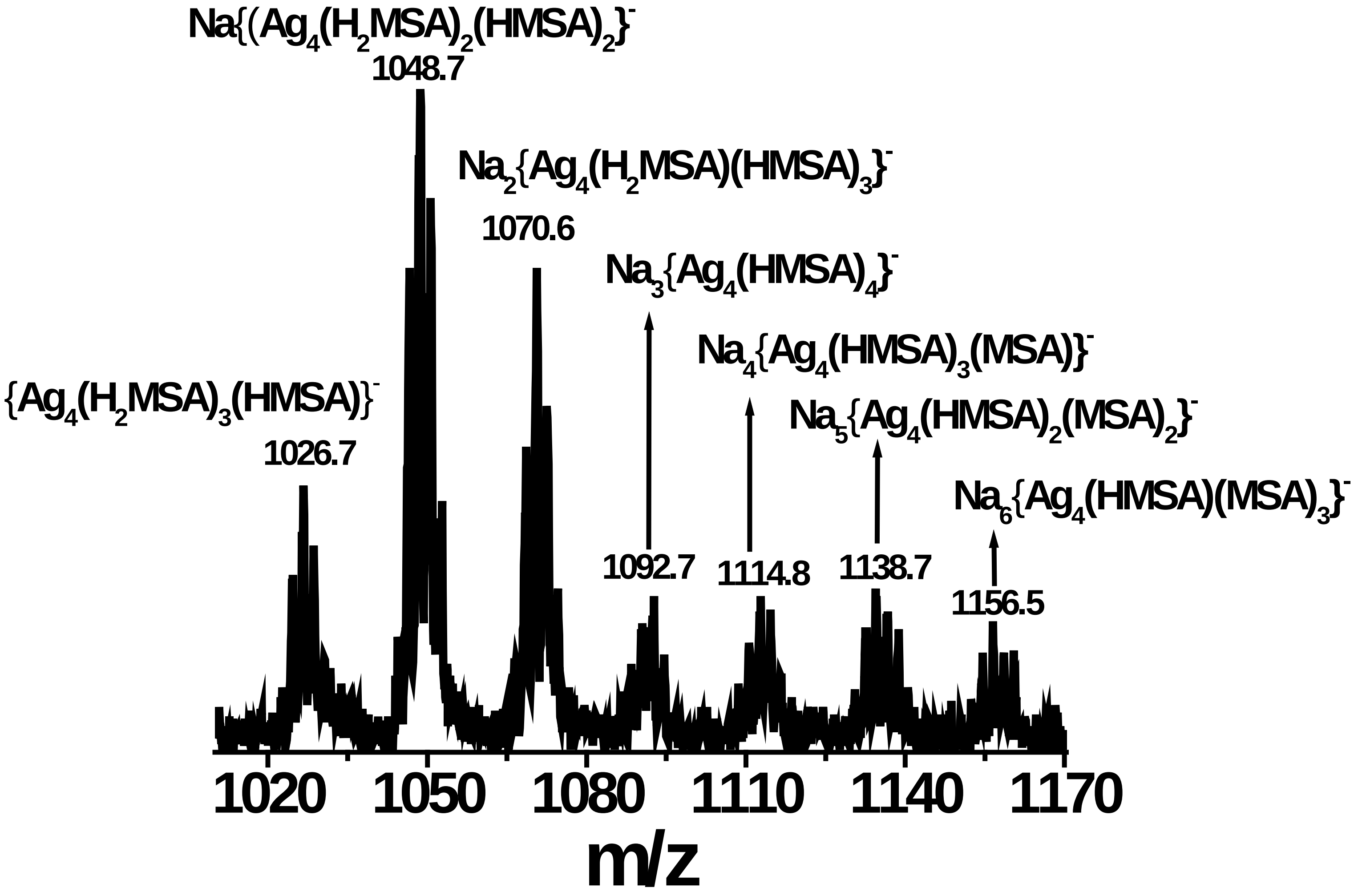
Na{(Ag4(H2MSA)2(HMSA)2}-
1048.7
Na2{Ag4(H2MSA)(HMSA)3}-
1070.6
Na3{Ag4(HMSA)4}-
Na4{Ag4(HMSA)3(MSA)}-
{Ag4(H2MSA)3(HMSA)}-
1026.7
Na5{Ag4(HMSA)2(MSA)2}-
Na6{Ag4(HMSA)(MSA)3}-
1092.7
1114.8
1138.7
1156.5
1020
1050
1080
1110
1140
1170
m/z

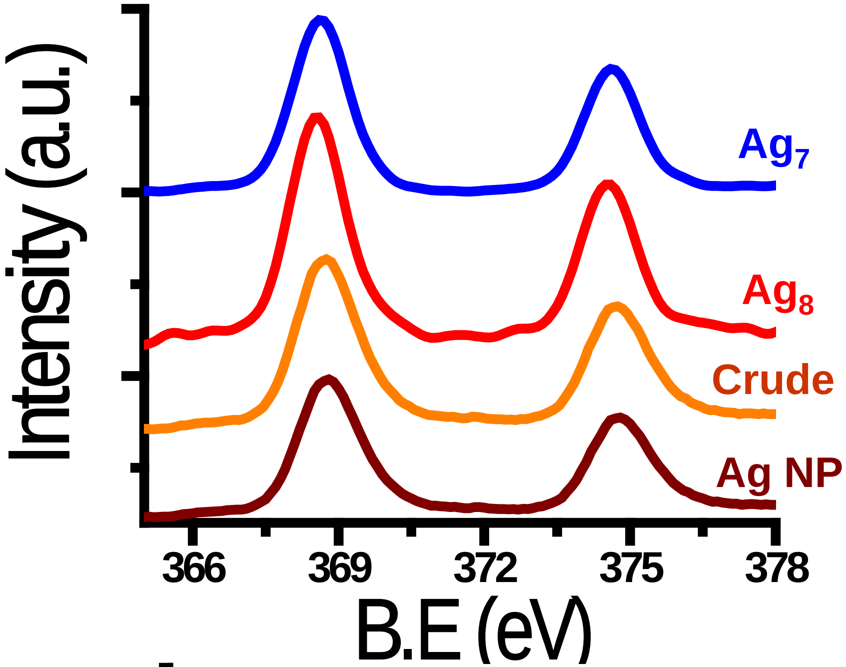
Intensity (a.u.)
Ag7
Ag8
Crude
Ag NP
366
369
372
375
378
B.E (eV)

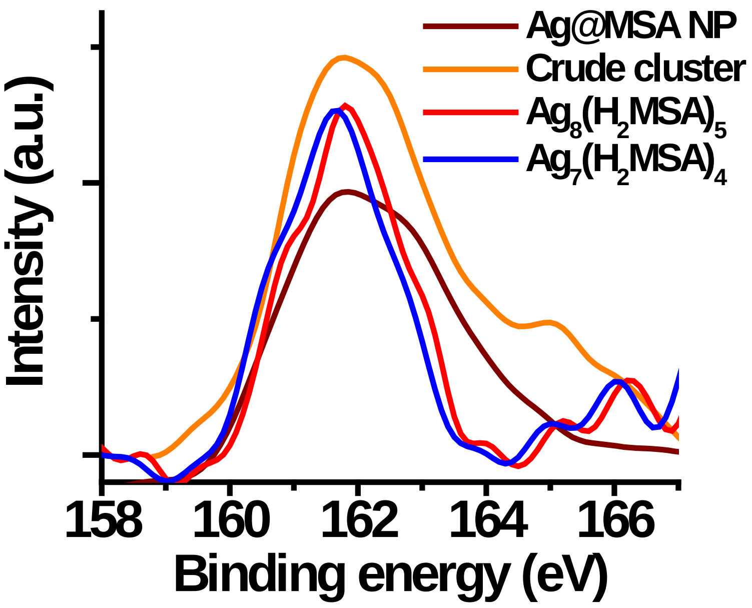
Ag@MSA NP
Crude cluster
Ag8(H2MSA)5
Ag7(H2MSA)4
Intensity (a.u.)
158
160
162
164
166
Binding energy (eV)

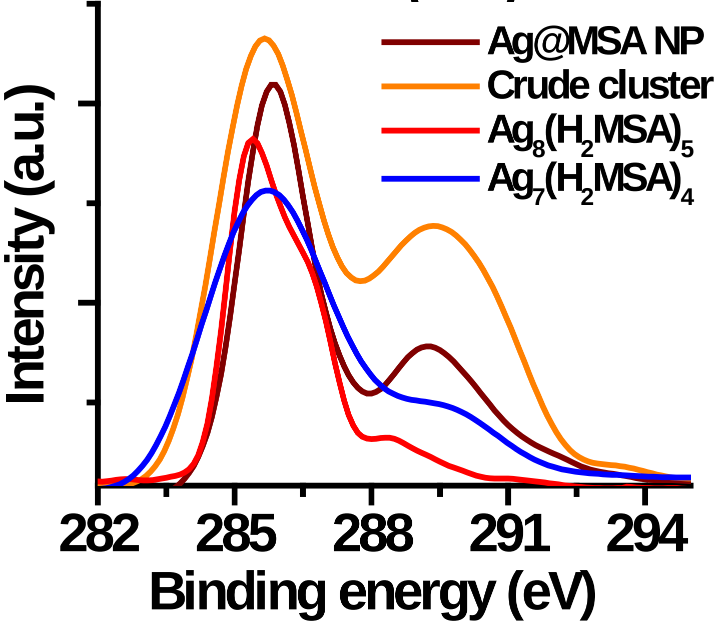
Ag@MSA NP
Crude cluster
Ag8(H2MSA)5
Ag7(H2MSA)4
Intensity (a.u.)
282
285
288
291
294
Binding energy (eV)

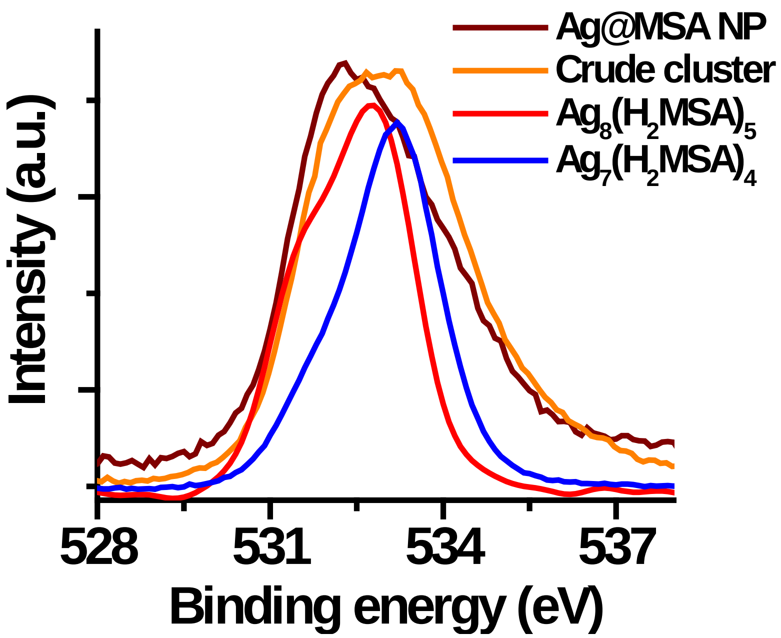
Ag@MSA NP
Crude cluster
Ag8(H2MSA)5
Ag7(H2MSA)4
Intensity (a.u.)
528
531
534
537
Binding energy (eV)

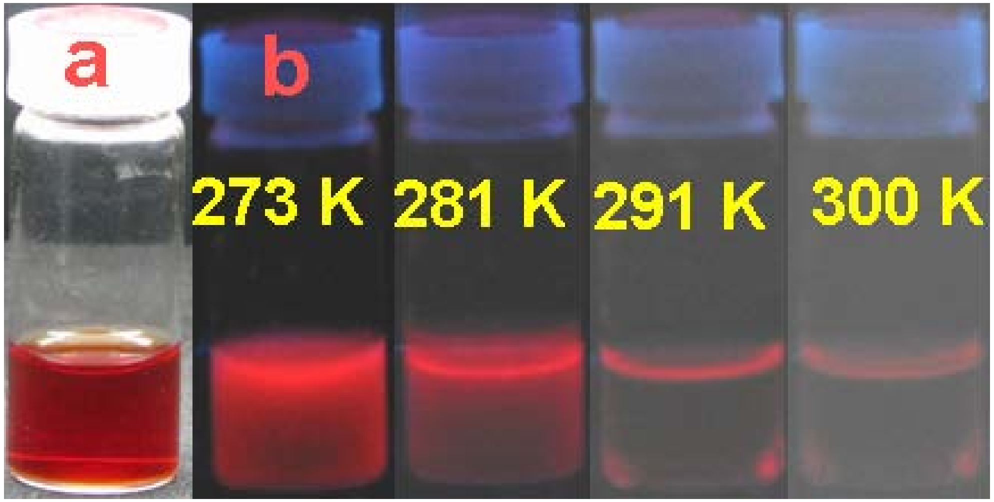

White light
RT

UV light T →

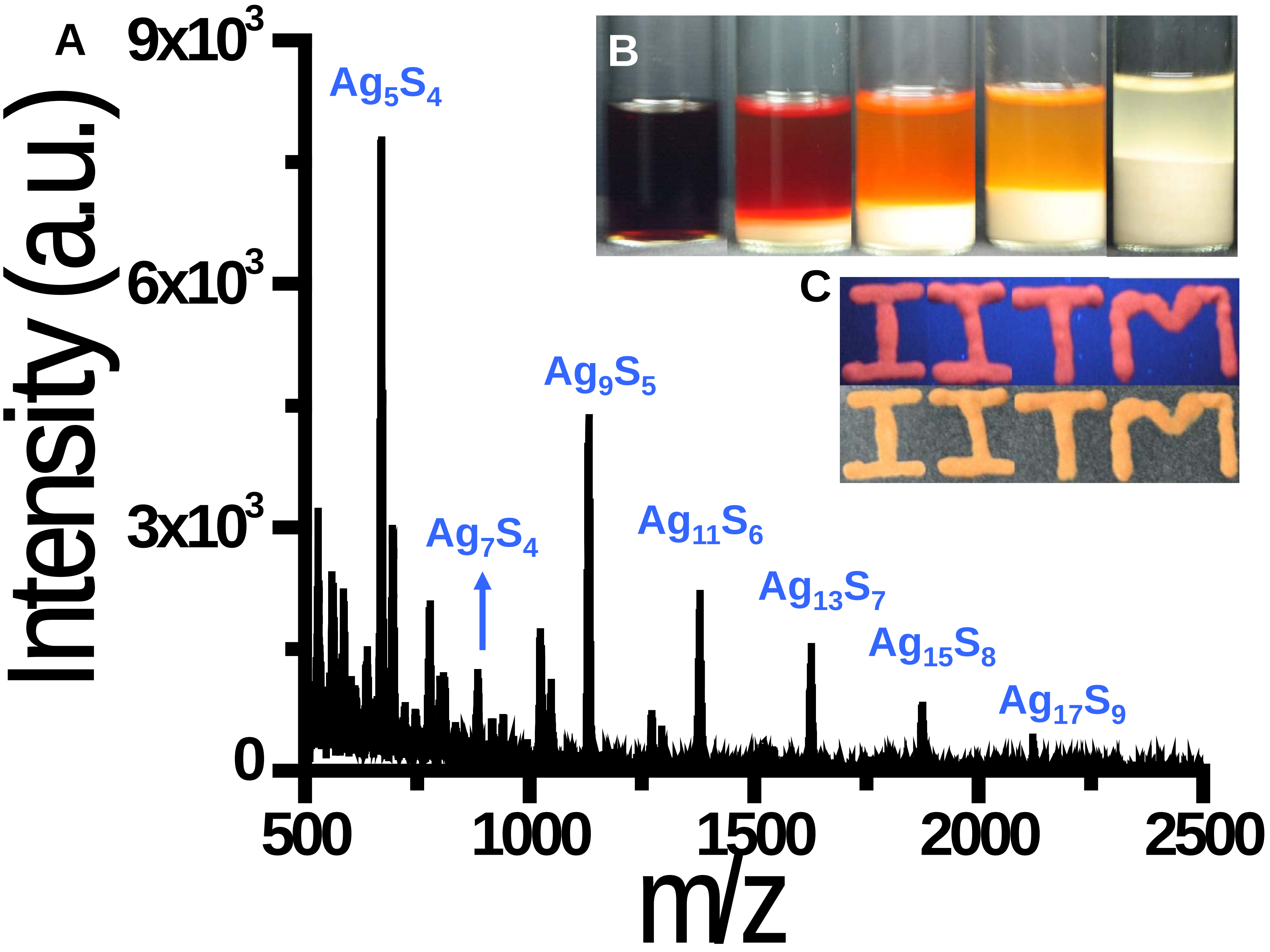
A
B
C
Intensity (a.u.)
9x10³
6x10³
3x10³
0
500
1000
1500
2000
2500
m/z
Ag5S4
Ag7S4
Ag9S5
Ag11S6
Ag13S7
Ag15S8
Ag17S9
IITM
IITM

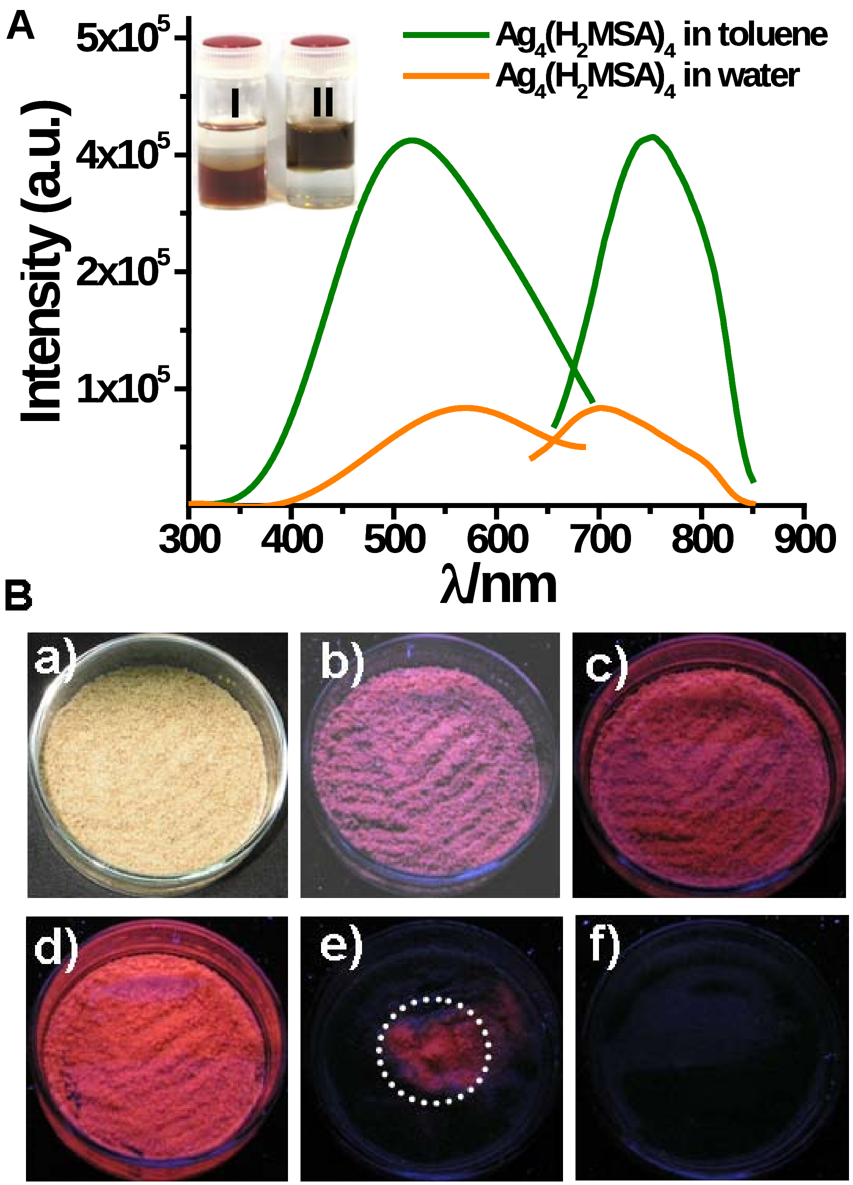
A
Ag4(H2MSA)4 in toluene
Ag4(H2MSA)4 in water
I
II
Intensity (a.u.)
5x10^5
4x10^5
2x10^5
1x10^5
300
400
500
600
700
800
900
λ/nm
B
a)
b)
c)
d)
e)
f)

Clusters in proteins

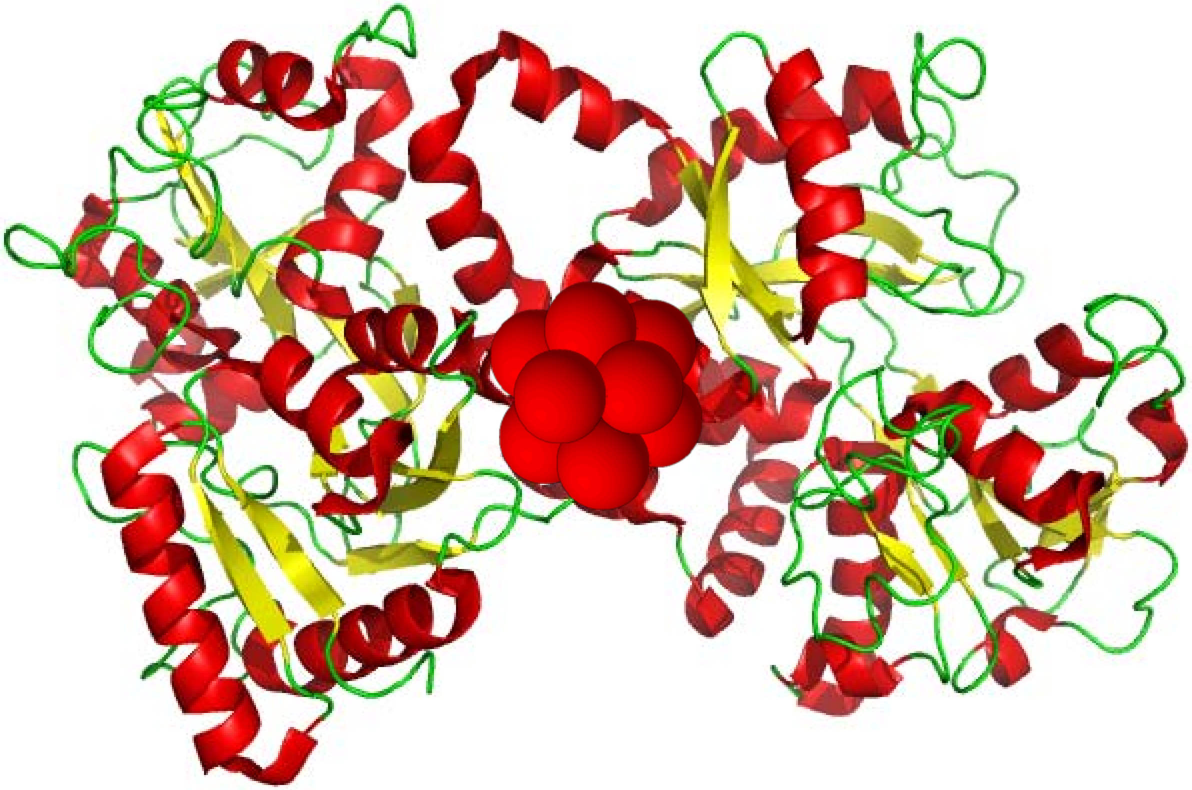

Lourdu Xavier, Kamalesh Choudhari

Nothing Gold Can Stay

Robert Frost (1923)

Nature’s first green is gold,
Her hardest hue to hold.
Her early leaf’s a flower;
But only so an hour.
Then leaf subsides to leaf.
So Eden sank to grief,
So dawn goes down to day.
Nothing gold can stay.

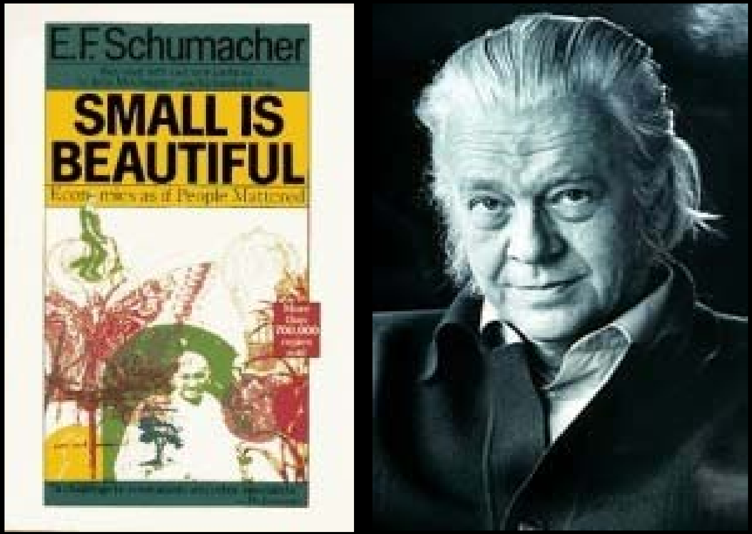

E. F. Schumacher

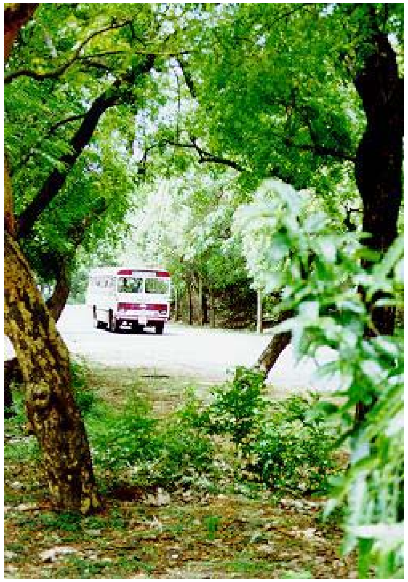

Nano Mission, Department of Science and Technology

IIT Madras

Thanks!

Na Guror Adhikam Tatwam
Na Guror Adhikam Tapa:
Tatwa Gnyaanaat Param Naasti
Tasmai Sri Gurave Nama: